

DEVELOPMENT AND EVALUATION OF A NATURAL-CONVECTION SOLAR DRYER  
FOR MANGO IN RURAL HAITIAN COMMUNITIES

By

DREW FRANK SCHIAVONE

A THESIS PRESENTED TO THE GRADUATE SCHOOL  
OF THE UNIVERSITY OF FLORIDA IN PARTIAL FULFILLMENT  
OF THE REQUIREMENTS FOR THE DEGREE OF  
MASTER OF SCIENCE

UNIVERSITY OF FLORIDA

2011

© 2011 Drew Schiavone

To my wife, Jessica, who lovingly supported and encouraged me throughout the long hours of work and preparation involved with this study

## ACKNOWLEDGMENTS

I would like to thank my advisor Dr. Teixeira as well as my committee members, Dr. Bucklin and Dr. Sargent, for their support and guidance throughout my research. I would also like to thank the technicians whose work allowed for the construction of the prototype system. The assistance, suggestions and engineering work that James Rummel and Steve Feagle conducted were instrumental in accomplishing this study.

Furthermore, I am thankful for the support of WINNER through the UF/IFAS Office of International Programs in allowing this project to be undertaken. Finally, I would like to thank all my family and friends who supported me during this work with their presence and encouragement. I could not have made it through this degree program without the support of everyone mentioned here and the blessings lavished on me by Jesus Christ, who is my Lord and Savior and the Foundation and Perfector of my faith. None of this would have ever been possible without the Author of Salvation.

## TABLE OF CONTENTS

	<u>Page</u>
ACKNOWLEDGMENTS.....	4
LIST OF TABLES.....	8
LIST OF FIGURES.....	9
LIST OF ABBREVIATIONS.....	13
ABSTRACT .....	16
CHAPTER	
1    INTRODUCTION .....	18
2    OBJECTIVES .....	22
Task 1: Mango Fruit.....	22
Task 2: Dryer Design .....	22
3    LITERATURE REVIEW OF SOLAR DRYERS .....	23
Background.....	23
Post Harvest Losses.....	23
Biological Degradation.....	24
Drying Review .....	25
Traditional Drying Methods.....	30
Industrial Drying Methods.....	32
Solar Drying Methods.....	33
Solar Dryers.....	36
Active and Passive Mode .....	36
Direct Mode Dryers .....	38
Indirect Mode Dryers .....	41
Large-Scale Dryers .....	51
Case Studies .....	53
Direct Solar Dryer Designs .....	55
Indirect Cabinet Designs (Passive) .....	57
Indirect Cabinet Designs (Active) .....	59
Supplemental Heat Dryers .....	63
Desiccant-Integrated Dryers.....	70
Indirect Tunnel Dryers .....	71
Large-Scale Solar Dryers .....	74
Construction.....	74
Evaluation .....	75
Product Evaluation .....	76

Dryer Parameter Evaluation .....	79
Performance Evaluation .....	81
Evaluation Procedure .....	84
<b>4 MATERIALS AND METHODS .....</b>	<b>143</b>
Task 1: Sorption Isotherm.....	143
Task 2: Dryer Design .....	148
Design Features and Considerations .....	149
Mathematical Procedure.....	149
Construction.....	156
Absorber.....	156
Cabinet.....	158
Dryer Operation .....	159
General Overview.....	159
No Load.....	159
Load .....	160
Evaluation.....	162
<b>5 RESULTS AND DISCUSSION .....</b>	<b>168</b>
Sorption Isotherm .....	168
Solar Dryer Design.....	169
Dryer Operation .....	169
No-Load.....	169
Load Experiments .....	172
Evaluation.....	176
Dryer Efficiency.....	176
Product Quality .....	176
<b>6 CONCLUSION .....</b>	<b>189</b>
<b>7 FUTURE DEVELOPMENTS.....</b>	<b>191</b>
<b>APPENDIX</b>	
<b>A DRYING PARAMETERS .....</b>	<b>193</b>
<b>B STANDARD OPERATING PROCEDURES.....</b>	<b>194</b>
Product Preparation.....	194
Dryer Operation .....	194
Maintenance/Cleaning .....	195
<b>C OPERATING SCHEDULE .....</b>	<b>196</b>
<b>LIST OF REFERENCES .....</b>	<b>197</b>

BIOGRAPHICAL SKETCH..... 205

## LIST OF TABLES

<u>Table</u>		<u>Page</u>
3-1	Estimated postharvest losses of fresh produce in developed and developing countries.....	94
3-2	Moisture absorption capability .....	95
3-3	Commonly used materials for solar dryers in developing countries.....	142
3-4	Optimum tilt angles for solar collectors.....	142
4-1	Design parameter input for natural-convection solar dryer .....	165
5-1	Estimated parameters of sorption isotherm models of mango slices.....	179
5-2	Design parameter output for natural-convection solar dryer .....	179
A-1	Mango drying parameters and storage conditions.....	193

## LIST OF FIGURES

<u>Figure</u>		<u>Page</u>
3-1	Drying curve .....	94
3-2	Psychrometric chart showing a drying process.....	95
3-3	Traditional open-air sun drying .....	96
3-4	Working principle of direct solar dryer .....	96
3-5	Working principle of indirect, active solar dryer .....	97
3-6	General classification of solar dryers.....	98
3-7	Working principle of direct-type, solar dryer.....	99
3-8	Typical direct-type, tent solar dryer.....	99
3-9	Typical direct-type, seesaw dryer .....	100
3-10	Typical direct-type, box dryer.....	100
3-11	Typical indirect-type cabinet dryer .....	101
3-12	Airflow principles in assorted solar collectors .....	101
3-13	Typical indirect-type, tunnel dryer.....	102
3-14	Typical large-scale, greenhouse solar dryer .....	102
3-15	Roof-integrated solar drying system .....	103
3-16	Drying cabinet and solar collector of in-house dryer.....	103
3-17	Solar dryer categorization overview.....	104
3-18	Schematic of direct, box dryer .....	105
3-19	Box dryer with H <sub>2</sub> O heater.....	106
3-20	Box dryer with limited tracking .....	107
3-21	Detailed schematic of box dyer.....	108
3-22	Box dryer with variable inclination .....	109
3-23	Box dryer. A) Pictorial. B) Side view schematic.....	110

3-24	Simple cabinet dryer.....	111
3-25	Cabinet dryer schematic.....	112
3-26	Cabinet dryer with multiple solar collectors.....	113
3-27	Reverse absorber cabinet dryer, RACD .....	114
3-28	Cabinet dryer with top absorber.....	115
3-29	Simple active cabinet dryer, schematic .....	116
3-30	Active cabinet dryer, schematic.....	117
3-31	Active cabinet dryer with absorber mesh, schematic.....	118
3-32	Active cabinet dryer with piping .....	119
3-33	Rotary column cylindrical dryer, RCCD .....	120
3-34	Large-scale cabinet dryer with heater array.....	121
3-35	Cabinet dryer with thermal, gravel storage .....	122
3-36	Cabinet dryer with thermal, rock storage .....	123
3-37	Cabinet dryer with thermal , PCM storage.....	124
3-38	Cabinet dryer with thermal, silica gel storage .....	125
3-39	Cabinet dryer with interchangeable thermal, sand storage.....	126
3-40	Cabinet dryer with auxiliary heater .....	127
3-41	Cabinet dryer with auxiliary heating channel .....	128
3-42	Cabinet dryer with heating elements, schematic .....	129
3-43	Cabinet dryer with exhaust recirculation.....	130
3-44	Indirect cabinet dryer with biomass burner.....	131
3-45	Direct cabinet dryer with biomass burner .....	132
3-46	Cabinet dryer with biomass burner and thermal storage.....	133
3-47	Forced cabinet dryer with integrated desiccant .....	134
3-48	Cabinet dryer with integrated desiccant.....	135

3-49	Cabinet dryer with integrated desiccant and mirror .....	136
3-50	Simple tunnel dryer schematic.....	137
3-51	Tunnel dryer schematic .....	138
3-52	Tunnel dryer with biomass burner .....	139
3-53	Greenhouse dryer schematics.....	140
3-54	Greenhouse dryer.....	141
4-1	Natural-convection solar dryer featuring a solar collector and separate drying cabinet with five trays .....	164
4-2	Schematic of solar collector, cross section.....	166
4-3	Solar convection dryer on UF campus in Gainesville, FL .....	166
4-4	Trays loaded within the cabinet section of the solar convection dryer .....	167
5-1	Sorption isotherm for mango at 71°F (22°C) .....	178
5-2	Solar collector schematic.....	180
5-3	Drying cabinet with chimney, shutter and trays (schematic) .....	180
5-4	Incident solar radiation recorded at weather station .....	181
5-5	Temperatures recorded within the solar dryer. ....	182
5-6	Cabinet temperatures based on average temperatures between all trays.....	183
5-7	Relative humidity as recorded near chimney exhaust .....	183
5-8	Exhaust air velocity recorded at chimney exhaust.....	184
5-9	Temperatures within the solar dryer at various locations.....	184
5-10	Temperatures of incoming air in the plenum and rock bed.....	185
5-11	Temperatures recorded at the exhaust outlet.....	185
5-12	Relative humidity of ambient air as recorded at weather station and in chimney/exhaust.....	186
5-13	Moisture content of mango slices in solar dryer over 2 full days of sunlight with batch mode of operation.....	186

5-14	Moisture content of mango slices in solar dryer over 2 full days of sunlight with continuous mode of operation.....	187
5-15	Photograph of solar dried mangoes compared with commercially-available mango slices.....	188

## LIST OF ABBREVIATIONS

A	aperture area of dryer, cross-sectional flow area
$A_c$	solar collector area
$A_{cs}$	cross-sectional, tray area
$a_w$	water activity
B	surface heat constant
C	constant, discharge coefficient
$C_p$	specific heat of air
D	diffusion coefficient
d	slice thickness
E	total useful energy
G	mass flow rate of air per unit of collector area
g	gravitational acceleration
H	height (head)
h	vertical distance between trays, height of chimney
$h_{as}$	absolute humidity of the air entering dryer at the point of adiabatic saturation
$h_{final}$	final enthalpy
$h_i$	absolute humidity of air entering the drying chamber
$h_{initial}$	initial enthalpy
I	total solar energy incident upon plane of collector per unit time per unit area
$k_1, k_c$	rate constant of constant rate period
$k_2, k_E$	rate constant of falling rate period
L	latent heat of vaporization of water, length of sample

$M_C$	final moisture concentration of constant rate period
$M_E$	final moisture concentration of falling rate period
$M_{EQ}$	equilibrium moisture content
$M_f$	final moisture content (wb)
$M_i$	initial moisture content (wb), initial moisture concentration
$M_o$	monolayer moisture
$M(t)$	absorbed moisture concentration
$m_a$	airflow rate
$m_{dr}$	average drying rate
$m_{fruit}$	weight of whole fruit
$m_p$	weight of sliced fruit
$m_w$	mass of water to evaporate
$N_{fruit}$	number of whole fruit
$N_{trays}$	number of trays
$n$	numbered day of year
$P_{ATM}$	ambient air pressure
$P_i$	internal air pressure
$Q$	chimney effect (flow rate)
$T_{atm}, T_{ATM}$	ambient air temperature
$T_{AVG}$	average temperature between $T_o$ and $T_i$
$T_{da}$	temperature of drying air
$T_{max}$	maximum allowable temperature
$T_o$	absorber outlet temperature, average ambient temperature
$T_i$	absorber inlet temperature, average internal temperature
$t, t_d$	drying time (sunshine hours)

$t_C$	drying time of constant rate period
$t_E$	drying time of falling rate period
$v_{wind}$	wind speed
$V$	volumetric air flow rate
$V_a$	volumetric airflow rate
$W$	weight of water evaporated from the product
$W_f$	final humidity ratio
$W_i$	initial humidity ratio
$\beta$	collector angle/slope
$\delta$	angle of declination
$\Delta P$	air pressure difference
$\eta, \eta_{COLLECTOR}$	collector efficiency
$\eta_{PICK-UP}$	pick-up efficiency
$\eta_{SYSTEM}$	system efficiency
$\rho, \rho_{air}$	density of air
$\phi$	latitude
$\phi_{atm}$	ambient relative humidity
$\phi_f$	equilibrium relative humidity

Abstract of Thesis Presented to the Graduate School  
of the University of Florida in Partial Fulfillment of the  
Requirements for the Degree of Master of Science

DEVELOPMENT AND EVALUATION OF A NATURAL-CONVECTION SOLAR DRYER  
FOR MANGO IN RURAL HAITIAN COMMUNITIES

By

Drew Frank Schiavone

December 2011

Chair: Arthur Teixeira

Major: Agricultural and Biological Engineering

A natural-convection solar dryer capable of producing dried mango slices in rural communities of Haiti was designed and evaluated. Studies of both the mango fruit and the mathematical design of the drying system were undertaken to develop an adequate and effective system capable of preserving mango fruit slices. The design, construction and operation of this newly developed dryer is described in this report based on a variety of factors including the physical properties of mangoes, Haitian environmental conditions and the local production capabilities of small Haitian villages.

Moisture equilibrium data for desorption of water from mango slices were used for the development of a sorption isotherm to determine target levels of moisture content and water activity. A mathematical procedure for solar dryer design was adopted and modified for the development of this dryer and schematics were created based on the results. The dryer consists of two primary components; the solar collector which produces thermal energy and the drying chamber which houses five trays loaded with product. Fabrication of the dryer was carried out using locally available material such as plywood for the frame, a corrugated aluminum absorber, polycarbonate glazing, rock wool insulation and wire mesh for trays. The 18.4 ft<sup>2</sup> solar collector was designed

to allow flow on both sides of the absorber. A 0.67 x 0.67 x 2.2 ft<sup>3</sup> chimney was built into the upper portion of the 2 x 2 x 3.125 ft<sup>3</sup> cabinet to dissipate heat and moisture with a thin steel shutter for airflow regulation. Additionally, a 2 ft<sup>3</sup> thermal rock bed was integrated into the bottom of the cabinet to provide heat during inclement weather and during the night.

Evaluation of the solar dryer in Gainesville, Florida found temperatures inside the cabinet significantly elevated compared to environmental air with temperature increases of up to 58.3°F (32.4°C) and 72.1°F (40.0°C) depending on airflow and loading. Loading tests conducted with an average of 21.6lbs (9.80kg) of fresh mango slices resulted in effective drying within two days from a moisture content of 84% (wb) down to approximately 9.4% (wb) and 11.1% (wb) for batch and continuous modes of operation respectively. The collector efficiency, drying efficiency and system efficiency were 29.5%, 10.8% and 33.9% respectively. These results indicated sufficient drying and preservation of mango slices within two full days of sunlight. The quality of solar-dried product was competitive with commercially-available mango slices.

## CHAPTER 1

### INTRODUCTION

Many rural areas in developing nations suffer substantial losses of vital agricultural products. In fact, it has been reported that Haiti loses between 20 to 40% of their mango harvest each year (Castañeda et al., 2011; Lush, 2010). While there are several contributing factors which account for this loss, spoilage due to insufficient postharvest management plays a key role particularly in provincial communities. Mechanical injury of the fruit actually begins with inadequate and limited harvesting practices and continues throughout transportation and sorting processes (Medlicott, 2001; Yahia, 1999). Additionally, the fruit is quickly lost to fungal and microbial degradation due to the high humidity levels associated with tropical environments (Dauthy, 1995; Enebe and Ezekoye, 2006). Limited resources and a complete lack of electricity in many rural locations, leaves farmers with few options to preserve their crops.

While education and improvement of proper postharvest practices can be of benefit, processing operations are needed in close proximity to the harvesting areas in order to minimize losses associated with spoilage (Singh, 1994). While sophisticated cooling and mechanized-drying methods have high rates of performance (Buteau, 2009; Chua and Chou, 2003), they are unfeasible due to the energy requirements which are unavailable in many rural communities. In contrast, traditional open-air and smoke drying preservation methods result in contamination by animals, insects, dust, and microorganisms due to the extensive environmental exposure times of the products (Bakeka and Bilgen, 2008; Bhandari et al., 2005; Kandpal et al., 2006). Developing countries with humid environments and limited resources like Haiti, pose unique

challenges in quickly and efficiently removing moisture from agricultural crops to reach adequate preservation standards by drying.

For these reasons, the use of a natural convection-type, solar dryer is proposed for rural communities of Haiti. The operation of solar dryers is dependent entirely on solar energy, which is a widely available resource in tropical communities. In principle, air is heated by solar radiation and naturally circulated by pressure gradients which promote vertical airflow. Consequently, these dryers require no electrical or mechanical components because the natural convection driving force is based only on temperature difference or changes in air density. Thus, product quality can be improved while reducing wasted produce and minimizing the use of traditional fuels. For these reasons, solar dryers are often considered more effective than sun drying with operating costs generally lower than mechanized dryers (Chen et al., 2009).

The ease of construction of previously reported designs has indicated the potential for adoption into small, rural communities where financial and material resources are limited (Chen et al., 2009). Studies further show that prolonged product shelf life is achieved while significantly reducing both the product volume and weight. By establishing these conditions, packaging, storing and transportation costs are effectively minimized (Chaudhri et al., 2009). The controlled environment of solar dryers also ensures that food remains unaffected by water intrusion, convective heat losses and contamination by foreign particles thereby reducing the likelihood of fungal and microbial growth.

Additionally, these advantages benefit the end user by limiting the work needed for protecting the crop from these threats. Moreover, solar drying results in improved

quality which enhances the product marketability. Thus, the application of this drying process allows for improved financial opportunities for farmers compared with traditional drying methods. To this end, the application of solar dryers has been shown to be practical, economical and environmentally responsible in the conservation of agricultural products (Buchinger and Weiss, 2002). However, significant amounts of mango fruit continue to spoil under mango groves in remote areas of Haiti despite the potential of solar drying technology. This may be attributed to the development of inappropriate solar dryer designs, elevated construction costs or the inaccessibility of resources needed for construction (Akoy et al., 2006).

To promote drying processes in these developing communities, an inexpensive, natural-convection solar dryer capable of producing dried mango slices was proposed for development. An ideal region for implementation of this system has been identified as the mountainous, Saut-d'Eau region of Haiti which is a major mango harvesting area outside of the Haitian power grid. Considering the limited resources in rural locations, the widely available energy source of solar radiation has significant potential for implementation. This resource can easily undergo conversion into low-grade heat for evaporation of moisture from agricultural products. In this manner, moisture content can be reduced until deterioration is effectively slowed. Air flow must also be established by the natural convection principle to remove heated water vapor and help prevent accumulation of emerging vapors on the product surface.

The application of drying systems in developing communities can greatly reduce post harvest losses of agricultural commodities and significantly contribute to food availability in these areas. Additionally, this technology has potential to generate local

employment opportunities depending on the size and scale of operation. Increased revenue is also possible as otherwise spoiled product is dried and either sold domestically or exported. This is a significant realization considering that dried mango is currently the highest value mango product according to a recent assessment of the Haitian mango industry (Castañeda et al., 2011). All of these factors must be recognized in order to meet the needs as well as the limitations of developing communities.

## CHAPTER 2 OBJECTIVES

The overall objective of this project was to design, construct, and make operational a natural convection-type, solar dryer for use in the tropical weather conditions of rural Haitian communities. To accomplish this task, studies of both the mango fruit and the drying system were undertaken to develop an adequate preservation system. Each of these project components was comprised of integral steps, procedures, and considerations which required meeting the following specific directives.

### **Task 1: Mango Fruit**

The objective of Task 1 was to construct a sorption isotherm for mango fruit slices from which the target values of moisture content and water activity could be determined. These target values were to be determined by analysis of commercially-available, dried mango slices serving as a standard. Equilibrium moisture data was also collected for fresh mango. An appropriate sorption isotherm model describing the equilibrium moisture data was then determined.

### **Task 2: Dryer Design**

The objective of Task 2 was to design, fabricate and operate a natural-convection, solar dryer, and evaluate its operating performance in the dehydration of mango fruit slices.

## CHAPTER 3

### LITERATURE REVIEW OF SOLAR DRYERS

#### Background

##### **Post Harvest Losses**

Compared to industrialized nations such as the United States, many rural areas and developing nations suffer substantial postharvest losses of vital agricultural products. In fact, postharvest losses in developing countries are estimated over a wide range, generally in the order of 40% but in certain areas these losses may exceed 50% (National Academy of Sciences, 1978). While significant postharvest losses do exist in developed countries, the primary difference in developing communities is that more of the product is lost before reaching retail sites as shown in Table 3-1.

High moisture content products, such as fruit and vegetables, are quickly lost to fungal and microbial degradation in these developing communities due to the lack of appropriate preservation and storage systems. This degradation begins shortly after harvesting and is greatly increased in areas with high levels of humidity. The development of processing facilities in close proximity to harvesting areas is crucial to reducing these losses. However, limited resources and a complete lack of electricity in many rural areas, leave farmers with few options to preserve their crops.

According to Bhandari et al. (2005), the primary requirement of agricultural producers is to secure a surplus of fresh produce from being wasted through spoilage, so that it can be preserved for extended periods of time. This allows for consumption of the preserved product in off-seasons as well as increasing the marketability of the product which serves to uplift the local economy. Additionally this agricultural production stimulus stands to assist national development. However, according to Amir et al.

(1991), agricultural crops must meet high quality standards in order to be made available in the world market. Otherwise, “the price will decline resulting in low profits for the exporting country and the producing farmer” (Amir et al., 1991). For these reasons, a great challenge is posed in efficiently and appropriately preserving agricultural goods.

### **Biological Degradation**

A general understanding of the biological processes which lead to spoilage is necessary for the consideration, development and implementation of appropriate preservation systems that will effectively slow deterioration and maintain product quality. It should be noted that in addition to quantitative losses, qualitative losses contribute to the overall loss of agricultural goods during postharvest processes. Therefore a brief description of these processes is provided here.

As mentioned previously, high moisture content products quickly spoil as microorganisms thrive in such environments. Additionally, deterioration is known to be caused by a range of biological processes including mechanical injuries, physiological disorders, pathological breakdown, respiration rate, ethylene production and action, sprouting and rooting, water stress and rates of compositional changes which are associated with qualitative characteristics such as nutritive value, flavor, color and texture (Kader, 2005). The actual rate of deterioration is dependent upon environmental conditions such as air velocity, sanitation procedures, temperature, atmospheric composition and relative humidity (Kader, 2005).

To counteract this susceptibility to deterioration, Chaudhri et al. (2009) suggests that harvested products should optimally be preserved, sold, or processed as quickly as possible after harvesting. To overcome this problem, drying processes

have been widely implemented as prerequisite for the storage of agricultural products. Drying improves the preserved shelf life and significantly reduces the product volume and weight while minimizing packaging, storage and transportation costs (Chaudhri et al., 2009). Thus, wastages can easily be prevented by applying proper drying procedures.

### Drying Review

Effective drying of agricultural goods is essentially the evaporation of moisture from the crop, thus reducing the product's moisture content so that deterioration no longer occurs. Each agricultural crop has different experimentally determined levels of moisture content that is considered safe for preservation (see Appendix for specific information pertaining to the safe moisture levels of mango fruit). In a normal drying process, the product is placed in an environment in which supplied heat evaporates moisture from the product and air flow then removes the water vapor.

Without an air current, emerging vapors will accumulate on the product surface which hinders further transport of moisture from within the fruit. The amount of heat needed for water removal from the product is equal to the latent heat of vaporization of water (Arata and Sharma, 1991). It follows that elevated temperatures, along with increased airflow rates and reduced levels of relative humidity, permit higher rates of food drying. These conditions apply as long as the diffusion rate is not the rate controlling process for the removal of water vapor. However, at lower moisture content, airflow rate is much less important than temperature. In this case, higher temperatures lead to higher rates of diffusion within the product which corresponds to the falling rate portion of the drying curve as shown in Figure 3-1.

During the drying process, water at the product's surface evaporates first. As additional heat is absorbed by the product, water then begins to migrate from within a crop's interior to the product surface. The ease of this migration is dependent on characteristics such as the diffusion rate which is affected by the porosity of the substance and the surface area exposed to the environment. It should be noted that only the physically held water is removed during drying while the chemically bound water remains in the product.

Drying continues until reaching a point where the moisture vapor pressure within the product is equivalent to the pressure of atmospheric moisture. This corresponds to an equilibrium state in which moisture absorption and desorption occur at the same rate and is known as the equilibrium moisture content.

Drying kinetics are often presented by measuring the average product moisture content as a function of time. This relationship is known as a drying rate which is shown in Figure 3-1. During the initial drying stages, excess moisture on the product surface results in a rapid rate of moisture removal. Subsequent drying of the material depends on the product-dependent rate at which internal water migrates to the product surface via diffusion (Chen et al., 2009).

Figure 3-1 shows multiple rates at which biological products undergo the drying process. The first period is described by Arata and Sharma (2009) as the constant rate of drying where moisture on the product surface is evaporated. A vapor pressure gradient is established which is greatly influenced by the air temperature and air flow rate.

Vapor pressure is essentially the partial pressure of water vapor in a known volume of air and is a function of the humidity ratio which describes the relationship between the mass of water vapor that is actually present in moist air and the mass of dry air. Saturated vapor pressure is the maximum vapor pressure which is a function of temperature. The vapor pressure deficit essentially describes the difference between actual vapor pressure and saturation vapor pressure evaluated at the same temperature which serves as a good indicator of the evaporative capacity of the air. As water is evaporated by the heated air, less potential is established as evaporative cooling effects which introduce additional pressure drops.

The rate of evaporation during the constant rate period is determined by the humidity ratio, ambient temperature and air circulation (Arata and Sharma, 2009). The second portion of the drying curve, in which the moisture removal rate decreases, is known as the falling rate period. This is a result of the diffusion rate which is slower than evaporation at the surface of the product. The nature and attributes of the drying curve are analogous for both hygroscopic and non-hygroscopic material until all of the unbound moisture within the material is removed. Beyond this point, a fraction of the bound water is actually removed from hygroscopic material.

Figure 3-2 depicts a simple psychrometric chart that demonstrates a drying process. In this example, ambient air is assumed to have a dry bulb temperature corresponding to the point labeled as '1' in Figure 3-2. As this ambient air is heated, the humidity ratio remains constant until reaching the heated temperature described by the point labeled as '2'. In this process, the relative humidity is reduced. If the heated air is then used to remove moisture from agricultural products until equilibrium is reached, the

temperature of the drying air will be reduced to the point labeled as '3'. During this drying process, the enthalpy remains constant. The final humidity ratio can then be assessed at point '3'. The difference in the final and initial humidity ratio allows for the determination of the amount of water removed from the product.

The moisture loss occurring in the constant rate period can be described by Equation 3-1 while the moisture loss occurring in the falling rate period can be expressed by Equation 3-2.

$$\frac{M(t) - M_C}{M_i - M_C} = \exp(-k_1 t_C) \quad (3-1)$$

$$\frac{M(t) - M_E}{M_C - M_E} = \exp(-k_2 t_E) \quad (3-2)$$

The variable  $M(t)$  refers to the absorbed moisture concentration which is a function of time.  $M_i$  is the initial moisture concentration,  $M_C$  is the final moisture concentration directly following the constant rate period and  $M_E$  is the final moisture concentration after the falling rate period. The variables,  $t_C$  and  $t_E$  are the drying times for the constant rate and falling rate periods, respectively. The rate constants,  $k_1$  and  $k_2$  are defined by the general expression described in Equation 3-3.

$$k = \frac{\pi^2 D}{4L^2} \quad (3-3)$$

The variable  $D$  refers to the unique moisture diffusion coefficient that depends on which drying rate period is being investigated. The variable  $L$  refers to length of the sample.

Safe storage of biological materials is particularly difficult in environments with high relative humidity. This challenge becomes even more difficult if the required equilibrium moisture content of the material is sufficiently low. For this reason, a

significant dilemma in developing communities, particularly in tropical environments, lies in the removal of moisture from agricultural products to reach adequate preservation states in a timely manner. If the drying process is too slow, growth of microorganisms will occur due to the conditions associated with high ambient temperature and relative humidity.

The primary objective of a dryer system is to provide increased temperatures to the product that are higher than the ambient conditions. By doing so, the vapor pressure of moisture within a product is sufficiently raised, while the relative humidity is lowered. However, vapor pressure is only a function of the humidity ratio as it does not change with temperature. The saturation vapor pressure that drives the drying process is what actually changes. This expression is essentially defined as the difference between vapor pressure and saturated vapor pressure. This condition ensures sufficiently low equilibrium moisture content by increasing the moisture carrying capacity of the air since heated air is able to retain larger quantities of moisture than cool, ambient air. The manner in which temperature and humidity affect the potential moisture absorption of air is shown in Table 3-2.

The application of such dryer systems in developing countries can greatly reduce post harvest losses of agricultural commodities and significantly improve the availability of food in these areas. However, appropriate systems must be considered that meet the needs as well as the limitations of the community. A brief outline of drying practices is mentioned here in order to demonstrate the necessity of an appropriate level of technology for developing nations. After identification, this technology will be elaborated on and reviewed in this report. This broad overview of

dryer sophistication levels ranges from simple, traditional practices to advanced, industrial practices.

## **Traditional Drying Methods**

Open-air sun drying is one of the most common and long practiced methods of food preservation among a large number of countries due to its simplicity and the abundance of solar irradiance (Bhandari et al., 2005; Chen et al., 2009; Kandpal et al., 2006; Sreekumar et al., 2008). In this process, the food product is spread into thin layers on the ground, on mats, or on trays as is shown in Figure 3-3. The uneven crop surface is thereby exposed to short wavelength solar energy which is converted into thermal energy after being absorbed. However, only a portion of this energy is actually absorbed by the product while the remaining radiation is reflected. Additionally, air flow across the product surface results in convective heat loss and can introduce moisture. The products are rarely pretreated and must be turned frequently in order to sufficiently dry.

Open-air sun drying has diminished over time as the limitations associated with this process are further recognized. In fact, it is widely acknowledged “that this method is unhygienic since the crops are easily contaminated” (Enebe and Ezekoye, 2006) by atmospheric dust, pollution, intrusion by animals, infestation by birds or insects, and animal droppings that all lead to infestation by fungi, bacteria, and other microorganisms. Additionally, this method is known to be labor and time intensive as crops need to be covered at night and during inclement weather. Further, the crops must be continually watched to prevent contamination from animals and birds. Additionally, the products must be turned frequently to attain adequate drying.

Moreover, this process requires significant land area and prolongs the drying period which may result in deterioration of crop quality.

Due to the hygroscopic properties of agricultural products, crops exposed to environmental conditions stand the risk of being rewetted, particularly at night when ambient temperature is lowered and humidity increases. In these situations, remoistening effects occur by condensation or by vapor diffusion induced via osmotic forces. This poses significant problems in humid, tropical regions where certain crops are grown and processed during rainy seasons (Buchinger and Weiss, 2002). Non-uniform and insufficient drying also leads to spoilage and deterioration of the crop during storage. Additionally, many products are known to exhibit discoloring when exposed to direct UV radiation. Furthermore, direct sun exposure during high temperature days is known to contribute to case hardening, in which hard shells form on the exterior surfaces of agricultural products (Chen et al., 2009). This shell subsequently traps moisture inside and thus extends the product's exposure to moisture.

All of these issues result in the deterioration of food quality in terms of a loss of nutritional value, adverse enzymatic reactions, loss of germination and an overall deterioration of the product (Bhandari et al., 2005). Under these conditions, studies have shown that agricultural losses can actually rise as high as 40-60% of the total harvest production (Chaudhri et al., 2009). For these reasons, it has been determined that “open-air sun drying does not fulfill the international quality standards and therefore it cannot be sold in the international market” (Chen et al., 2009).

Smoke drying is another traditional method of preservation used in tropical countries. In this process, heat is generated by biomass combustion of such materials as timber, coconut shells, rice husks and other agricultural wastes (Amir et al., 1991). Although this technique is weather independent and preserves crops to an extent, it also contaminates the product with combustion residues and thus severely diminishes the product quality. It has been noted that the quality of such products "are not good enough to attract the market and hence are to be consumed locally only" (Bhandari et al., 2005).

### **Industrial Drying Methods**

In industrialized regions, traditional drying methods have been replaced by mechanical dryers that exhibit faster drying rates, require less land, and provide higher quality product. These industrialized areas employ advanced drying equipment such as steam dryers, infrared, fluidized bed, spouted bed, drum dryers and freeze dryers to process commercial products. However, this equipment is expensive and energy intensive since it requires relatively significant amounts of energy in the form of electricity or fuel to operate. While companies that generate substantial revenues can reasonably afford this technology, most small-scale organizations or communities that are directly involved with the farms are unable to afford implementation of these technologies (Chen et al., 2009). Only large plantations or commercial establishments find these technologies economically viable in developing countries (Buchinger and Weiss, 2002).

Additionally, many rural areas in developing countries have limited resources. Construction supplies may be limited and energy sources such as fossil fuels and

electricity may be unreliable or totally absent. Studies have shown that even small, simple oil-fired batch dryers are not applicable for rural farmers in these regions (Buchinger and Weiss, 2002). Hence, there is a need to identify an intermediate, practical drying technology that can easily be implemented in developing regions to ensure food supply to a growing population. Furthermore, appropriate drying technology can enable farmers to produce high quality, marketable goods (Buchinger and Weiss, 2002).

### **Solar Drying Methods**

Solar drying has been described as “a potential decentralized thermal application of solar energy particularly in developing countries” (Chen et al., 2009). In fact, the use of solar thermal systems has been shown to be “practical, economical and environmentally responsible” in conserving agricultural products (Buchinger and Weiss, 2002). Moreover, solar heating systems are capable of improving product quality while reducing wasted produce and minimizing the use of traditional fuels. “The justification for solar dryers is that they may be more effective than sun drying, but have lower operating costs than mechanized driers” (Chen et al., 2009).

The application of equipment for collecting solar radiation serves to differentiate solar drying from traditional methods such as open-air sun drying. As noted by Arata and Sharma (1991), the superiority of solar drying has already been established over open-air sun drying through many solar drying studies. In solar drying operations, a portion of shortwave solar radiation is first received by an absorber as it travels through a transparent cover. The radiation is subsequently converted into low-grade heat after striking an opaque wall. Since long wavelength

radiation is unable to travel back across the transparent cover, the heat becomes trapped within the dryer as shown in Figure 3-4. In this way, radiative energy is harnessed for drying applications as opposed to directly exposing the product to the environment.

By enclosing the product inside a controlled environment, the food is less likely to be contaminated by animals, birds, insects and dust thereby reducing the likelihood of fungal and microbial growth. This also limits the intrusion of water in poor weather conditions and reduces the direct convective losses to the ambient environment. These improvements directly benefit the end user by limiting the work that must be done to protect the crop from these threats and results in a higher quality product.

Additionally, solar drying results in quicker drying rates by achieving higher temperatures, lower humidity, and increased air movement (Buchinger and Weiss, 2002). Hence, foods can be dried over shorter periods of time which increases the efficiency of the process by allowing less time for spoilage to occur. More complete, uniform drying is also possible which allows for better preserved quality and longer storage potential. Increased product throughput is also possible with increased drying rates.

Nutritional values of the products are also better preserved by drying food items in short times and optimal temperatures. Additionally, research has shown that solar drying can improve the quality of a product in regards to color, flavor and appearance which enhances the product's marketability and consequently allows for improved financial opportunities for farmers (Chen et al., 2009). Although solar dryers are capital

intensive, it has been discussed that “the unit cost of solar drying is expected to be a small fraction of the selling price of the product” (Kandpal and Kumar, 2005).

Furthermore, numerous studies have noted the financial attractiveness of solar dryers to the operators as fabrication is simple and commercial fuels are substituted (Kandpal et al., 2006). Several additional aspects must also be considered when comparing solar drying to conventional dehydration processes. For instance, solar dryers must be able to provide the equivalent performance of a conventional process in terms of capacity, labor input, product quality, and reliability.

However, the performance of solar dryers is still largely dependent on weather conditions because the heat required to remove moisture is often generated by solar energy only. Weather conditions also significantly influence the capacity of the product that can be dried within a given time period. The drying time is short under sunny conditions and is extended during adverse weather. Considering this dependence on weather, the utilization of solar energy as the only energy source is recommended for small-scale dryers where the risk of large quantities of spoilage in inclement weather is low. It is recommended that large-scale dryers used for commercial purposes, are equipped with back-up heaters to ensure drying during inclement weather (Buchinger and Weiss, 2002).

The drying behavior of agricultural crops is also dependent on the product size and shape, initial moisture content, final moisture content, bulk density, layer thickness, mechanical or chemical pretreatment, turning intervals, product temperature, temperature and humidity of the drying air, and the air velocity. To

improve these conditions, dryers must be designed to ensure that drying air flows through the chamber while contacting as much of the product surface as possible. The product surface area is increased by thinly slicing the food before placement on drying racks that allow for maximum contact between the heated air and product. As the heated air flows over the trays, the product becomes loaded with moisture. The moist air is then exhausted from the dryer while fresh air is subsequently drawn in.

Solar dryers are generally classified according to the manner in which solar heat is applied and used during the drying process. Generally, dryers are categorized into two broad groups; active dryers (conventional) and passive dryers (natural-circulation) (Sreekumar et al., 2008). Active dryers are systems which induce forced air circulation, while passive dryers only make use of the natural convection principle which generates movement of the heated air. The following section of this review serves to identify and elaborate on these two types of solar dryers. Additionally, a classification scheme for solar dryers is developed and the distinctions made are described in further detail with actual examples of drying systems.

## **Solar Dryers**

### **Active and Passive Mode**

Passive solar dryers are also called natural circulation or natural convection systems. Their operation depends completely on solar energy. Air in these systems is heated and naturally circulated by pressure gradients established by wind and temperature-induced buoyancy forces. As a result, these dryers do not require electrical or mechanical components such as fans or blowers because the natural convection driving force is based on temperature difference or changes in air density. The

difference in specific weight between the ambient air and the drying air promotes a vertical air flow independent of electrical supply.

Studies have shown that in general, solar dryers can be easily maintained and constructed from inexpensive, locally available materials. Consequently, it has been determined that solar dryers are appropriate for small farms where financial and material resources are limited (Chen et al., 2009). Likewise, it has been shown that the natural convection solar dryer has potential for implementation in the tropic and subtropic communities of the developing world. In fact, Sharma et al. (1995) showed that these dryers were suitable at household levels for drying small batches of high moisture content produce, despite limitations due to the dependence on temperature difference and pressure drop of air as it is forced through the crop.

A primary concern of the performance of solar dryers is that the airflow in these systems is not sufficient in penetrating higher crop bulks (Buchinger and Weiss, 2002). Furthermore, the air flow comes to a standstill during night and adverse weather conditions. These limitations elevate the risk of product deterioration from mold attack and increased enzymatic reactions. Therefore, it has been concluded that “successful use of natural-convection dryers is restricted to the drying of small batch loads in areas with high insolation” (Amir et al., 1991).

Alternatively, forced-convection solar dryers have been introduced in order to maintain continuous ventilation and air flow. Since these dryers utilize solar energy as well as motorized fans or blowers for air circulation, they generally have the advantages of high reliability and efficiency. On the other hand, the requirement of electricity for fans or blowers, limits implementation of these devices since

electricity is non-existent in many rural areas. Even when electricity is available, the incomes of potential energy consumers are often too low to make application feasible. In this case, the cost of electricity must be balanced with an improved system performance such as greater drying capacity, reduced drying time, and improved product quality. According to Mrema et al. (1987), natural convection dryers typically exhibit overall drying efficiencies of about 10-15% while forced-convection dryers are generally 20-30%.

Figure 3-5 shows a schematic of the main components of an active solar food dryer. Active dryers such as these, use fans or blowers to move solar-heated air from solar collectors to drying chambers. High moisture content products such as fruits and vegetables are often processed with active dryers.

### **Direct Mode Dryers**

Dryer configurations can be further differentiated into sub-classes of integral type (direct) and distributed type (indirect) dryers depending on whether the product is exposed directly to solar radiation or dried in the shade. Integral type (direct) dryers consist of a single drying unit, often with the solar collector forming the roof or wall of the chamber. With direct mode, the product itself serves as the absorber. The heat transfer is affected not only by convection but also by radiation according to the albedo of the product's surface (Buchinger and Weiss (2002)).

In contrast, distributed-type (indirect) dryers often consist of two separate units. A solar collector first heats the air which is then forced through the product in a separate drying chamber. Figure 3-6 depicts a general overview of dryer types based on these distinctions.

Direct solar dryers hold the product within an enclosure that is often shielded with a thin, transparent cover formed out of plastic or glass. The drying chamber itself is essentially an insulated, rectangular box that allows for airflow through small holes in the top and bottom. Perforated trays are used to hold the product as the air flows through both the trays and the product. Several direct dryer designs reviewed in this report are the tent dryer, the seesaw dryer and the box dryer. A typical direct dryer (box-type) is shown below in Figure 3-7.

These direct dryers are designed so that heat is not only generated by solar radiation absorption on the surfaces of the drying chamber, but also on the product itself. Direct passive dryers have been shown to successfully dry small batches of high moisture content produce such as banana, carrots, french beans, mango, pineapple, and potato (Jayaraman et al., 2000).

However, when using integral (direct) mode of drying, it should be noted, that sunlight may affect certain essential components in the product. In fact, direct exposure to sunlight often results in discoloration, vitamin loss and undesirable temperature rises in the thin, top layer of the product (Sreekumar et al., 2008). Due to these limitations of the bulk depth, such dryers need frequent crop turning to attain uniform drying and large surface areas to spread the product. Therefore, if grounds are scarce, indirect mode type of dryers are preferred for drying larger quantities. Also, moisture evaporated from the food may condense on the inside of the absorber cover, thus reducing the transmittivity.

Tent solar dryers, as shown in Figure 3-8, are inexpensive and simple in construction. These units consist of a plastic sheet covering a frame that is fabricated

with wooden poles. Black plastic sheeting is preferred on the side opposite of sunlight exposure to absorb more heat. Within the frame, a rack is situated to hold the food. However, studies have shown that drying times are hardly improved compared with open-air sun drying (Buchinger and Weiss, 2002). Rather, the primary purpose of tent dryers may only serve to protect the product from potential contaminants such as dust, rain, or predators where wastage is otherwise high. Tent dryers are also able to be stored when not in use and they are typically used to dry crops with low density and porosity.

The traditional seesaw dryer consists of a stiff, rectangular frame supported about an axis. The support is designed to allow tilting of the frame to track sunlight throughout the day. The product is enclosed in the frame on a number of mesh trays which allows vertical air circulation and subsequently promotes evaporation. Corrugated iron sheet is often used with wooden supports to absorb heat. These surfaces are painted black for improved heat absorption. Additionally, thermal insulation can be integrated into the frame with the use of wood fiber, polystyrene, corrugated cardboard or other insulating material. The product is placed on removable trays that are positioned above the corrugated iron in either continuous rows or with space between them, which allows for improved heating of air. A typical seesaw dryer is shown in Figure 3-9.

A greenhouse effect is observed with the inclusion of a transparent plastic sheet above the trays. Air circulation is driven by the natural convection principle while fresh air enters the lower end of the drying chamber and escapes at the upper end. Air circulation is improved with a wider air outlet opening compared to the air inlet opening.

This allows for a gradual widening of the cross-sectional area of the frame which improves convection.

The box-type solar dryer has been extensively implemented in small scale food drying processes. The general design is comprised of a wooden box with an inclined, transparent lid made of glazing material. The internal collector walls are painted black to absorb incoming radiation and the product is held on mesh trays. Holes in the bottom and front of the dryer frame allow air to enter the dryer while heater air is exhausted from vents located at the upper end of the back wall. Figure 3-10 illustrates the elemental features and design of a standard solar box dryer. These types of dryers are capable of achieving higher temperatures and consequently shorter drying times than tent dryers. However, drying rates are still relatively low and products often exhibit discoloration. Due to the small drying capacity of these dryers, their use is generally limited to domestic use (Bhandari et al., 2005).

### **Indirect Mode Dryers**

Indirect solar dryers are generally less compact than direct dryers, but often exhibit improved efficiency (Chen et al., 2009) and are capable of drying larger quantities of food product (Buchinger and Weiss, 2002). The primary distinction with indirect dryers is that, unlike direct dryers, the product is not exposed directly to solar radiation. This minimizes the possibility of decomposition such as discoloration, surface cracking and inadequate internal drying, which arise from direct radiation exposure. The primary indirect dryer designs investigated in this review are known as cabinet and tunnel dryers.

The solar collectors in these distributed systems must be appropriately positioned in order to optimize the collection of solar energy. This requires the determination of a suitable inclination as greater amounts of solar energy are gathered with the surface of the collector positioned perpendicularly to the sunlight. A tilting of the solar collector also assists in air flow via the natural convection principle in which warmer, less dense air rises through the system.

The solar cabinet dryer is considered more sophisticated as compared to typical box dryers as they generally consist of two separate components: a collector which heats air with solar radiation and; a drying chamber that houses trays or shelves of product. The principle of operation is similar to that of the box dryer where ambient air is drawn in as hot, moist air is expelled from vents at the height of the dryer. A standard solar cabinet dryer is shown in Figure 3-11. While the higher complexity of design results in a relatively costlier option, these dryers are still considered suitable for small-scale, income generating communities (Bhandari et al., 2005).

These dryers are designed to operate with solar radiation serving as the main energy source, although back-up heaters are used when radiation is inadequate due to poor weather conditions and during the night so that continuous drying is made possible. Radiation first passes through the transparent cover of these dryers, where it is absorbed by the interior surfaces of the solar collector. The heat generated results in an increased temperature of the surrounding air. Natural convection causes the heated air to rise and is thus forced through the drying trays where moisture is collected. The moist air then exits through vents located at the top of the dryer which reduces internal

cabinet pressure. Consequently, ambient air is continually drawn into the dryer. The airflow can be regulated by varying the outlet vent size.

Airflow in a natural convection system is established by the solar heated air becoming lighter or less dense than the ambient air. A small pressure difference is thus created by the density gradient which draws air through the collector, drying chamber, and crop. This effect increases with greater heights between the inlet and bed, as well as the outlet and bed. However, “the effect on an increased height of the outlet is less than that of an increased height of bed because the air is cooled as it passes through the bed” (Buchinger and Weiss, 2002). The moist air is then discharged through air vents or a chimney located above the drying chamber. The optimization of chimney height for natural convection solar dryers is discussed by Irtwange and Adebayo (2009).

The cabinet component of these dryers is essentially a large wooden or metal box which is properly insulated to minimize heat loss. Water resistant cladding is often used in the construction of these dryers. Internal runners are fitted inside the cabinet to support the trays of food being processed. The drying trays slide on these runners so they can easily be removed for loading, unloading and cleaning. A “general rule of thumb is that a one  $m^2$  tray area is needed to lay out 10kg of fresh produce” (Buchinger and Weiss, 2002).

The basic components of a solar air collector are a cover, absorber, air passage and insulation. As solar radiation is transmitted through the cover, the absorber is heated, which in turn heats the air in the air passage. While air has a relatively low heat capacity compared with water, these solar air collectors are

preferred as they require less technical equipment than water-based collector systems and will not malfunction when small leaks exist (Buchinger and Weiss, 2002). The result of this compromise is that higher volume flow rates must be attained with air collectors.

A large variety of flat plate collectors which are utilized in agricultural drying processes have been reviewed by Shove (1977). The basic collector type is the bare plate which is comprised of an air chamber between insulation with the uppermost surface acting as the absorber plate. Preference is given to bare plate collectors as they are easily incorporated into the roofs of storage buildings. Alternatively, covered plate collectors exhibit improved collection efficiency but result in higher cost and complexity. This sophistication and higher cost arises from the addition and utilization of translucent covers above the absorber plates.

More sophisticated designs have also been developed including the flow-on-both-sides absorber in which an air channel is formed between two plates of metal (Buchinger and Weiss, 2002). The upper sides of the plates are coated black and a glass cover is mounted above. Suspended plate collectors are known to exhibit higher levels of efficiency than both the bare and covered plate collectors, but require a more complex fabrication as air is allowed to flow on both sides of the plate. Figure 3-12 shows several air flow principles of solar collectors.

Additionally, attention has been given to the integration of sidewall collectors into dryer walls. However, these designs are often expensive and are usable for only two or three seasons (Chen et al., 2009). Plastic film solar collectors have also been presented by Keener et al. (1977) and Chau et al. (1980).

A solar chimney increases the buoyancy force within the dryer and thus provides a higher velocity of air current. This results in an increased rate of moisture removal. However, it has been shown that the implementation of a chimney only becomes useful when the incoming air is heated in excess of 10-30°C (Buchinger and Weiss, 2002). Otherwise the chimney makes no significant improvement unless it efficiently raises air temperature by serving as a solar collector. It should be noted that passive dryers achieve only minimal pressure difference per unit of chimney height even when high density differences are attained (Buchinger and Weiss, 2002). In contrast, forced convection systems operate at much higher magnitudes of pressure differences.

The chimney effect is essentially the movement of air into and out of the chimney and is driven by buoyancy forces resulting from temperature and moisture differences. Greater thermal differences and chimney heights result in greater buoyancy forces and an increased chimney effect. Thus, the draft flow rate that is induced by the chimney effect involves large temperature differences between heated air and ambient air. This term is defined by Equation 3-4, where Q is the chimney effect (flow rate), C is the discharge coefficient, A is the cross-sectional flow area, g is the gravitational acceleration, h is the height of the chimney,  $T_i$  is the average internal temperature and  $T_o$  is the ambient air temperature.

$$Q = CA \sqrt{2gh \frac{T_i - T_o}{T_i}} \quad (3-4)$$

Although the reported performance of natural convection cabinet dryers is acceptable, there are many inherent constraints. The main limitation of these systems is inadequate air flow which reduces the drying rate and poor moist air removal which results in crop spoilage. These conditions occur when the flowing air becomes nearly saturated to the extent that the temperature is nearly equal to that of the ambient air. This results in considerably small buoyancy differences, and as a result, low air flow rates (Mumba, 1996). On the other end of the spectrum, exceptionally high internal temperatures can result in overheating of the product. In fact, temperatures as high as 70-100°C may be reached with these dryers which are excessive levels for most products (Buchinger and Weiss, 2002).

An extensive range of design improvements have been suggested in response to these limitations. One such design enhances ventilation with the introduction of wind-powered rotary vanes installed on the top of chimneys (Buchinger and Weiss, 2002). Dampers are used to control the temperature and air flow rates of these dryers. However, these systems have been shown to be essentially ineffectual between wind peaks and exhibited complete inactivity during abeyances in the wind. Hence, this dryer design is limited to use in areas with relatively high, sustained winds.

The incorporation of forced convection components has also been given considerable attention in improving the temperature and flow rate control of solar cabinet dryers. In these hybrid solar cabinet dryers, optimum air flow can be provided in the dryer throughout the drying process to control temperature and moisture independent of weather conditions. Furthermore, the bulk depth is less restricted.

Hence, the capacity and the reliability of these dryers are increased considerably compared to natural convection dryers. For these reasons, well designed and executed, forced-convection dryers are considered to be more effective and exhibit a higher level of control than the natural-circulation type. In fact, it has been shown that drying times can be reduced by up to three times while the required area for the collector can be reduced by up to 50% with the use of forced convection (Buchinger and Weiss, 2002). It follows that forced-convection dryers are able to process the same amount of product as natural convection dryers that have collector areas that are six times larger (Buchinger and Weiss, 2002).

Considering these conditions, it is clear that air flow rate is crucial to the overall system performance. Too high an air flow consumes excessive fan power and too low of a flow rate causes poor thermal performance. Additionally, the effect of leakages increases with the air flow rate (Buchinger and Weiss, 2002). In general, the pressure drop should also be low to keep the necessary electrical power for the fans as low as possible.

When fans are implemented to improve circulation, the design of the dryer requires a slight modification since the chimney may no longer be necessary (Mrema et al., 1987). In fact, forced circulation cabinet dryers without chimneys have been shown to significantly improve the rate of drying, which “minimizes the chances of crop damage due to irregular drying” (Mumba, 1996). Even so, the establishment of fixed-speed air flow significantly reduces the dryer performance compared with more sophisticated, controlled air speed systems which use electronic controllers (Mumba,

1996). However, these electrical sources are either unavailable or unaffordable for small scale farmers in the developing world.

For this reason, photovoltaic (PV) cells have received considerable attention as an energy supply for fans. In fact, the performance of PV-driven systems exhibits an advantage of dependability over grid-driven systems in some developing communities (Buchinger and Weiss, 2002). In these PV-powered systems, fans are directly coupled to solar panels which results in simple and reliable systems that operate without the integration of sophisticated accumulators or load controllers. A fluctuating air flow rate is thus established as changes in solar radiation result in acceleration or deceleration of the fan.

While this system has the advantage of a simple temperature control, the control of air flow rate is lost. Thus a compromise must be made in design complexity and the ability to control air flow.

However, the cost of solar drying systems greatly increases with the integration of PV cells. This significantly limits the implementation of PV-driven systems in developing communities as the investment capital of the dryer becomes too high. Therefore, it is widely accepted that when grid power is available, it provides a cheaper electricity source (Buchinger and Weiss, 2002).

The ability to continually process crops is important, however, a significant disadvantage of solar dryers is that their use is limited during inclement weather and the drying time is consequently extended. In addition to limited throughput, solar dryers can also result in decreased product quality. A range of improvements have been proposed and tested for this purpose. In fact, focus has been applied in

addressing the low heat transfer coefficient between conventional air collectors and the flowing air stream. Improvements have been made by adding fins, making the absorber V-corrugated, or by roughing the surface of the absorber (Buchinger and Weiss, 2002). Additionally, absorbers have been equipped with thermal storage components such as rock beds, water, desiccant, or concrete. These storage components collect and store heat while solar radiation is acting on the system. This heat is then dissipated into the dryer during poor weather conditions. Goswami (1986) recommended a storage volume of 0.15 to 0.35m<sup>3</sup>.

Another method of ensuring adequate heat absorption is the integration of back-up heating components. Additional heat is useful because warmer air can absorb more moisture and it helps to raise the product temperature which improves water migration to the product surface. Agricultural wastes such as peels, husks and shells can be used in combustion processes, but as Buchinger and Weiss (2002) noted, "biomass, particularly fuel wood, is the most common source of energy in rural areas of developing countries". However, in many current implementations, the fuel wood is burned inefficiently. Thus, the development of simple and affordable combustion systems is necessary to complement solar drying technologies when exposure to radiation is minimal.

However, improvements in solar drying systems increase the cost and the complexity of the design. As a result, the use of these more sophisticated solar dryers becomes limited in developing countries with the increased dependence on imported commercial components and materials (Bakeka and Bilgen, 2008). Due to

these constraints, and the subsequent compromise in maintaining the small capacity of the dryers, they are limited to small scale operations.

The solar tunnel dryer is effectively an intermediate-stage dryer in terms of its sophistication. With the integration of forced convection processes, the tunnel dryer is dependent on electrical power; therefore it only suited for intermediate sized farms or small cooperatives where electricity is available or where investment capital allows for implementation of alternative energy sources. The forced convection control in the tunnel dryer increases the drying rate and results in a higher quality product than is achieved in traditional, open-air methods. In fact, some studies have shown that compared with traditional methods, high moisture content fruit can be dried in half the time (Buchinger and Weiss, 2002).

The major components of the tunnel dryer are a solar collector and a dryer compartment. Additionally, tunnel dryers are equipped with airflow systems which circulate air with the use of fans powered by a PV panel, a generator or central utility. The principle mode of operation for these dryers is similar to that of cabinet dryers. Tunnel dryers essentially use blowers or fans to force air into the solar collector where solar radiation is used to raise the temperature. The air continues flowing through the food drying compartment where moisture is removed. Some tunnel dryer designs incorporate the use of gas powered heating units to promote drying even during inclement weather. The drying chambers are often accessed by removing the covering manually, although some designs are equipped with hand cranks. The product is spread on mesh which is suspended across the length of the dryer compartment. A typical tunnel dryer is depicted in Figure 3-13.

Tunnel dryers can either be constructed as a permanent installation on top of a foundation or in a portable design for mobility depending on the local needs and circumstances of the target community (Chen et al., 2009). The advantage of forced circulation tunnel dryers is that air throughput can be altered by the speed of the fans depending on the amount of solar radiation available. Uniform drying is also established without the need for turning the crop (Buchinger and Weiss, 2002). These dryers can easily be adapted to the local climate and manufacturing demands of specific countries, however the integration of forced convection fans and gas-powered back-up heating results in higher investment.

### **Large-Scale Dryers**

Solar dryers of more sophisticated designs will only be briefly mentioned in this report as these elaborate designs do not fall into the context of small-scale systems for use in developing communities. These complex solar drying systems require significant financial investment and considerably intensive construction processes. Additionally, many of these designs incorporate the use of mechanized systems, highly dependent on electricity which is often limited or absent in rural areas of developing nations. The small-scale systems described earlier in this review are considered better suited for farm-level or cooperative use in rural communities of developing countries. Hence, these more sophisticated systems, which include greenhouse dryers and in-house dryers, should only be considered in large-scale, commercial applications of developing countries.

The basic design of natural circulation, solar greenhouse dryers consists of drying racks made of wire mesh spread across wooden beams. These racks are

arranged in parallel rows with space between allowing easy access to the product.

These racks are located under fixed, slanted glass roofs which allow solar radiation over the product and frame where it is absorbed by black-coated internal walls. Ridged caps are formed over the roofs to provide exit vents for air which is often regulated by shutters. A typical greenhouse dryer as described here is shown in Figure 3-14.

Another type of large-scale, solar drying system is the in-house dryer which has significant construction requirements, complicated operation processes and relatively high investment compared to previously discussed solar dryers. These in-house dryers consist of roof-integrated solar collectors, drying bins and electric motors operated with axial flow fans. A typical in-house dryer is shown in Figure 3-15. Auxiliary heat sources such as LPG gas burners have been integrated in some designs (Smitabhindu et al., 2008).

These dryers are capable of accommodating large numbers of stacked trays as shown in Figure 3-16 and therefore have greater processing loads than small-scale dryers. The experimental performances of some in-house dryers have also demonstrated significant reductions in drying times compared with open-air sun drying. Additionally, the dried products of these systems have been determined to be of higher quality. Furthermore, uniform air temperature and product moisture content can be acquired with electric blower integration (Janjaia et al., 2008).

As was discussed, solar drying technology provides an attractive option for food preservation purposes that is “clean, hygienic and establishes sanitary conditions that meet national and international standards” (Chen et al., 2009). This is accomplished with either zero or limited energy use with active and passive mode dryers respectively.

However, solar drying is more than just a substitution for fossil fuels, but is a technology based process for producing dried materials of the required quality. It also saves “time, occupies less area, improves product quality, makes the process more efficient and protects the environment” (Chen et al., 2009).

The capacity of a solar dryer mainly depends on the crop itself and the shape. On the one hand, it should be small enough to ensure the product has adequate time for preparation such as washing and slicing. On the other hand, it should be big enough to enable the user to generate income. Additionally, solar dryer systems influence the marketing capacity and income generating potential, since a higher price can be obtained for products of improved quality. Therefore, the opportunities provided through the development of low cost and locally manufactured solar dryers, offer an auspicious option that promises to significantly reduce losses associated with post harvest degradation.

For these reasons, efforts have been made over the last three decades to develop, design, and construct solar dryers. In fact, solar drying technology is currently used throughout the world to dry a wide range of food products. The following discussion of this report serves to outline and describe the diversity of solar dryers currently in use.

### **Case Studies**

A wide range of small-scale dryer designs have been suggested for adoption and implementation in developing communities depending on the type of materials that are locally available as well as the mode of heat transfer employed by the dryer. The use of solar dryers has in fact been implemented in the drying application of various products

in order to meet the needs of small-scale farmers from around the world. Therefore, a comprehensive review of the distinctive designs, principles of operation, details of fabrication, and drying characteristics of previously reported solar dryers is presented here.

The proposed solar dryers reviewed in this report were selected for discussion because of their low initial capital costs. Additionally, these systems were determined to meet relatively simple fabrication requirements often with the use of unconventional, local materials. Furthermore, these systems are considered easy to operate as they require no sophisticated mechanical or electrical components. Thus, the designs discussed here are easily maintained and require only simple replacement of parts during repairs. Furthermore, consideration was given to identify dryers which effectively promote improved drying kinetics and result in a higher quality product than is achieved via open-air, sun drying. Hence, this review identifies and provides brief surveys of solar dryers that satisfy these criteria.

To present this information, a systematic approach for solar dryer classification is proposed here. In this context, three generic groupings of solar dryers have been identified; simple or direct solar dryers, conventional or indirect solar dryers and large-scale dryers. Several types of simple (direct) dryers are outlined here including the box, tent and seesaw dryers. However, these dryers are mentioned here only briefly since many of these designs are considered to be relatively inefficient and result in a degraded product quality compared with the conventional, indirect systems.

For this reason, emphasis is placed on the conventional dryers, particularly cabinet dryers since these designs represent a reasonable compromise between

sophistication and efficiency. The conventional dryers elaborated in this review are the cabinet dryer and the tunnel dryer. Large-scale systems are briefly reviewed in this report; however, the high investment, sophisticated design, and increased power demand of these designs do not fall into the scope of small-scale, cooperative use. An overview of dryer categorization for this discussion is depicted in Figure 3-17.

### **Direct Solar Dryer Designs**

Sodha et al. (1985) designed and proposed the use of a solar box dryer as shown in Figure 3-18. The results show that high moisture content fruit such as mango flesh, with a thickness of 1cm and an initial moisture content of approximately 95% (wb), could be dried to 13% (wb) in only 12 hours of sunlight exposure. Therefore, it was determined from this study that the use of box type dryers could be effective in domestic applications for processing high moisture content products such as fruits and vegetables. The overall efficiency of the box type dryer was improved compared to the efficiency of open-air sun drying while the quality of the product was also better preserved.

Pande and Thanvi (1991) evaluated a solar dryer in conjunction with a water heater as shown in Figure 3-19. In this sense, the system they developed was able to be used for either drying high moisture content produce or for water heating purposes exclusively. Experiments showed that between 10-15kg of high moisture content products could be dried in only 3-5 days. It was surmised that the dryer could process approximately 500 kg of product annually.

Mwithhiga and Kigo (2006) developed and evaluated a solar box dryer which was designed with limited, solar radiation tracking ability as shown in Figure 3-20. The

solar absorber plate was fabricated from mild steel with a transparent cover of polyvinyl chloride (PVC). The tracking capabilities allowed the system to be adjusted in 15° increments to follow the sun throughout the day. Evaluation of the dryer performance was conducted with either one, three, five or nine adjustments of the angle made each day with either no load conditions or loaded with coffee beans. The drying chamber was found to reach 70.4°C which allowed for coffee beans to be lowered from an initial moisture content of 54.8% (wb) to approximately 13% (wb) in only 2 days. These results indicate an improvement over open-air sun drying which requires approximately 5-7 days. However, it was determined that no significant improvement in drying duration was observed with the solar tracking ability of the dryer.

A domestic solar dryer was designed, constructed, and characterized by Enebe and Ezekoye (2006) for the drying of pepper and groundnuts during high humidity and low temperature periods in Nigeria. The dryer was fabricated from locally available material in Nigeria such as hardwood, Perspex® glass for glazing, angle iron for skeleton, screws, wire mesh and plywood as shown in Figure 3-21. The effective collector area was  $1.255\text{m}^2$  and was tilted 22.9° while the volume of air needed for drying was  $.0.24\text{m}^3$ . The optimal temperature of the dryer was determined to be 67°C with a relative humidity of 43%, corresponding to an ambient temperature of 31°C. Experimentation resulted in the drying of pepper to a moisture content of 56.2% (wb) and groundnuts to 40.53% (wb) in 8 days and 5 days respectively. The average collector efficiency was estimated to be 10% while the dryer efficiency was found to be significantly improved at 22%.

This study exhibited the advantage of processing at low temperatures which effectively prevented cracking and subsequent exposure to fungal, bacterial and insect infestation. The product was also shown to maintain its natural color. The potential for large-scale, commercial use of the dryer by enlarging the collector area and increasing the number of trays was also noted.

Singh et al. (2006) designed a multi-shelf solar dryer which consisted of three perforated trays with adjustment capabilities to allow variable inclination for different seasons as shown in Figure 3-22. Intermediate heating between the trays allowed for uniform drying and experiments determined that a maximum stagnation temperature of 100°C was established during the drying of 1kg powder forms of chili, garlic, ginger, mango, coriander, onion, and fenugreek leaves. The use of this dryer was found suitable for domestic level purposes under hygienic conditions.

Singh et al. (2004) also designed and evaluated a portable solar box dryer with a multi-shelf design with drying air intermediately heated between the trays as shown in Figure 3-23. This design promoted uniform drying among the trays and experimentation determined a maximum stagnation temperature of 75°C was established during drying of fenugreek leaves which were effectively preserved to a shelf life greater than one year. The dryer was found to be economically viable and could potentially enable farmers in remote places to increase the value of their produce.

### **Indirect Cabinet Designs (Passive)**

A simple solar dryer was designed and constructed by Bolaji and Olalusi (2008) consisting of a black painted, aluminum plate heat absorber mounted on a well-seasoned wood frame as shown in Figure 3-24. Foam material with thermal

conductivity of  $.043\text{ W/mK}$  was placed in the space between the inner and outer box and a mesh screen was placed halfway between the transparent, glass cover and the absorber plate to provide improved air heating by absorbing additional solar radiation. Experimentation found hourly variation of the internal cabinet temperature to be significantly elevated compared with ambient air and was actually observed to attain an excess of 74% after several hours. The drying rate and collector efficiency for drying yam chips in this study were  $0.62\text{ kg/hr}$  and 57.5%), respectively. The results of this evaluation demonstrated sufficiency in quickly drying food products to adequately preserved moisture levels.

Ezekwe (1981) evaluated a typical cabinet dryer modified with a wooden plenum that served to guide incoming air. An extended chimney was also incorporated in this dryer to increase the natural circulation. The resulting rate of drying was found to be approximately five times greater than open-air sun drying.

Othieno et al. (1981) developed an indirect solar dryer which consists of a single-glazed air heater with effective area of  $1\text{ m}^2$  for the absorber. A drying chamber equipped with a chimney was constructed from hardboard and was connected to the air heater. The air heater was modified to accommodate several layers of absorber mesh by increasing the width of the air gap. Tests conducted with 90kg of wet maize resulted in drying from 20% to 12% (wb) within 3 days.

Pangavhane et al. (2002) proposed, designed and evaluated the use of a solar dryer with an aluminum foil absorber, glass cover and a drying chamber made of GI sheet as shown in Figure 3-25. Grapes were successfully dried in 4 days compared

with traditional methods such as open-air sun drying which resulted in 7 days of drying which corresponds to a reduction in drying time of 43%.

Li et al. (2006) investigated a solar dryer as shown in Figure 3-26 which was designed with an effective collector area of  $6\text{m}^2$  for the drying of salted greengages. During experimentation, fully wet product was isolated from semi-dried product to improve efficiency. Results indicated that effective drying of salted greengages was reduced to 15 days compared with 48 days necessary for open-air sun drying.

Goyal and Tiwari (1999) proposed and analyzed a modified, indirect system referred to as the reverse absorber cabinet dryer (RACD) in which a downward facing absorber and a cylindrical reflector were placed below the drying chamber. A single wire mesh tray held the product in the drying chamber and the glass absorber cover was inclined at an angle of  $45^\circ$  to receive maximum radiation. The cylindrical reflector redirected the solar radiation toward the absorber where incoming air was heated as shown in Figure 3-27.

### **Indirect Cabinet Designs (Active)**

Sreekumar et al. (2008) developed and evaluated an efficient cabinet dryer with a product load arrangement beneath the absorber plate which prevents discoloration by avoiding direct solar irradiation as shown in Figure 3-28. While this design is similar to integrated box dryers, it is mentioned here in this report due to the essential separation of the heating and drying components. Two axial flow fans were used to accelerate the drying rate, a collector glazing was inclined for maximum absorption of solar radiation, and six perforated trays were used for material loading. Tests resulted in a temperature of  $97.2^\circ\text{C}$  attained by the absorber plate under no load conditions,

which corresponded to a maximum dryer temperature of 78.1°C. It was determined that within 6 hours, 4kg of bitter gourd could be dried from an initial moisture content of 95% to 5% (wb) without the loss of product color, whereas open-air sun drying required 11 hours.

Chen et al. (2007) evaluated the performance of a forced-flow cabinet dryer for preserving banana chips. The banana chips were reduced from a moisture content of 75-85% (wb) to approximately 7-8% (wb) in 5 sunlight days with a thermal efficiency of the dryer reported to be 30.86%. Better quality product was achieved compared with product evaluated with open-air sun drying. Shorter drying periods were also accomplished.

Tiris et al. (1995) designed and evaluated a solar dryer as shown in Figure 3-29 using chili peppers, sweet peppers, sultana grapes and green beans. The results of this study indicated that the dryer could significantly reduce the duration of drying and essentially provide a higher quality product than open-air sun drying. The thermal efficiency of the drying chamber and the solar air heater were discussed in relation to the physical parameters of the dryer as well as the resulting product quality at different air flow rates. The results indicated that overall drying performance was increased with higher flow rates and the drying system was found to have a thermal efficiency in the range of 0.3 to 0.8.

Mohanraj and Chandrasekar (2008) developed a forced-convection solar dryer as shown in Figure 3-30 which consisted of a 25°-tilted, flat plate collector of area  $2\text{m}^2$  connected to a drying chamber for drying copra. A centrifugal fan was used to force air between the glass cover and the absorber below. To ensure air circulation was uniform

across the absorber, a divergent entry was formed for the solar air heater. It was determined that in 82 hours copra could be dried from an initial moisture content of 51.8% to 9.7% and 7.8% (wb) at the top and bottom of the dryer respectively, while the thermal efficiency was determined to be 24%.

Mumba (1996) designed and evaluated the performance a solar cabinet dryer as shown in Figure 3-31 which was equipped with a PV-powered DC fan that permitted passive control of the temperature of drying air. The solar collector was tilted 15° and was comprised of blackened sisal absorber mesh which helped to improve heat transfer. Additionally, three transparent covers of a Tedlar®/Teflon® combination allowed for high shortwave transmittance and reduced heat loss from the upper surface. Furthermore, transparent insulation material (TIM) was placed between the absorber and the covers to assist in raising the temperature. Dry wood shavings were used for the air heater wall insulation and all surfaces were painted black to increase the heat gain.

It was determined that the drying air temperature of this system had an upper limit of approximately 60°C which effectively prevented overheating and cracking of the grain. From performance testing, it was determined that the system could dry a batch of about 90kg maize from 33.3% (db) moisture content to below 20% (db) in only a day. The thermal efficiency was 77% and the optimum ratio of PV to solar heater area was determined to be 0.22 to achieve a cost effective dryer design. This dryer resulted in a better preserved product compared with open-air sun drying, therefore, this dryer was determined to be suitable for

application in rural communities where electricity and fuel is unavailable or the cost is too high.

Al-Juamly et al. (2007) developed a solar dryer system as shown in Figure 3-32 which was comprised of a drying cabinet, solar collector and an air blower connected with piping for processing high moisture content produce such as fruits and vegetables. The absorbers of the solar collector were V-corrugated and had glass covers providing an effective area of  $2.4\text{m}^2$ . Results indicated that apricots were reduced from an initial moisture content of 80% to 13% (wb) within 1.5 days, grapes from 80% to 18% (wb) in 2.5 days, and beans from 65% to 18% (wb) in only 1 day. It was determined that the primary factor affecting the drying rate is the temperature of the drying air whereas the airflow variation was discovered to be negligible since the relative humidity of exhausted air was only between 25 and 30%.

Sarsilmaz et al. (2000) investigated the use of a rotary column cylindrical dryer (RCCD) with a fan and rotor system to rotate product trays within the cabinet as shown in Figure 3-33. The optimal airflow and speed of rotation for processing apricots was determined in order to reduce drying times and maintain uniform and hygienic conditions. It was found that 2-3kg trays of apricots were effectively dried to a moisture content of 25% (wb) in half the time needed to dry them compared to open-air sun drying. The products were also found to be more attractive in color with uniform quality among trays. However, this design is limited in use due to the additional power demand of the rotary system.

Pawar et al. (1995) developed and tested a large-scale solar dryer as shown in Figure 3-34 that was loaded with coriander powder for performance

analysis. The drying system consists of 3 cabinets and an array of 40 solar collectors with an integrated blower to establish air flow. This dryer was shown to be feasible and results indicated that substantial amounts of fuel could be saved compared with larger, industrial systems. Additionally, the dried product was found to be untainted and was actually dried quicker than with open-air sun drying. As a result, the use of forced-convection solar dryers was found to be suitable for use in the food industries of developing communities.

### **Supplemental Heat Dryers**

A laboratory scale, passive dryer, as shown in Figure 3-35, was developed by Irtwange and Adebayo (2009) and was comprised of a solar collector, a drying chamber made of wood and a thermal storage unit. The collector was constructed from corrugated zinc roofing sheet and covered with a glass sheet for glazing while the chimney was fabricated from metal tube and corrugated roofing sheet. The thermal storage unit consists of black painted gravel for better heat absorption and trays were made of stainless steel wire to avoid rusting.

The dryer was evaluated using 10 kg of maize which took 4 days to dry from an initial moisture content of 32.8% to 13.1% (wb). Compared with open-air sun drying which took 8 days to dry to 13.4% (wb), this dryer system clearly resulted in a faster drying rate. It was noted that the dryer could be enlarged for community level, cooperative use and for further improvement; the airflow rate could be increased.

Ayensu (1997) developed an inexpensive, solar dryer that operates at low temperature and is considered simple to operate. The dryer consists of a thermal, rock storage component and a drying chamber equipped with a chimney as shown in Figure

3-36. Only locally available materials such as wood and scrap metal were used in the fabrication of the dryer. Chicken wire mesh was used to form a double layer food bed. Plywood access doors were overlapped to prevent air leakage and a glazing was integrated on top of the drying chamber to provide additional heat. It was found that the solar collector transferred approximately  $118\text{W/m}^2$  of thermal power to the drying air, which allowed heating of the air to  $45^\circ\text{C}$  at 40% relative humidity from ambient conditions of  $32^\circ\text{C}$  and a relative humidity of 80%. Consequently, various crops (cassava, groundnuts, okra, etc.) were dried to moisture content levels below 14% (wb) which enabled preservation in excess of one year without biological degradation.

Enibe (2002) designed a passive air heating system consisting of a heat storage system integrated into the solar collector as shown in Figure 3-37. The storage system was comprised of distinct modules of phase change material (PCM) that were equally spaced across the absorber plate and served as parallel air heating channels. Testing of the system was conducted over environmental temperature ranging from  $19\text{-}41^\circ\text{C}$  while global irradiation was measured between  $4.9\text{-}19.9\text{MJ/m}^2$ . Results indicated successful application for crop drying.

Ezeike (1986) developed a modular, solar dryer with a dehumidification chamber and a triple-pass air collector as shown in Figure 3-38. The dehumidification chamber is essentially a frame containing perforated trays that are loaded with silica gel. The collector surface was equipped with baffles to assist in uniformly distributing the heated air. The cabinet was modified with wall collectors to provide additional heat gain. Through experimentation, the outlet temperatures were found to be between 90 to  $101^\circ\text{C}$  with wind speeds of up to  $3.5\text{m/s}$ . The dryer efficiency was determined to be

between 73-81% for the drying of rice paddy from 25.93% to 5.31% (wb) in 10 hours and yam slices from 64.90% to 10.66% (wb) in 31 hours. An open-air sun drying control resulted in significantly increased drying time and lower quality product.

EI-Sebaii et al. (2002) developed and evaluated a natural convection dryer as shown in Figure 3-39 which consisted of a drying cabinet connected to a flat plate air heater that was designed to allow interchanging of storage material to improve performance. Testing was performed with and without sand as a storage material for an assortment of vegetables and fruits such as apples, figs and grapes. The storage material was found to reduce the drying process by 12 hours in some cases with 10kg of product loaded.

Mohamed et al. (2008) investigated the drying kinetics of edible red algae using an indirect, forced-convection solar dryer as shown in Figure 3-40. The dryer was equipped with a circulation fan and an auxiliary heater to gain greater control over the drying parameters. Experiments were conducted at a range of temperatures and some variation in relative humidity and airflow rate was introduced. Most drying was observed within falling rate period and it was concluded that the temperature of the drying air was the primary influence on the drying kinetics.

Zomorodian et al. (2007) introduced an active solar dryer with a semi-continuous, timer-assisted discharging system as shown in Figure 3-41. Multiple solar air heaters, tilted at 45°, were employed in this design to provide a total area of 12m<sup>2</sup>. The system also consisted of an air distribution system and an auxiliary heating channel. A timer-controlled, electrical rotary discharging valve was installed at the bottom of the dryer.

Experiments were conducted with rough rice kernels in order to investigate the effect of both the rate of airflow and the discharging time interval on the drying rate. The capacity of the dryer was approximately 132kg of rough rice with 27% (db) initial moisture content, which required 3 hours to achieve a moisture content of 13% (db). The overall dryer efficiency was 21.24% and the average temperature of the drying air was determined to be 55°C. Furthermore, it was found that the auxiliary heating channel used only a fraction of the solar energy (6-8%).

A small-scale dryer consisting of a drying, heating and plenum chamber was realized by Singh (1994) as shown in Figure 3-42. Aluminum sheets, mineral wool insulation and galvanized iron sheet formed the walls of the drying chamber which contained 20 aluminum-framed, nylon mesh trays stacked in two rows. To assist in uniform distribution of air; wire mesh was incorporated between the drying chambers and plenum. This mesh also prevented foreign contaminants from entering the system. Mild steel sheeting was used to form the heating chamber which housed 16 heating elements controlled by thermostat. Additionally, an electric motor was used to drive a blowing unit and thus establish control of the airflow.

Testing was carried out while maintaining a constant air intake of  $0.33\text{m}^3/\text{s}$ . Under this condition, it took 11 hours to lower the moisture content from 92.5% to 8.69% (wb), 14 hours from 92.65% to 8% (wb), and 12 hours from 90% to 7.5% (wb) respectively for 50kg batches of cabbage, cauliflower and onion slices. The overall drying efficiencies for processing these crops were 28.21%, 30.83% and 29.51% respectively.

Sarsavadia (2007) developed a forced convection dryer as shown in Figure 3-43 for drying onions with recirculation of exhaust air under controlled rates of airflow and air temperatures. It was determined that the energy needed for drying was reduced as air temperature increased. Conversely, higher flow rates caused an increase in the energy needed for drying. The total energy required to dry onions from 86% (wb) to 7% (wb) without recirculation, ranged from 23.548 to 62.117 MJ/kg water. The contribution of energy from the electrical heater, the solar air heater and the blower were found to range from 41.0% to 66.9%, 24.5% to 44.5% and 8.6% to 16.3% respectively.

Chaudhri et al. (2009) designed a solar cabinet dryer for processing onion flakes using a packed rock, thermal storage bed to supply heat and re-circulated exhaust to dry the product. The absorber was created with corrugated galvanized iron (GI) sheet painted black with a cover made of UV-stabilized plastic sheet. It was determined that onion flakes could be dried from 85.5% to a moisture content between 9.56% and 6.76% (db) for cases with and without recirculation respectively, in under 7 hours. These results indicate that under recirculation conditions, less moisture is removed. Therefore it was concluded that the drying potential was reduced regardless of the temperature when exhaust air was recirculated. The efficiency of the dryer was determined to be 19% and 23% for the cases of with and without recirculation respectively.

Furthermore, it was noted that a 74% increase in thermal efficiency was observed in the case without recirculation. The dried onion quality was also found to be of higher quality in terms of color for the without recirculation test. From these results, it was concluded that recirculation procedures may only be feasible for processing products with low moisture content or with the introduction of desiccated material.

A solar biomass cabinet dryer as shown in Figure 3-44 has been developed by Bhandari et al. (2005), which consists of two solar collectors, a drying chamber, a heat exchanger, a chimney, a flue gas outlet and a mild steel biomass stove that was installed adjacent to the collector system. The solar collector was comprised of a corrugated aluminum absorber plate, a glass window glazing, and a collector box formed with glass wool sandwiched between GI sheets. Nine stainless-steel, wire mesh trays were supported by a wooden drying cabinet over which the chimney was formed from GI sheet. The roof of the drying chamber was equipped with an additional solar collector to provide supplemental heating. All surfaces in contact with the heat air were painted black to increase heat absorption.

Stove-heated flue gas heats the incoming, ambient air as it passes through the heat exchanger. The flue gas then exits from an outlet pipe, while the heated, ambient air passes into the drying chamber, is forced through the product and exits out the chimney. The heat exchanger was fabricated from aluminum sheet and was provided with fins to improve heat transfer, while the flue gas outlet was formed from GI sheet. Rubber gaskets were used on all the joining components of this system to ensure airtight joints.

The effective drying time of 10kg of cauliflower was determined to be 10 hours over the span of two days with a dryer efficiency of 16.32%. Therefore, this dryer was found to be efficient and technically feasible when compared to similar dryer types with reported dryer efficiency of only 9%. The dried product was also found to be higher quality with this dryer compared to traditional techniques.

Prasad et al. (2006) designed and evaluated a hybrid, biomass dryer as shown in Figure 3-45 that could generate continuous heated airflow between 55 and 60°C for processing turmeric rhizomes. The quality of dried products was evaluated with both water-boiling and slicing pre-treatments. The products of both pre-treatment methods were found to be similar in respect to physical characteristics and required only 1.5 days to dry. The efficiency of the dryer was determined to be 28.57%, while open-air sun drying took 11 days to dry and resulted in a lower quality product.

Madhlopa and Ngwalo (2007) developed an indirect solar dryer equipped with a biomass heater and a solar collector with a thermal storage system as shown in Figure 3-46. The biomass burner was designed with a small, rectangular duct leading to a flue gas chimney for exhaust, while a conventional chimney provided exhaust above the drying chamber. The collector was equipped with a flat absorber made of black-painted concrete. Additionally, an integrated rock pile was incorporated to serve as thermal storage. Results indicated that the thermal rock pile was able to effectively store heat from the biomass burner and absorbed solar energy.

Drying of 20kg batches of fresh pineapple was successfully conducted under exclusively solar operation, biomass-only operation, and a hybrid mode of operation. It was observed that drying proceeded during inclement weather only with use of the biomass heater. The pineapple slices were reduced from a moisture content of 66.9% to about 11% (db) with the biomass burner mode of operation. During the last day of processing, the average efficiencies of moisture pickup were recorded as 15%, 11% and 13% for the exclusively solar, biomass-only and hybrid modes

respectively. Based on these results, it was determined that high moisture content products such as pineapples could be adequately preserved by the dryer.

### **Desiccant-Integrated Dryers**

Shanmugam and Natarajan (2006) developed a forced-convection solar dryer as shown in Figure 3-47 which was comprised of a flat-plate solar absorber and a desiccant component holding 75kg of CaCl<sub>2</sub>-based desiccant which is composed of bentonite, CaCl<sub>2</sub>, vermiculite and cement mixed in the ratio of 6:1:2:1. Experiments were carried out under hot, humid conditions for the preservation of green peas at various airflow rates and the results indicated that equilibrium moisture content could be reached between 14 to 22 hours depending on the airflow. A pickup efficiency of 63% was observed while the performance of the system was found to be satisfactory for uniform desiccant drying.

Thoruwa et al. (1996) developed and evaluated a solar cabinet dryer as shown in Figure 3-48 which was capable of holding 32.5kg of bentonite (CaCl<sub>2</sub>) desiccant enclosed in individual 250g bags. A maximum of 14.6kg of water was expected to be absorbed by the desiccant as determined with preliminary experiments. To achieve the optimal solar collection, the desiccant bed and Tedlar® glazing panel were inclined at 15°. This angle also assisted in the prevention of rain leakage.

Experiments were conducted without load in order to access the dryer's ability to deliver dehumidified air which could subsequently be used in external applications. While exposed to solar radiation, a small, PV-powered fan drew air through an entry port where it passed through the desiccant bed before being

exhausted into the ambient air. During periods of no solar radiation exposure, this valve was closed, thus forcing the dried air over the food product.

Shanmugam and Natarajan (2007) also developed and evaluated an indirect forced-convection cabinet dryer as shown in Figure 3-49 which was equipped with a desiccant system for processing pineapple slices and green peas. The integration of a reflective mirror on the desiccant bed was found to significantly increase the drying potential. In fact, a 10°C temperature rise was achieved with the addition of the mirror. This temperature rise resulted in a reduction of the drying time for green peas by 2 hours and pineapple slices by 4 hours.

Compared to both open-air sun drying and other desiccant integrated processes, this system exhibited higher relative pick-up and average thermal efficiencies. Furthermore, the drying rate was comparatively quick and the products from this dryer were observed to be uniformly dried. Product quality was good in terms of both color and minimal microbial decay. Furthermore, continuous operation of the dryer in excess of one year was possible as the desiccant material remained stable.

### **Indirect Tunnel Dryers**

A forced convection solar tunnel dryer as shown in Figure 3-50 was developed by Hossain and Bala (2007) and was evaluated under tropical conditions in processing hot red and green chilies. Red chili was reduced from a moisture content of 85% to 5% (db) in only 20 hours whereas open-air sun drying was found to achieve 9% (db) in 32 hours. Green chili was also reduced from an initial moisture content of 76% to 6% (db) in 22 hours whereas open-air sun drying was found to achieve 10% in 35 hours. Thus, the use of the solar tunnel dryer following blanching pre-treatment, was found to reduce

drying time considerably. Additionally, this process was found to result in better quality color and pungency compared with products processed with open-air sun drying.

Bala et al. (2003) also investigated a solar tunnel dryer as for processing pineapple in Bangladesh. The dryer was comprised of a flat plate collector with a clear plastic cover and a tunnel connected in series. A solar module was used for operation of two DC fans to supply hot air. The loading capacity of the dryer was estimated between 120-150kg of pineapple and experiments resulted in greatly reduced drying times compared with open-air sun drying.

Datta et al. (1998) developed a thermal performance model for a tunnel dryer to assist in evaluating the drying behavior of high moisture content products. In essence, this study entailed the development of a transient, one-dimensional model for a tunnel dryer while the performance for natural convection mode was estimated. From the model, it was determined that large quantities of barley could be dried to equilibrium moisture content in the system within only two days of operation.

The proposed tunnel dryer was comprised of a solar collector and a connected drying chamber as shown in Figure 3-51. An absorber was fabricated from black polyester fabric with UV-stabilized polycarbonate sheet forming a cover. The performance analysis of this system was presented in terms of the air collector as well as the drying chamber. It was determined that approximately 1941 kg of barley could be processed from 34% moisture content to between 10-14% (wb) within only two days. The potential adaption of this system to drying processes of other crops in various locations was noted.

Amir et al. (1991) modified a multi-purpose solar tunnel dryer as shown in Figure 3-52 for locations with tropical weather conditions. This modified dryer was comprised of a solar collector, a centrifugal blower and a tunnel chamber built on a wooden structure which effectively prevented water intrusion. The dryer was also equipped with a biomass furnace and heat exchanger for operation during inclement weather. The absorber was fabricated from a thermo-stable, polyester fabric covered with UV-stabilized transparent foil. Additionally, palm fiber insulation was used to reduce heat loss and plastic foil was installed to minimize the leakage of water and heated air. Sealing foil and bamboo mats on the chamber floor, eased evaporation of water especially during the first drying stage.

Investigations of the system performance demonstrated a considerable reduction in drying time and product quality was improved overall. More specifically, results indicated that the drying time of cocoa, coconut and coffee was reduced by up to 40% compared with open-air sun drying. Furthermore, the products were found to meet both national and international market standards as well as the moisture content needed for storage. It was also determined that raising the ambient temperature from 30°C to 70°C in this system was possible at peak conditions. Furthermore, the heat storing capacity of the concrete foundation was found to contribute to a temperature rise during the night.

Further discussion was made regarding the potential adaptation of this system to different farm sizes and cooperative use areas. It was also suggested that alternative energy sources should be investigated in order to become independent from electricity.

## **Large-Scale Solar Dryers**

Smaller natural circulation greenhouse dryers have also been developed, constructed and tested by Koyuncu (2006). These dryers were comprised of corrosion-resistant plastic mesh, black-coated absorbers and polyethylene sheet on a frame of black-coated metal bars as shown in Figure 3-53. To determine effects on airflow, the dryers were tested both without chimneys and with galvanized iron chimneys.

It was determined that natural-circulation greenhouse dryers exhibited higher efficiencies than open-air sun drying by a factor of 2.5 for the drying of pepper. Additionally, it was found that the black-coated absorber and chimney improved the dryer performance.

Forced convection greenhouse dryers as shown in Figure 3-54 have also been developed and evaluated by Condori et al. (2001). The primary advantage of these dryers is that almost continuous production can be established since fresh product can be introduced as dried product is removed from the opposite end of the dryer. Additionally, these dryers result in lower labor costs than some simple systems since they are partly mechanized. The ease of conventional heater installation was noted which could assist in maintaining a constant production rate with significant reduction in energy consumption compared with other sophisticated dryers.

### **Construction**

Selection of an appropriate solar dryer for a given food product is dependent on product characteristics, quality requirements and relevant economic factors (Kandpal et al., 2006). Additionally, consideration should be given to material selection which directly impacts the quality of the product. Attention is given here to identify adequate

evaluation procedures of the product, dryer, and performance parameters that provide an overview of the necessary components of analysis which help in the selection of appropriate dryer systems. A synopsis for evaluation procedure is then outlined from the preparation of dryer, product and instrumentation; to the actual experimentation.

When selecting materials for dryer fabrication in developing countries, consideration must be given to the available resources, including equipment or tools, as well as the level of craftsmanship employable. Additionally, all materials should be resistant to heat, light and dampness to improve the lifetime of the dryer. Specifically, collectors and drying chambers should be watertight while absorber surfaces should be resistant to heat and moisture. Synthetic material used for covers or glazing must be resistant to UV light and high temperatures. Commonly used materials (as reported by studies reviewed in this report) are listed in Table 3-3.

### **Evaluation**

Sufficient testing of dryer systems is necessary to evaluate technical performance and establishes a basis for comparison to other dryer designs. Such analysis can assist in the selection of appropriate dryer designs given specific conditions which must be met. Furthermore, adequate evaluation can provide an indication of a dryer's performance in conditions different from those tested in. Leon et al. (2002) proposed a comprehensive procedure for the evaluation of solar dryer performance which provided methodology and test conditions in order to develop a standard practice of analysis. The procedure provides an explicit evaluation of solar dryer performance while facilitating in the comparison of different solar food dryers.

The parameters reviewed here provide a basis for comparison to different dryers and can assist in dryer selection to meet specific needs. Analysis of the product quality

involves evaluation of rehydration, sensory elements and chemical procedures.

Evaluation of dryer parameters should include consideration of dimensioning and sizing, solar collector, construction requirements, drying temperature, relative humidity and the airflow rate. Performance parameters include drying time, efficiency, maximum drying temperature and cost-associated factors which are all detailed further in this review.

## **Product Evaluation**

As mentioned earlier in this review, the physical properties of a product may be affected by drying and result in changes in size, shape, color, and texture while chemical and enzymatic conversions take place. For instance, adverse color changes occur in dried mango slices as a result of enzymatic browning. This discoloration is often prevented with careful control of temperature and moisture parameters particularly in more sophisticated drying systems. However, simple solar drying systems do not necessarily provide a significant level of control for these parameters. For this reason, sulfites and other preservatives are frequently employed to control the enzymatic browning of mango slices. Similarly, citric acid can be supplied from fresh lemons where commercially-available preservatives are unavailable.

The assessment of dried product quality is necessary to establish a basis of comparison between drying systems. However, as Kader (2005) noted, it is far more challenging to measure qualitative losses than quantitative. Analysis of quality characteristics such as consumer acceptability, edibility, caloric and nutritive value are often neglected in studies due to the challenge in developing and understanding adequate evaluation parameters.

"While reduction of quantitative losses is a higher priority than qualitative losses in developing countries, the opposite is true in developed countries where consumer dissatisfaction with produce quality results in a greater percentage of the total postharvest losses" (Kader, 2005). However, by reducing qualitative losses through better implementation of preservation processes, a higher quantitative level can be maintained. Thus the quantitative parameters worth mentioning here are rehydration, sensory evaluation and chemical tests.

A product's ability to regain the original volume, by soaking in water, serves as a good indicator of product quality since some dried products are consumed after rehydration. The common index used to express rehydration is the rehydration capacity, which is the ratio between the product weight after and before rehydration. The dried product will be graded best if it approaches the original fresh product volume. It has been generally observed that reducing the drying time and pre-treating the product using additives like salt, sugar and glycerol improves the rehydration quality of dried fruits and vegetables (Leon et al., 2002).

Rehydration tests can also serve to indicate the damage inflicted to the product caused by drying and pre-treatment. In fact, Khedkar and Roy (1990) observed a higher rehydration ratio in cabinet-dried raw mango slices compared to sun-dried slices, and attributed this to less rupture of cells during cabinet drying (36.4%) than sun drying (67.3%).

Although flavor loss of dried products is often due to volatile losses, chemical reactions such as oxidation and browning also contribute considerably. The size, shape, uniformity and absence of defects are all important in assessing product quality.

While the evaluation of these parameters is relatively straightforward, evaluation of color, aroma and taste are more difficult.

The change of color can influence a consumer's perception and may affect other attributes such as the flavor of the product. Measurement of product color implies either visual matching paired against standard colors or expression in terms of numerical dimensions using hue, saturation and lightness. Devices such as tintometers and spectrophotometers are relatively expensive, while visual matching against standard colors is more practical. The Munsell color-order system displays a collection of colored chips arranged with scales and thus provides a method of precisely specifying colors. Evaluation of color is particularly important in drying fruit slices as many products experience enzymatic color changes. Mangoes for example, undergo enzymatic browning which could be measured using some of these techniques. This information could be used to assess the need of preservatives such as citric acid or lemon juice which help in color retention. Color assessment could also help to estimate when drying of the fruit slice is complete.

Samples from the rehydration test may be salted to taste, and cooked in steam or in a microwave oven. Once the best cooking time for the product is established, it should be used for all samples of that particular product so that texture may be judged comparatively. Quality can be subsequently attributed on a specified grading scale.

Quality taste parameters such as sweetness can be evaluated with the use of hydrometers, oscillating U-tubes or refractometers which are calibrated to read in °Brix which refers to the sugar content in a solution. Nutritional attributes affected by

dehydration include chemical parameters such as ash and sugar content, ascorbic acid or Vitamin C,  $\beta$ -carotene content, and acidity content. Vitamins A and C are destroyed by heat but are better preserved with sulfite treatments. However this leads to thiamin degradation while the blanching of vegetables results in some vitamin and thiamin loss. High ash content indicates dust contamination while low sugar and Vitamin C content corresponds with degraded product quality due to high temperatures (Leon et al., 2002). The nutritive values, ash content and acidity can be determined by simple chemical analysis with the use of a standard index.

### Dryer Parameter Evaluation

The total area of the solar collector is an important consideration in the estimation of drying efficiency. In mixed-mode dryers, it should include the collector area and the spread area of the product receiving direct solar radiation. Apart from the size and physical characteristics of the collector, the system is largely dependent on the angle of inclination with the sun. In fact, the highest yield is attained with the collector oriented perpendicular to the sun and as a general rule; the optimum angle of tilt is equal to the degree of latitude of the site (Leon et al., 2002). Alternatively, Adegoke and Bolaji (2000) recommended an inclination of 10° more than the local geographical latitude while Enebe and Ezekoye (2006) proposed that the optimum collector slope could be determined by Equation 3-5.

$$\beta = \delta + \phi \quad (3-5)$$

The variable  $\phi$  represents the latitude at which evaluation is conducted and the angle of declination,  $\delta$ , is calculated with Equation 3-6.

$$\delta = 23.45\sin[0.9863(284 + n)] \quad (3-6)$$

The variable n refers to the numbered day of the year. Regardless of the method employed, a minimum angle of 15° should be maintained to assist the thermosiphon effect and to ensure adequate water runoff and air circulation (Buchinger and Weiss, 2002). Table 3-4 provides optimum tilt angles by latitude and season.

A chimney can be designed with consideration given to a proposed buoyancy force of air within the solar dryer. Air pressure generally increases with the establishment of greater density gradients through increased chimney heights according to Equation 3-7. The variable P refers to the pressure, g is the gravitational acceleration,  $h_1$  is the base height,  $h_2$  is the peak height and  $\Delta h$  is the difference in height between  $h_1$  and  $h_2$ . Additionally, the density of the air at  $h_1$  and  $h_2$  are given as  $\rho_1$  and  $\rho_2$ , respectively, where each is a function of temperature.

$$P = \rho_1 gh_1 - \rho_2 gh_2 = \Delta hg(\rho_1 - \rho_2) \quad (3-7)$$

Furthermore, consideration must be given to actual construction parameters and limitations that could restrict or prohibit the implementation of a specific dryer. For instance, the ease of construction indicates the feasibility of building a dryer based on the availability of materials, manpower and technical fabrication skills. These issues extend into the operation and maintenance as all of these conditions will be required for upkeep of the system. Available floor space should also be considered especially in hilly-terrain where flat land must be located for installation. Attention should also be given to the safety and reliability of the dryer.

The drying rate will be increased by raising the drying air temperature in two ways. First, this increases the ability of drying air to hold moisture. Secondly, the

heated air will heat the product, increasing its vapor pressure which will drive the moisture to the surface faster. However, there is a limit to raising the temperature of air in a dryer. The thermal sensitivity of food products limits the operation of dryers at significantly high temperatures as mentioned earlier in this report. A high drying air temperature could also result in more heat loss by conduction and radiation from both the collector and drying cabinet, resulting in overall reduction in system efficiency.

The humidity of the drying air is also crucial to the drying process. The ability of air to hold more moisture can be increased by either dehumidifying or heating the air as outlined earlier in this report. Recirculation of exhaust air also helps by utilizing the thermal energy of exit air as was detailed earlier.

Airflow is another parameter which influences the drying process by minimizing conduction and radiation losses through limitation of temperature rise. In natural circulation systems, airflow is primarily determined by the temperature rise in the collector. Higher flow may be used at the beginning of drying and lower flow when drying enters the falling-rate period (Leon et al., 2002). Furthermore, drying efficiency drops at significantly high airflow, since contact time with food is lowered. Alternatively, insufficient air flow can result in slow moisture removal.

## **Performance Evaluation**

One important parameter regarding the evaluation of dryer performance is the drying time. However, it may in fact be challenging to monitor the drying time closely and thus stop the process when the product reaches the same final moisture content value in all the trials or drying systems. Instead, a single final moisture value can be evaluated by analyzing the drying curve for each dryer. An estimation of the drying time

can then be made for the individual dryers to arrive at that specific moisture content.

Typically, this value can be taken as 15% (wb) for most fruits and vegetables.

Furthermore, drying times may be considerably reduced by decreasing the product dimensions through slicing or with the addition of a small amount of sulfite while chemical pretreatments increase the drying rate (Leon et al., 2002).

Drying system efficiency takes into account the weight of moisture evaporated from the product and the energy input to the drying system during the drying time. However, the efficiency of a dryer is often reported individually as collector efficiency, pick-up efficiency, and drying efficiency. Collector efficiency is a common measure of collector performance generally ranging between 40 to 60% for flat plate collectors and is expressed by Equation 3-8 (Ahmad et al., 1996).

$$\eta_{COLLECTOR} = \frac{GC_p \Delta T}{I} = \frac{GC_p(T_o - T_i)}{I} \quad (3-8)$$

The variable G is the mass flow rate of air per unit collector area,  $C_p$  is the specific heat of air evaluated at the average temperature within the solar collector,  $T_o$  is the temperature of air at the outlet of the absorber,  $T_i$  is the temperature at the absorber inlet, and I is the total solar energy incident upon the plane of the collector per unit time per unit area.

The pick-up efficiency determines the drying air's ability to remove moisture and is expressed by Equation 3-9 (Tiris et al., 1995).

$$\eta_{PICK-UP} = \frac{h_o - h_i}{h_{as} - h_i} = \frac{W}{\rho V t (h_{as} - h_i)} \quad (3-9)$$

The variables  $h_o$ ,  $h_i$  and  $h_{as}$  are the absolute humidities of air leaving the drying chamber, entering the drying chamber and entering the dryer at the point of adiabatic saturation, respectively. W is defined as the weight of water evaporated from the

product,  $\rho$  is the density of air evaluated at the average temperature of air within the dryer and  $V$  is the volumetric air flow rate.

Drying efficiency indicates the overall thermal performance of the system, including the dryer efficiency as well as the collector efficiency. This is essentially a measure of how effective the use of solar radiation is to the drying system. For natural convection dryers, the expression is defined by Equation 3-10 (Leon et al., 2002).

$$\eta_{\text{SYSTEM}} = \frac{WL}{IA} \quad (3-10)$$

The variable  $L$  is the latent heat of vaporization of water at the exit air temperature and  $A$  is the aperture area of the solar collector.

Temperatures in the range of 50–60°C are recommended for drying temperature-sensitive products like fruits and vegetables. While temperatures up to 65°C may be used initially, they should be lowered during drying to avoid quality degradation. Additionally, reports have shown that temperatures in excess of 55°C for at least the last hour of the drying period may degrade the quality (Leon et al., 2002). It is generally recommended that the maximum drying temperature, under no-load conditions, be used for dryer performance analysis since a consistent measure is unattainable under loaded condition due to product variability.

### **Financial Evaluation**

A financial analysis of solar dryers generally includes the cost or upfront investment in the dryer, the operating cost including maintenance, and the payback of the dryer. Since dryers are capital intensive, their use and implementation are only feasible if the operating cost can be balanced against fuel savings for which methods have been reported by Kandpal and Kumar (2005). While the fixed investment and

operation costs can be determined in a straightforward manner, the payback period is the measure of time required to recoup the total investment. Among many factors, the payback period also takes into account, the comparative product yield, the rate of drying, the cost benefits of improved quality and the price of the final product.

Additionally, the time for loading and unloading is an important consideration in the appropriate design of dryers because this may result in extended periods of time and labor that can significantly reduce throughput. In fact, some studies have noted that the loading and unloading of products is important in commercial dryers due to possibilities of contamination, cost of labor, and handling convenience (Leon et al., 2002).

### **Evaluation Procedure**

Product preparation may involve pre-drying processes, such as washing, peeling, cutting, slicing, coring, pitting, trimming, cutting, or chopping; and pre-treatment methods, such as blanching, sulfating, salting, alkaline dipping, heating, cooking, freezing or thawing. For instance, fresh mango fruit is often washed, peeled and cut before undergoing chemical pre-treatment for drying. Pre-treatment with ethylene action inhibitors and 1-methylcyclopropene is known to delay softening and browning in fresh mango fruit while maintaining improved appearance and textural quality. However, more common pre-treatments such as dipping in 0.5-1.0% ascorbic acid, citric acid (lemon juice), L-cysteine or N-acetylcysteine solution for 3 minutes is often employed due to the effectiveness and simplicity of these preservative treatments.

Product information, namely variety, kind or breed, maturity, and pre-treatment, should also be noted. Notes and details on the pre-drying processes and pre-treatment

methods are essential for maintaining consistency among the different products used in different dryers. Pre-heating the fruit slices by blanching or another method can also help to reduce the energy consumed by the drying system and minimize the drying time. All such product preparation should be documented to allow for proper analysis and comparison among studies.

Preparation of the dryer involves ensuring proper functioning of the dryer. Cover glazing must be thoroughly cleaned, and black coating for the solar collector should be checked and repainted if necessary. The dryer test site should be free from shadows during the testing period. Physical features of the dryer such as collector area, collector tilt, tray area and number of layers also need to be recorded. Loading density can be estimated by Equation 3-11 (Leon et al., 2002).

$$\text{Loading Density} = \frac{\text{Weight of fresh product loaded in the dryer (kg)}}{\text{Total solar aperture (m}^2\text{)}} \quad (3-11)$$

Instrumentation and measuring equipment on the dryer and at the test site generally include temperature and relative humidity sensors, pyranometers, anemometers and data-loggers among other devices. The following measurements are briefly described since they are essential in evaluating dryer performance. Common methods and devices utilized in each are mentioned when relevant and available.

Global solar radiation on solar collectors is measured using pyranometers which are commercially available at a wide range of prices depending on the precision demanded. Simple, dome solar meters are more commonly implemented as they are easy to use, and once calibrated, retain their accuracy for long periods (Leon et al., 2002). Furthermore, the wind speed or airflow rate can be measured with a hot-wire anemometer.

Temperature and relative humidity can be measured using appropriate sensors and recorded in a data-logger as closely as possible although typically every five minutes depending on memory constraints (Leon et al., 2002). Sensors should be installed at the air inlet, exit and several internal locations of the dryer. In cases where a data logger is not available, these data may be recorded manually every 30 min or in one hour intervals by a thermometer or air probe and a hygrometer, respectively (Leon et al., 2002). By measuring the temperature and relative humidity over time, the minimum, maximum and average of these values can be determined as well as the duration of air temperature above ambient.

The moisture content of the products can be determined with fixed surface probes inside the dryer or by testing a sample selected at regular intervals, such as on an hourly basis as suggested by Ranganna (1986). Samples should represent the average moisture content of the whole lot, and therefore care should be taken in making this selection. Special attention must be given in sample selection particularly if trays are interchanged during drying.

Additionally, the weight of fresh product loaded in the dryer must be noted as well as the weight of the dried product. This allows for determination of the moisture content of the fruit slices. The moisture content is essentially the amount of moisture in a product and is expressed as a percentage. In other words, moisture content is the ratio of the mass of water contained in a product over the total mass of the food sample. However, moisture content is often expressed in ‘dry weight’ as the mass of water divided by the mass of dry matter.

Common methods for measuring moisture content are either by direct techniques, such as drying, distillation or extraction; or by indirect techniques, such as spectroscopic measurements which do not actually remove water from the sample. Generally, the standard and easiest procedure employed in moisture content determination of a food sample is referred to as the gravimetric oven method. In this procedure, the initial weight of a sample is first determined. The sample is then placed in an oven where the product is periodically weighed while drying progresses. The change in weight will continue to be monitored until no further weight loss is observed. There are also a wide range of moisture meters that are available for determining the moisture content. These devices quickly determine the moisture content by rapidly evaporating moisture from the sample using infrared radiation.

Once equilibrium is reached in a drying process, the weight of the sample remains constant as no moisture in the food sample is lost or gained over time. At this point, the moisture content remains constant and is referred to as the equilibrium moisture content (EMC). The corresponding air relative humidity (RH) at which equilibrium is established is known as the equilibrium relative humidity (ERH). The degree of water availability within a food product is known as the water activity ( $a_w$ ) which is actually defined as the vapor pressure of water within a product divided by the vapor pressure of pure water. Thus, water activity is essentially the measure of the state of water in foods. This term is commonly used in discussing topics of food safety and quality. When a food product reaches equilibrium in respect to the atmosphere surrounding it, the water activity becomes equal to the relative humidity of the surrounding air.

The water activity scale extends from a completely dry state at 0 up to pure water at 1.0. While most microorganisms strive at water activities above 0.8, most microorganisms are unable to grow at levels below 0.6; however they can still survive at these reduced levels. If added to a suitable medium or rehydrated, these microorganism may be resuscitated and start to grow again.

Thus, drying techniques rely on lowering the water activity in order to minimize microbial growth rates and other adverse chemical reactions. The desired level of water activity must be selected to be sufficiently low in order to ensure spoilage reactions are unsupported by excess moisture. However, the precise level of water activity must also be sufficiently high in order to maintain a soft, flexible texture for the dried fruit slice. Therefore, by lowering the water activity to adequate levels, the product quality is maintained while greatly improving the shelf life through prevention of deteriorative reactions.

Water activity can be measured with a variety of methods including the use of desiccating jars which is often referred to as the isopiestic method. This approach to measuring water activity is frequently employed as it is rather inexpensive and straightforward to perform. In this method, a food product is brought into equilibrium with a closed atmosphere of known constant relative humidity which is established with either the use of calibrated saturated salt solution or a reference material of known moisture sorption isotherm . This approach requires knowledge of the initial moisture content and observations of the moisture loss over time. In this process, the weight of the sample will change as moisture is lost until equilibrium is reached with the relative

humidity of the surrounding air. Once equilibrium has been reached, the water activity of the product will be equal to the controlled constant relative humidity.

Water activity can also be measured with the use of a water activity meter or hygrometer. The most commonly used instrument for these measurements is known as a chilled mirror dew point hygrometer which determines vapor pressure based on fundamental thermodynamic principles. These instruments are accurate, precise, fast and simple to use. Dew point evaluation of air vapor pressure works on the basic principle that air can be cooled without changing the water content until it becomes saturated.

Dew point temperature essentially refers to the point at which air becomes saturated. In practice, this temperature is determined by assessing the precise point at which condensation begins to form on a chilled mirror. These devices are generally composed of a mirror, optical sensor, fan and infrared thermometer. Typical dew point instruments allow an agricultural product to come into equilibrium with the sealed headspace surrounding it. As a thermoelectric cooler controls the temperature of the mirror, a thermometer measures the temperature at which condensation begins to form. This condensate is detected with the use of an optical reflectance sensor. The temperature of the product is also measured simultaneously using an infrared thermometer. Both temperatures are then used to calculate the water activity using an integrated algorithm.

Measurement of water activity with these devices generally takes less than 5 to 10 minutes whereas the isopiestic techniques could require multiple weeks depending on the initial moisture content of the sample and calibrated solution.

The relationship between moisture content and water activity of an agricultural product is important. This relationship is often described in reference to moisture sorption isotherms. Sorption isotherms essentially represent the correlation between moisture content and water activity using a graphical plot. These graphical representations are generally expressed at a single, constant temperature over a range of water activities for a specific food material. The data points for moisture content and the corresponding water activities, generally fall on a smooth, sigmoidal curve for most agricultural products. The unique curve is considered a signature physical property for each specific food material at a given temperature. These tools illustrate the steady-state amount of water held by the agricultural products as a function of water activity.

In order to establish the critical moisture contents for agricultural products, the sorption isotherm must be adequately developed and understood for that particular product. This also helps to predict potential changes in food stability. Using an isotherm, you can predict how conditions such as high humidity will affect your products and determine the most stable point for your food product. The shape of a sorption isotherm also helps to predict the quality and physical characteristics of an agricultural material as a function of water activity.

To obtain a sorption isotherm, it is necessary to gather at least several data points relating moisture content to water activity. Thus, each point should be defined by the moisture content evaluated at a specific water activity. This data should be collected over a range of specified water activities to provide enough information to predict the specific shape of the curve. These data points are then fitted to sorption

isotherm models such as the GAB and BET models which have both been reported to be suitable for high sugar content fruits (Falade & Aworh, 2004) such as mangoes. While no isotherm model reported in literature is valid over the entire water activity range of 0 to 1, the GAB model is widely used with an approximate range of 0.10 up to 0.90, while the BET isotherm generally holds from 0.05 to 0.45 (Shyam et al., 2001).

This signature physical property of agricultural samples serves to specify the moisture content needed in order to reach adequate preservation standards in which microbial spoilage and deteriorative chemical reactions are prohibited. Thus, the sorption isotherm helps determine the amount of moisture needed to be removed in the drying process.

### **Summary of Solar Dryer Review**

Agricultural spoilage in developing countries is known to be significantly high particularly in moist, tropical regions. The various causes associated with product degradation have been reviewed in this report and a wide range of solutions have been described. Traditional drying processes such as open-air sun drying and smoke drying actually result in lower quality product due to microbial and fungal infestation while the implementation of sophisticated mechanized dryers in developing countries is scarce as finances and resources are limited. For this reason, small-scale solar dryers are considered and elaborated on in this review. Solar dryers essentially harness sunlight within enclosed environments thus protecting the product and minimizing the use of traditional energy sources.

A systematic classification scheme was developed in order to establish clear distinctions in the design of solar dryers. Generally, solar dryers are considered either

passive or active based on the utilization of forced convection. While passive systems are often easier to construct and relatively cheaper, they commonly exhibit lower quality product or decreased efficiency. Further distinction can be made considering the mode of solar radiation exposure. Direct dryers often result in downgraded product quality as direct exposure to radiation can hurt the product in a variety of ways. Indirect dryers are often slower but increase the quality substantially. Compromises must be made here to ensure adequate product quality and dryer efficiency while minimizing the complexity and investment in the dryer.

The wide selection of solar dryers reviewed here demonstrates the ongoing efforts to improve these drying systems. Modifications to solar dryers such as chimneys, ventilators, absorber improvements, thermal storage, and biomass burners, among many others are discussed in this review. While some of these modifications are found ineffective such as the wind ventilator, others show marked improvement. Some designs increase the solar absorption efficiency while others ensure heating continues during lulls in solar activity.

Materials for fabrication of solar dryers have also been reviewed here and a comprehensive list was created for the primary components. Additionally, discussion was presented on commonly evaluated parameters of solar dryers as well as parameters that are recommended for future evaluations which aim to improve characterization of dryers and allow for adequate comparison of different systems. Analysis procedures were briefly discussed with consideration given to instrumentation, the frequency of recording measurements and other useful guidelines. This review

should thus serve to sufficiently guide individuals in selecting appropriate dryer designs for given conditions and subsequently evaluating the performance of the system.

Table 3-1. Estimated postharvest losses of fresh produce in developed and developing countries

Locations	Developed Countries		Developing Countries	
	a Range (%)	Mean (%)	g Range (%)	Mean (%)
From production to retail sites	2-23	12	5-50	22
At retail, foodservice, and consumer sites	5-30	20	2-20	10
Cumulative total	7-53	32	7-70	32

Kader, A. A. (2005). Increasing food availability by reducing postharvest losses of fresh produce. International Postharvest Symposium, 5, Verona, Italy.

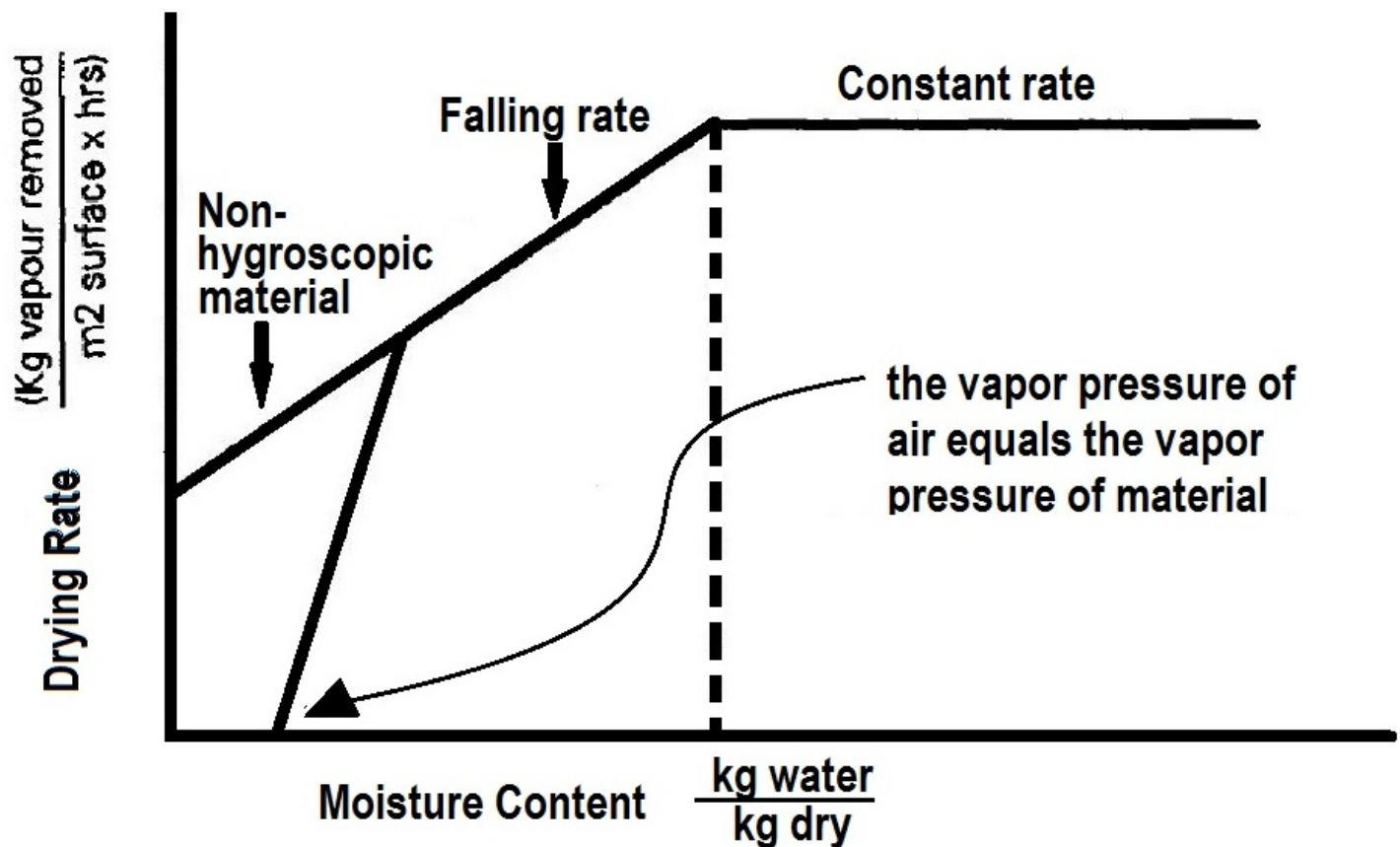


Figure 3-1. Drying curve

Table 3-2. Moisture absorption capability

Initial relative humidity	Moisture absorption capability (grams of $H_2O$ per $m^3$ of air) [ $g/m^3$ ]		
	Not heated	Heated to 40°C	Heated to 60°C
40%	4.3	9.2	16.3
60%	1.4	8.2	15.6
80%	0	7.1	14.9

(Buchinger and Weiss, 2002) Buchinger, J., & Weiss, W. (2002). Solar Drying. Austrian Development Cooperation: Institute for Sustainable Technologies.

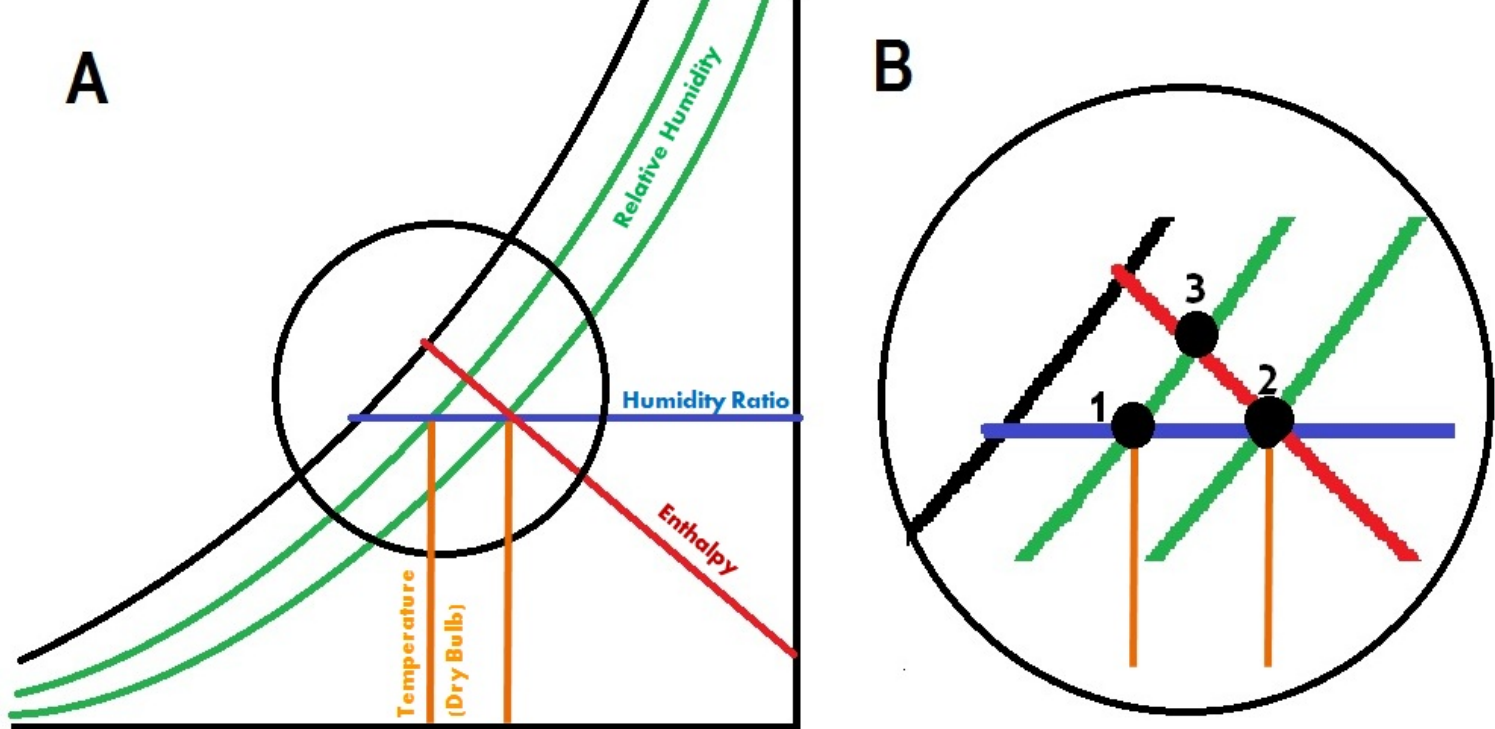


Figure 3-2. Psychrometric chart showing a drying process. A) Overview. B) Enlarged area of interest.



Figure 3-3. Traditional open-air sun drying [Reprinted with permission from Li et al., 2006 (Page 840, Figure 2).]

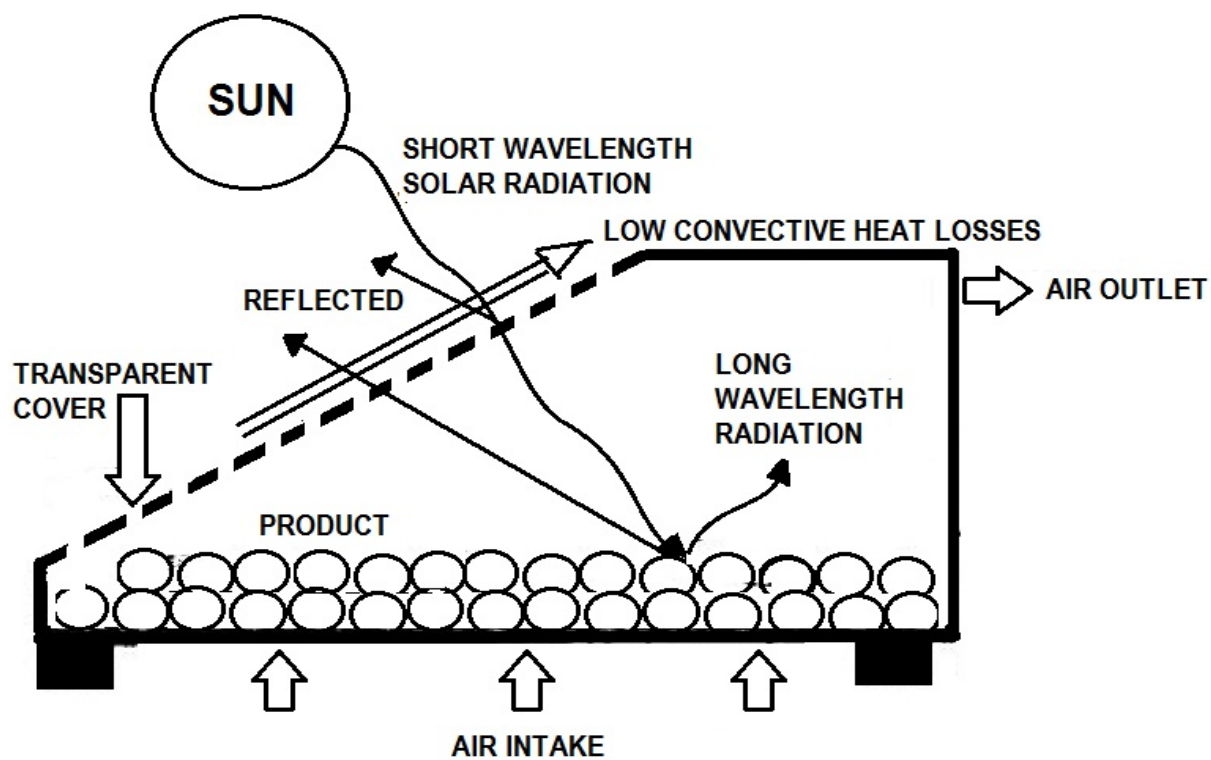


Figure 3-4. Working principle of direct solar dryer

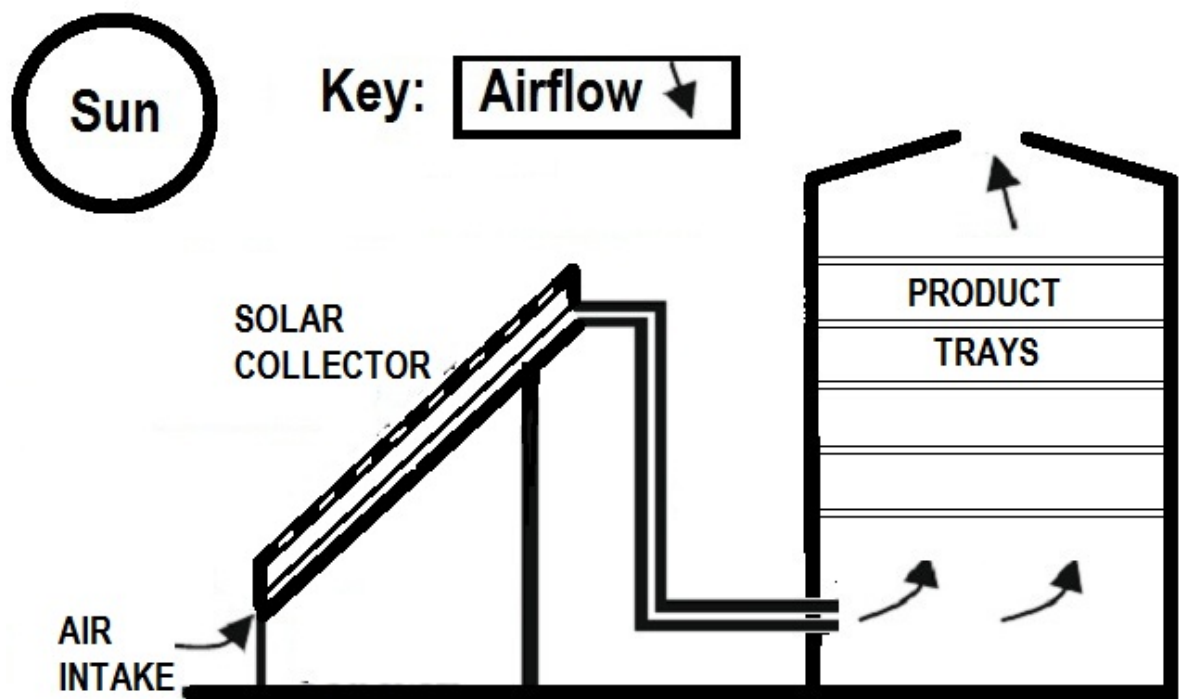
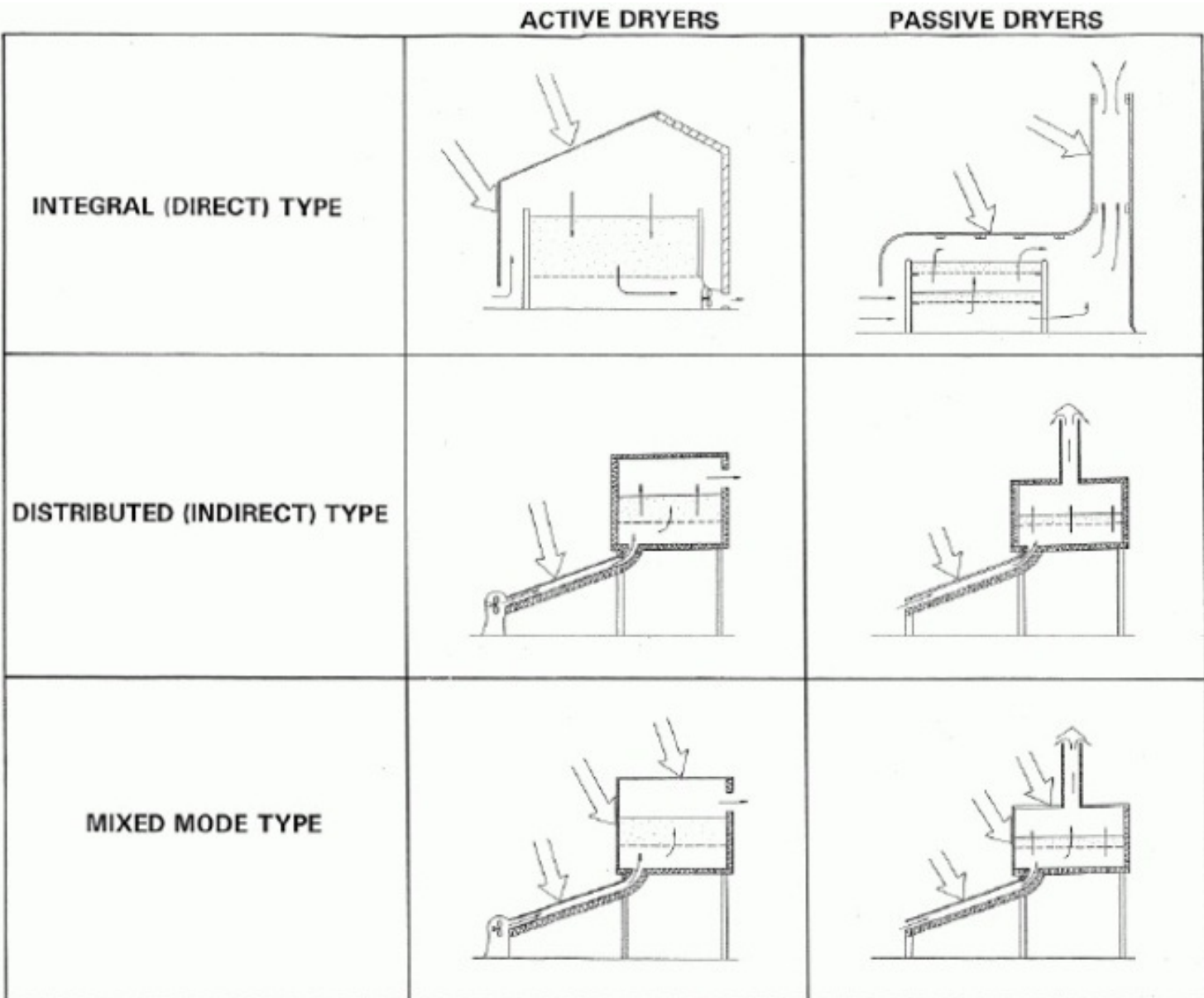


Figure 3-5. Working principle of indirect, active solar dryer



 SOLAR RADIATION  
 AIRFLOW

Figure 3-6. General classification of solar dryers [Reprinted with permission from Ekechukwu and Norton, 1999 (Page 620, Figure 2).]

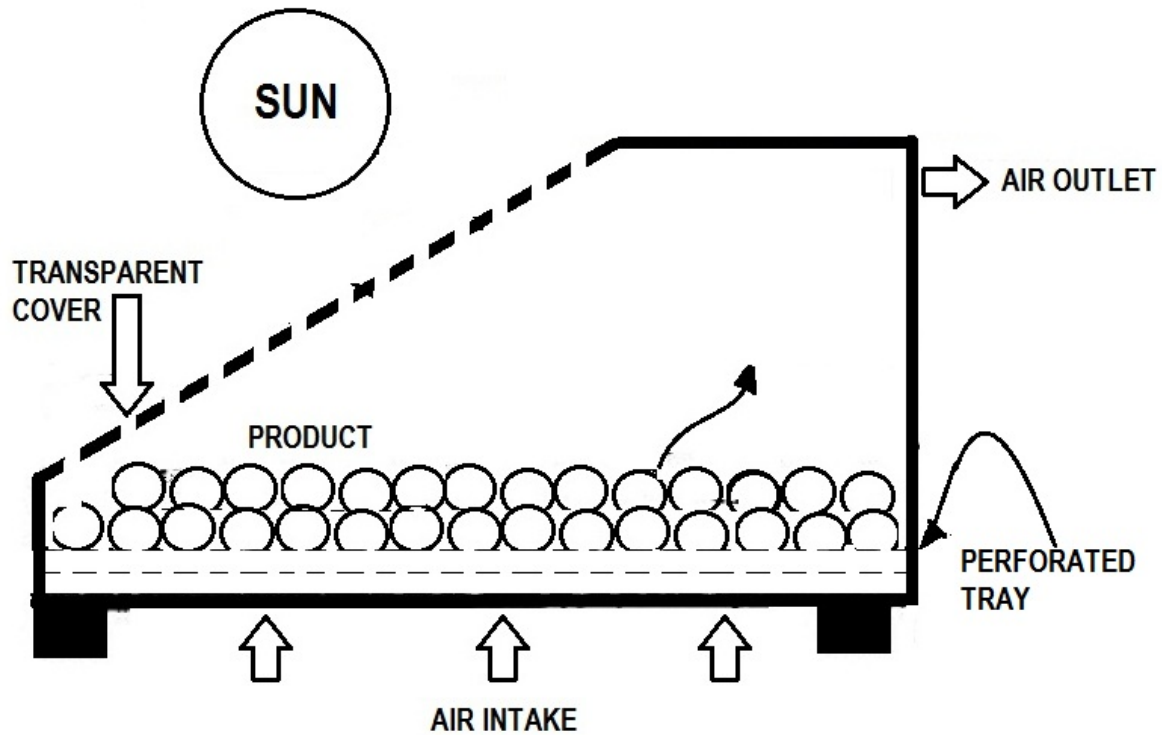


Figure 3-7. Working principle of direct-type, solar dryer

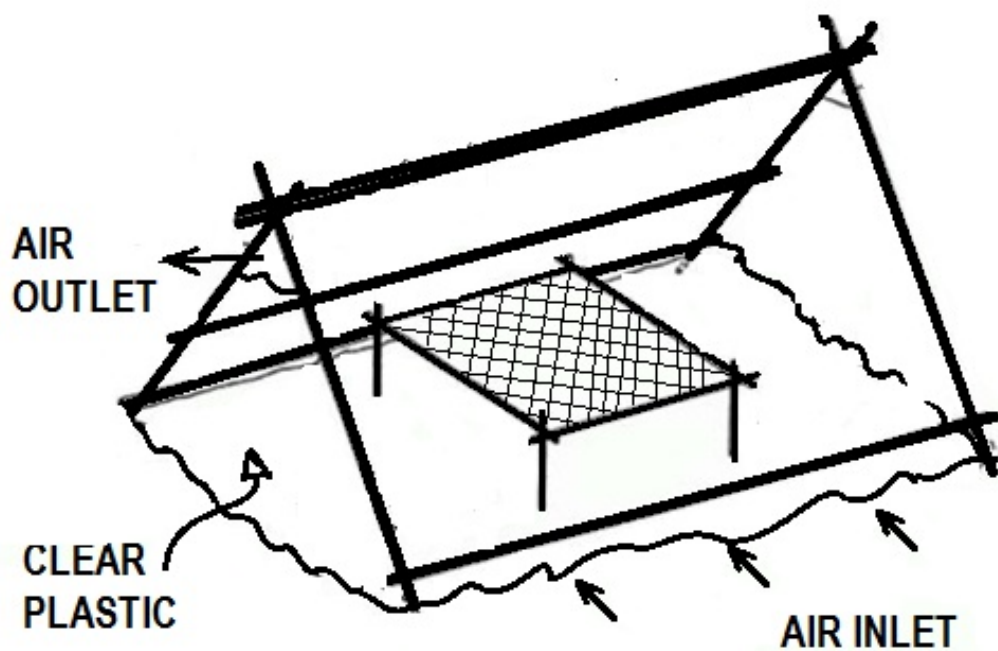


Figure 3-8. Typical direct-type, tent solar dryer

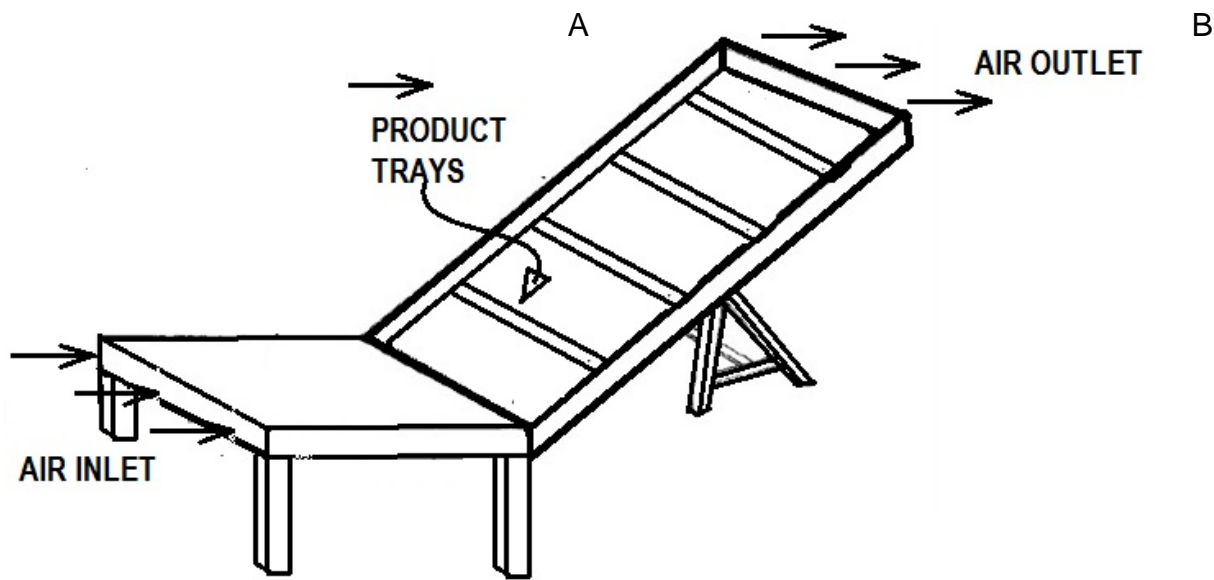


Figure 3-9. Typical direct-type, seesaw dryer

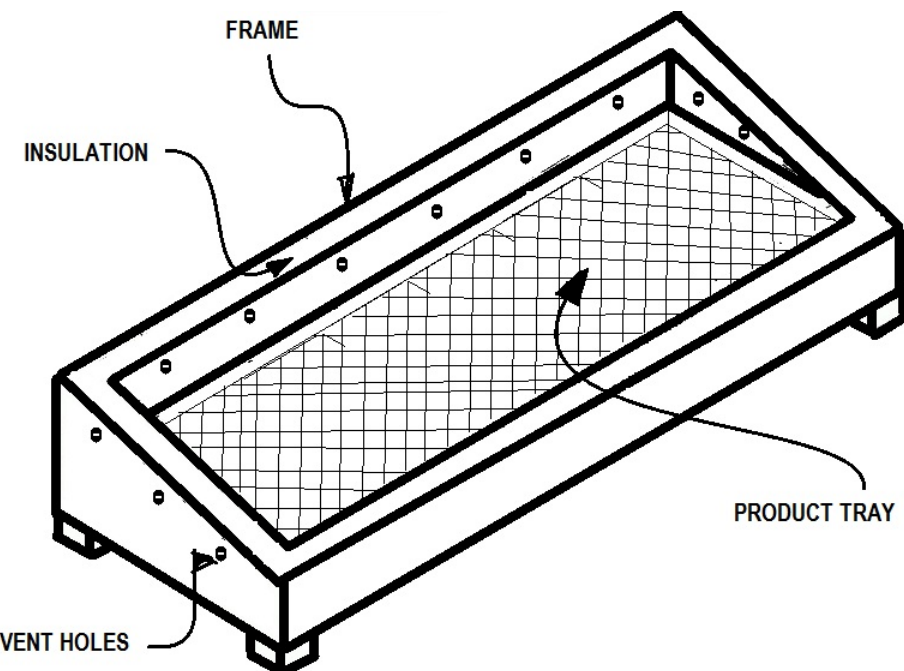


Figure 3-10. Typical direct-type, box dryer

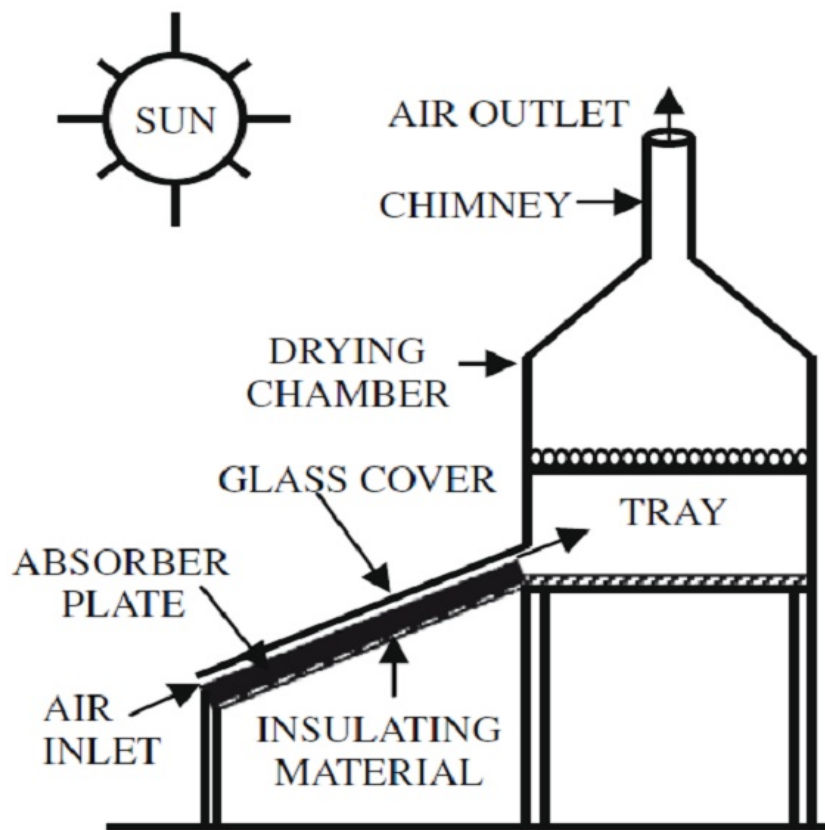


Figure 3-11. Typical indirect-type cabinet dryer [Reprinted with permission from Jairaj et al., 2009 (Page 1703, Figure 10).]

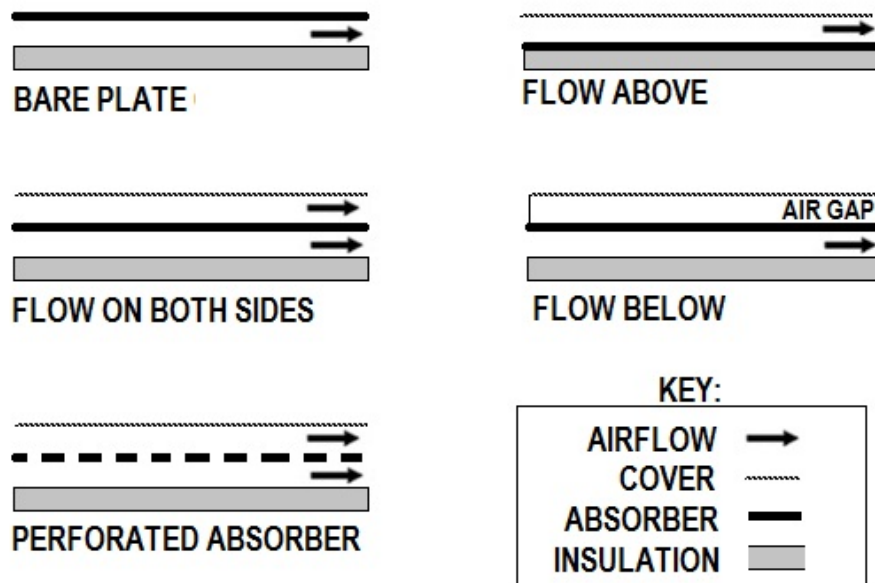


Figure 3-12. Airflow principles in assorted solar collectors

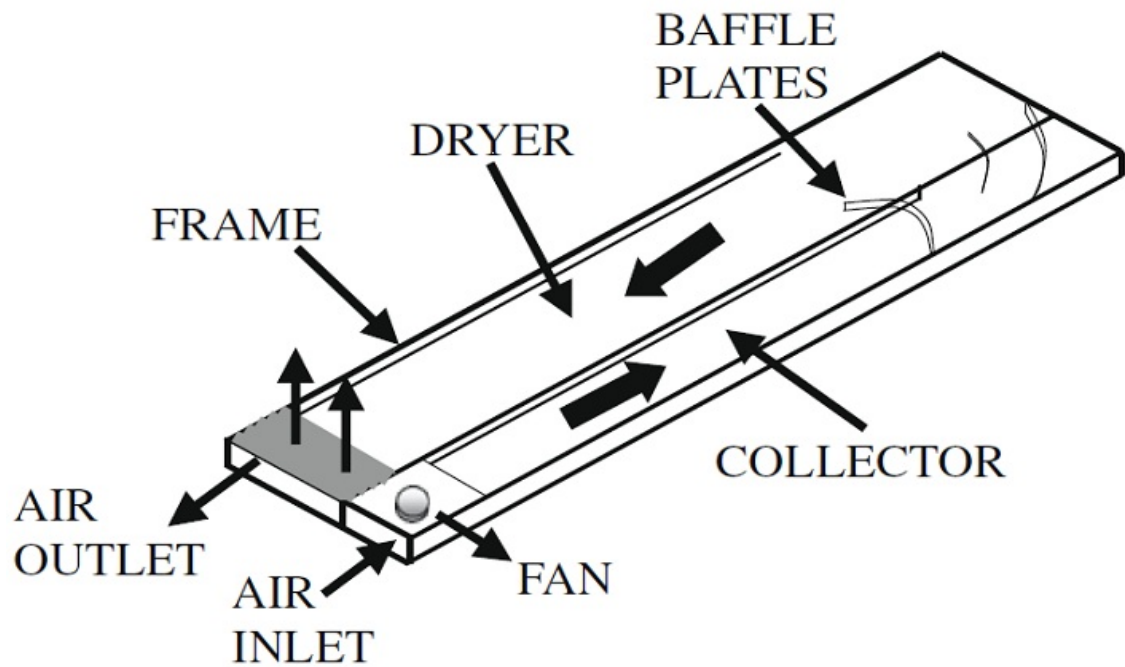


Figure 3-13. Typical indirect-type, tunnel dryer [Reprinted with permission from Jairaj et al., 2009 (Page 1705, Figure 18).]

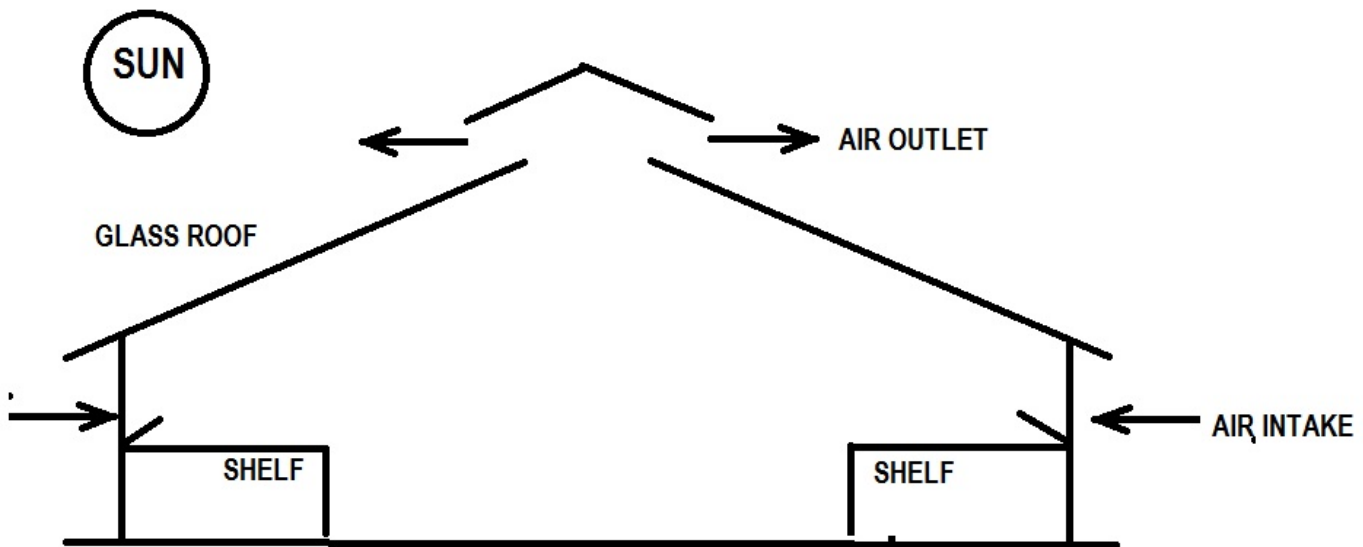


Figure 3-14. Typical large-scale, greenhouse solar dryer

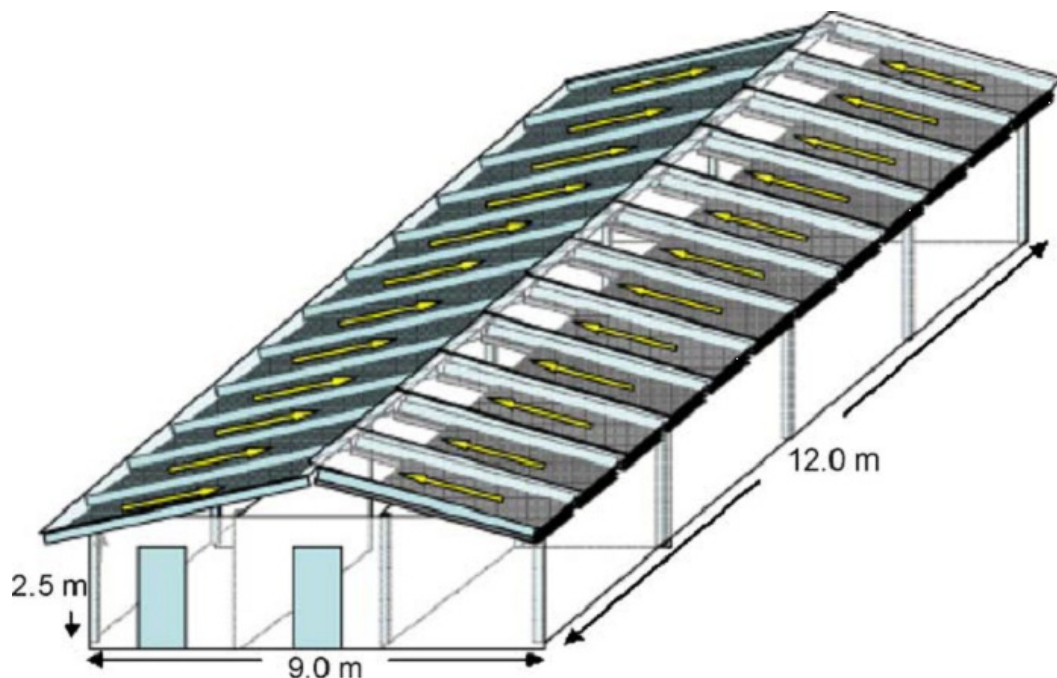


Figure 3-15. Roof-integrated solar drying system [Reprinted with permission from Janjai et al., 2008 (Page 93, Figure 1).]

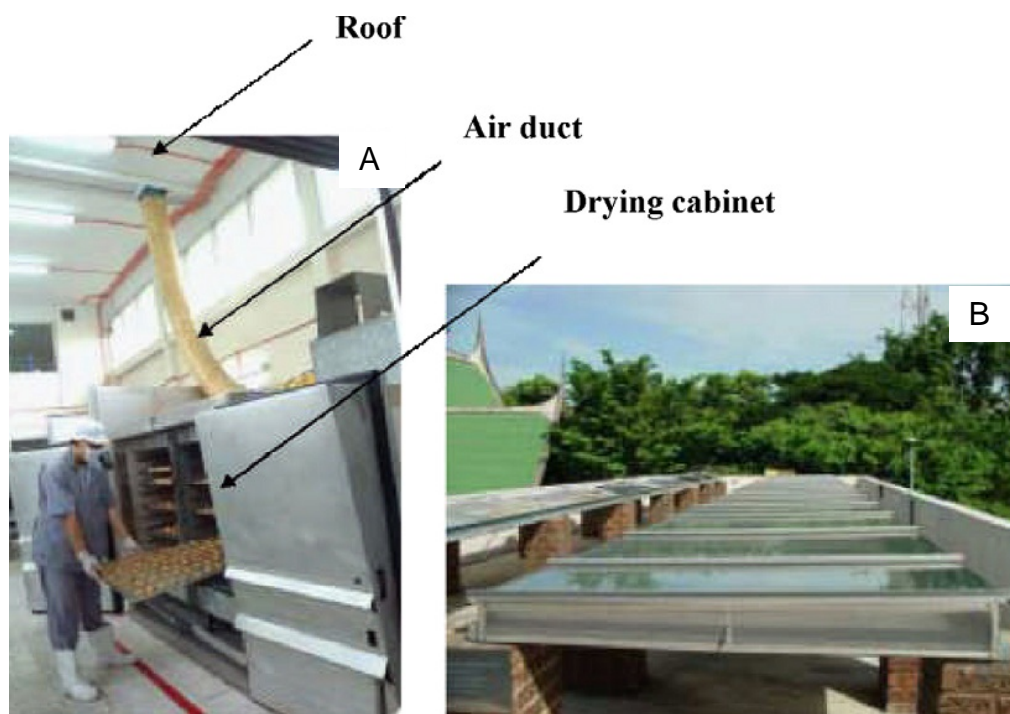


Figure 3-16. Drying cabinet and solar collector of in-house dryer. A) Operation of dryer with loaded trays. B) Roof-integrated solar collectors. [Reprinted with permission from Smitabhindu et al., 2008 (Page 1525, Figure 2).]

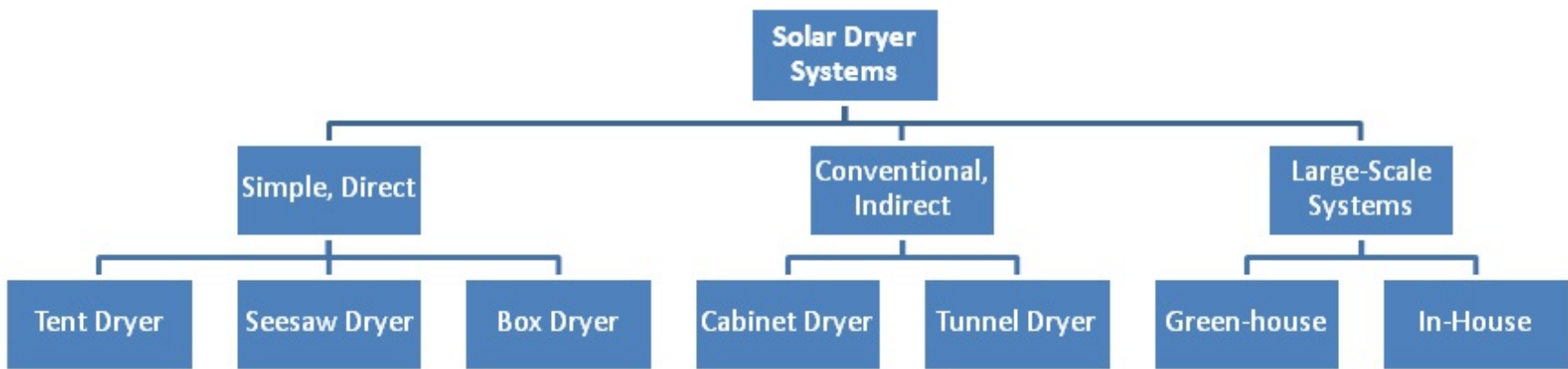


Figure 3-17. Solar dryer categorization overview

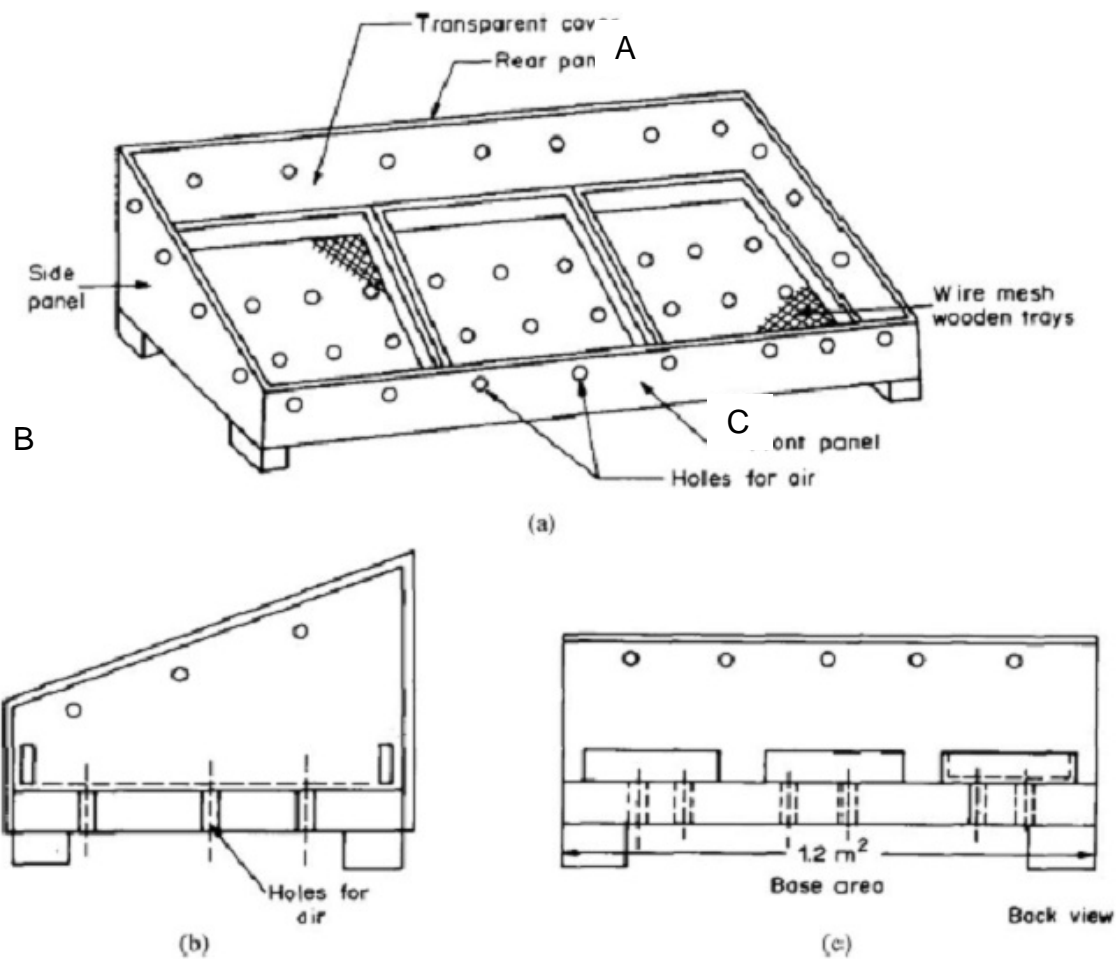


Figure 3-18. Schematic of direct, box dryer. A) Front. B) Side. C) Rear. [Reprinted with permission from Sodha et al., 1985 (Page 265, Figure 2).]

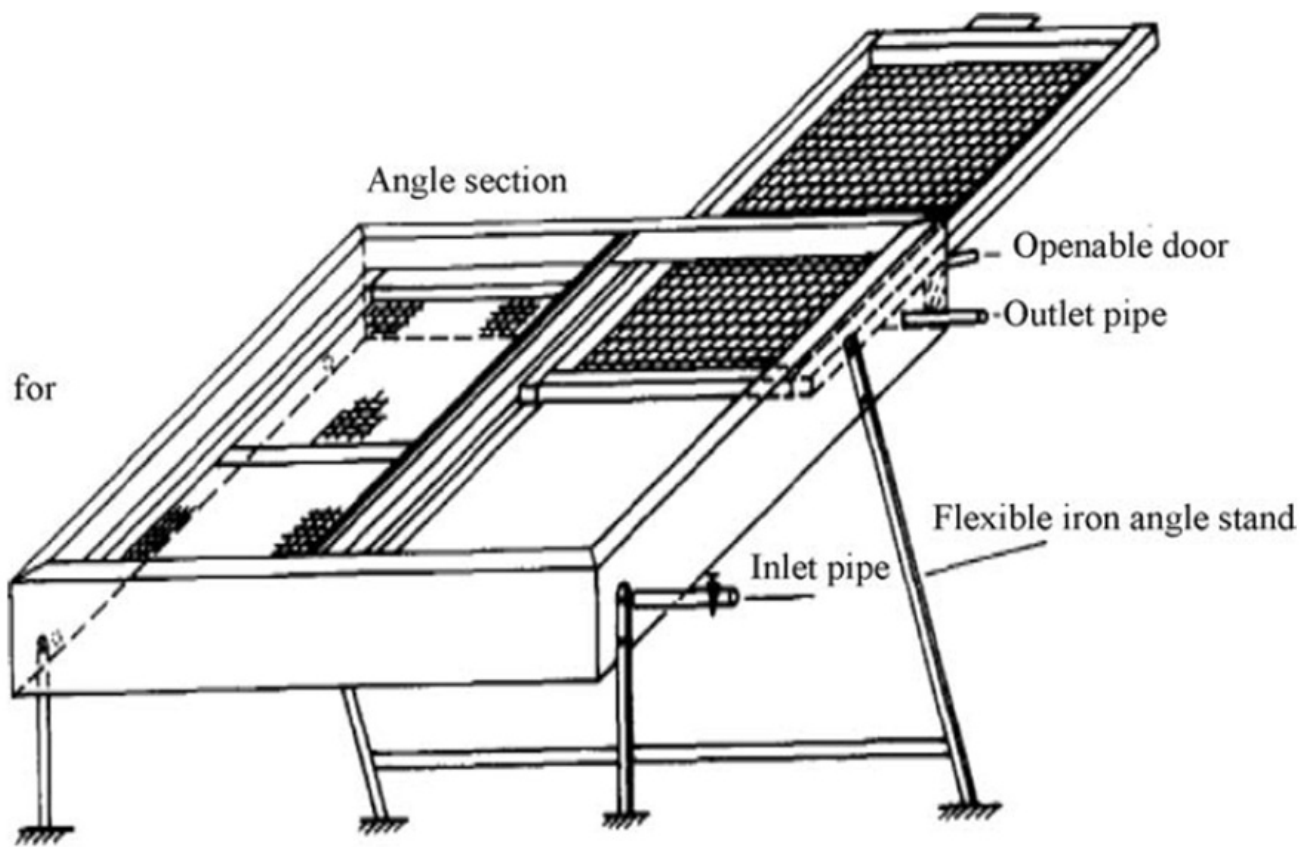


Figure 3-19. Box dryer with  $\text{H}_2\text{O}$  heater [Reprinted with permission from Pande and Thanvi, 1991 (Page 584, Figure 1).]



B

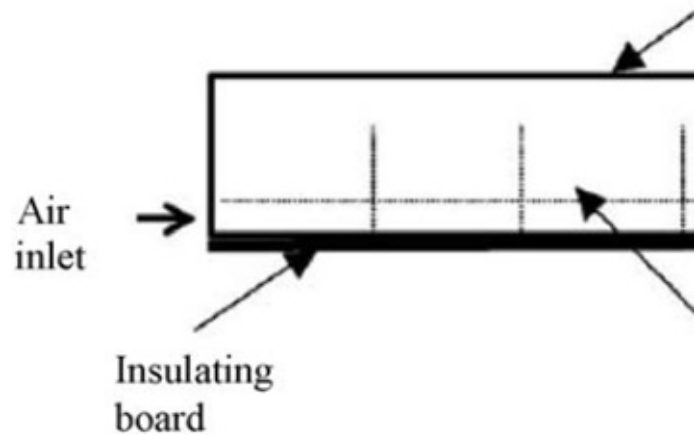
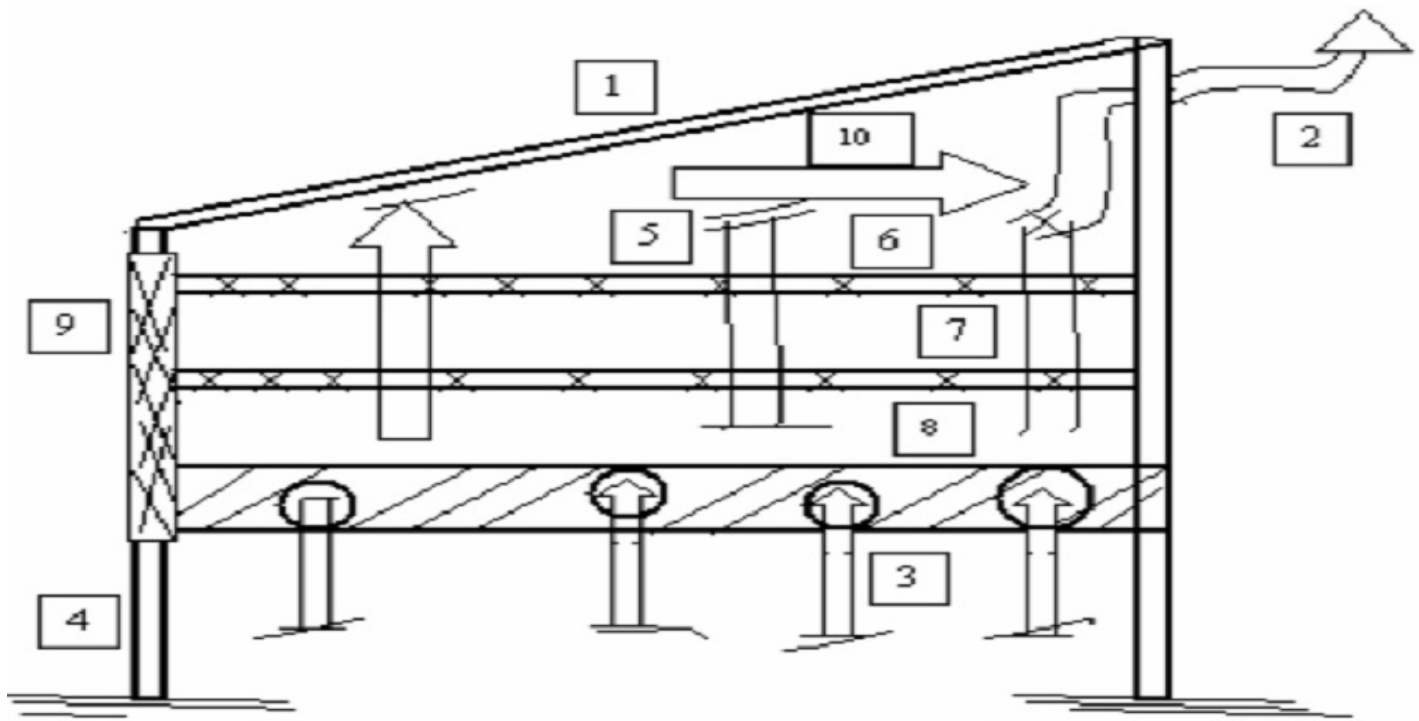


Figure 3-20. Box dryer with limited tracking. A) Pictorial. B) Cross-section schematic.  
[Reprinted with permission from Mwithiga and Kigo, 2006 (Page 248, Figure 1).]



### Components

- |                     |                 |
|---------------------|-----------------|
| 1. Top Glass Cover  | 6. Tray 1       |
| 2. Chimney          | 7. Tray 2       |
| 3. Air Vent (in)    | 8. Wooden Cover |
| 4. Iron Stand       | 9. Dryer Door   |
| 5. Side Glass Cover | 10. Air Flow    |

Figure 3-21. Detailed schematic of box dyer [Reprinted with permission from Enebe and Ezekoye, 2006 (Page 187, Figure 2).]



Figure 3-22. Box dryer with variable inclination [Reprinted with permission from Singh et al., 2006 (Page 1803, Figure 3).]

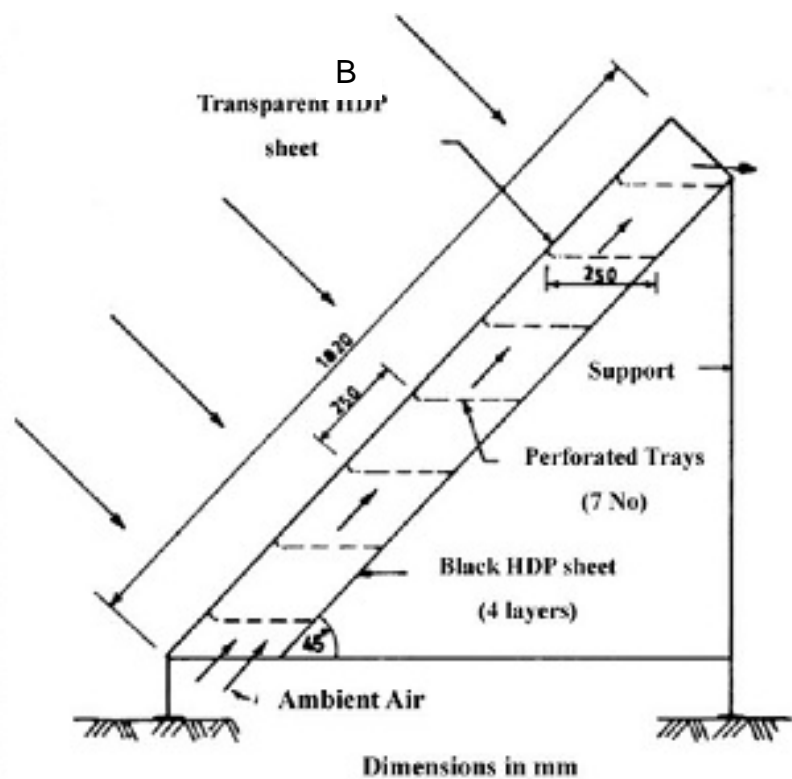
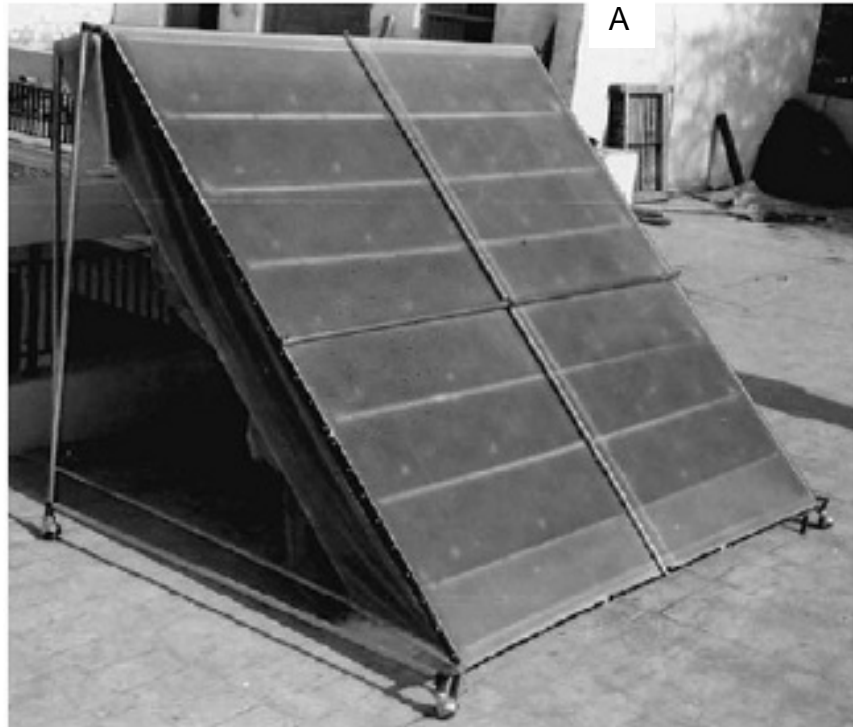


Figure 3-23. Box dryer. A) Pictorial. B) Side view schematic. [Reprinted with permission from Singh et al., 2004 (Page 756-757, Figure 1 and 2).]

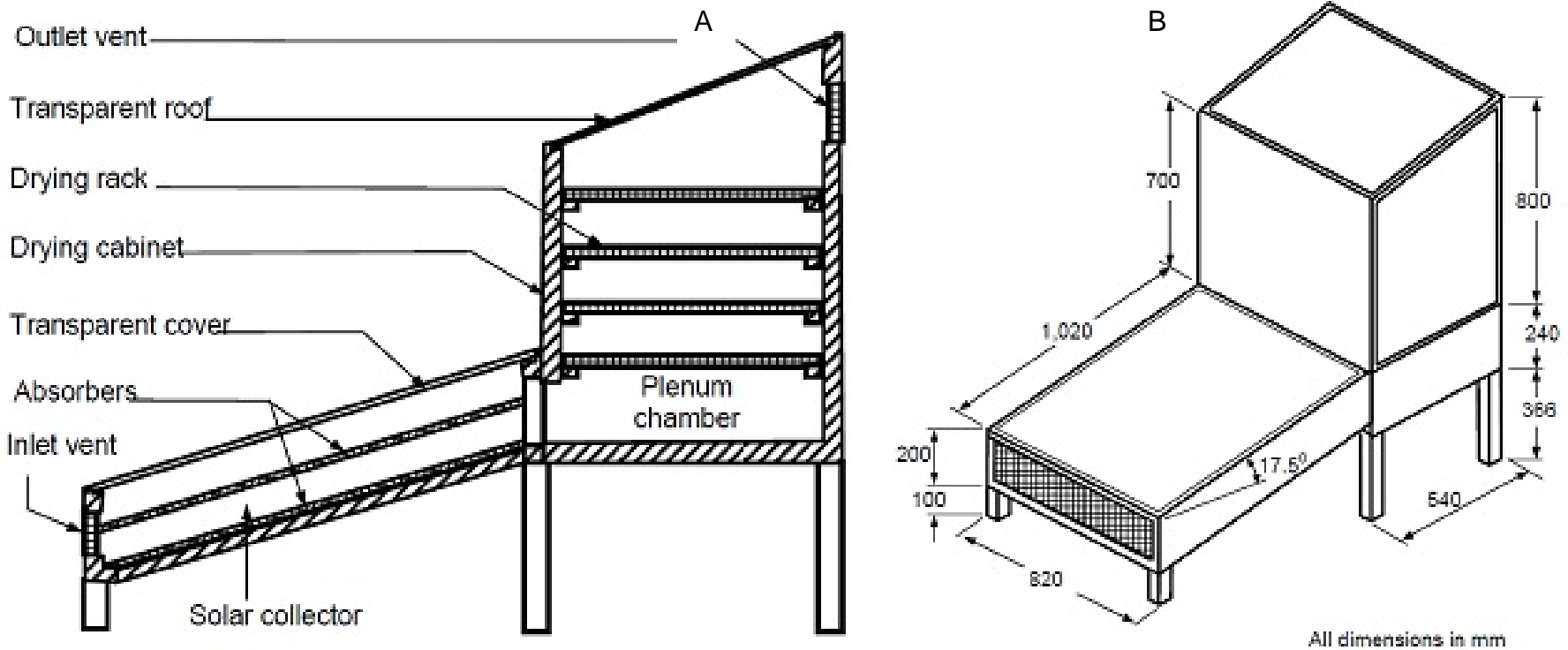


Figure 3-24. Simple cabinet dryer. A) Sectional view. B) Isometric view schematic. [Reprinted with permission from Bolaji and Olalusi, 2008 (Page 229, Figure 1 and 2).]

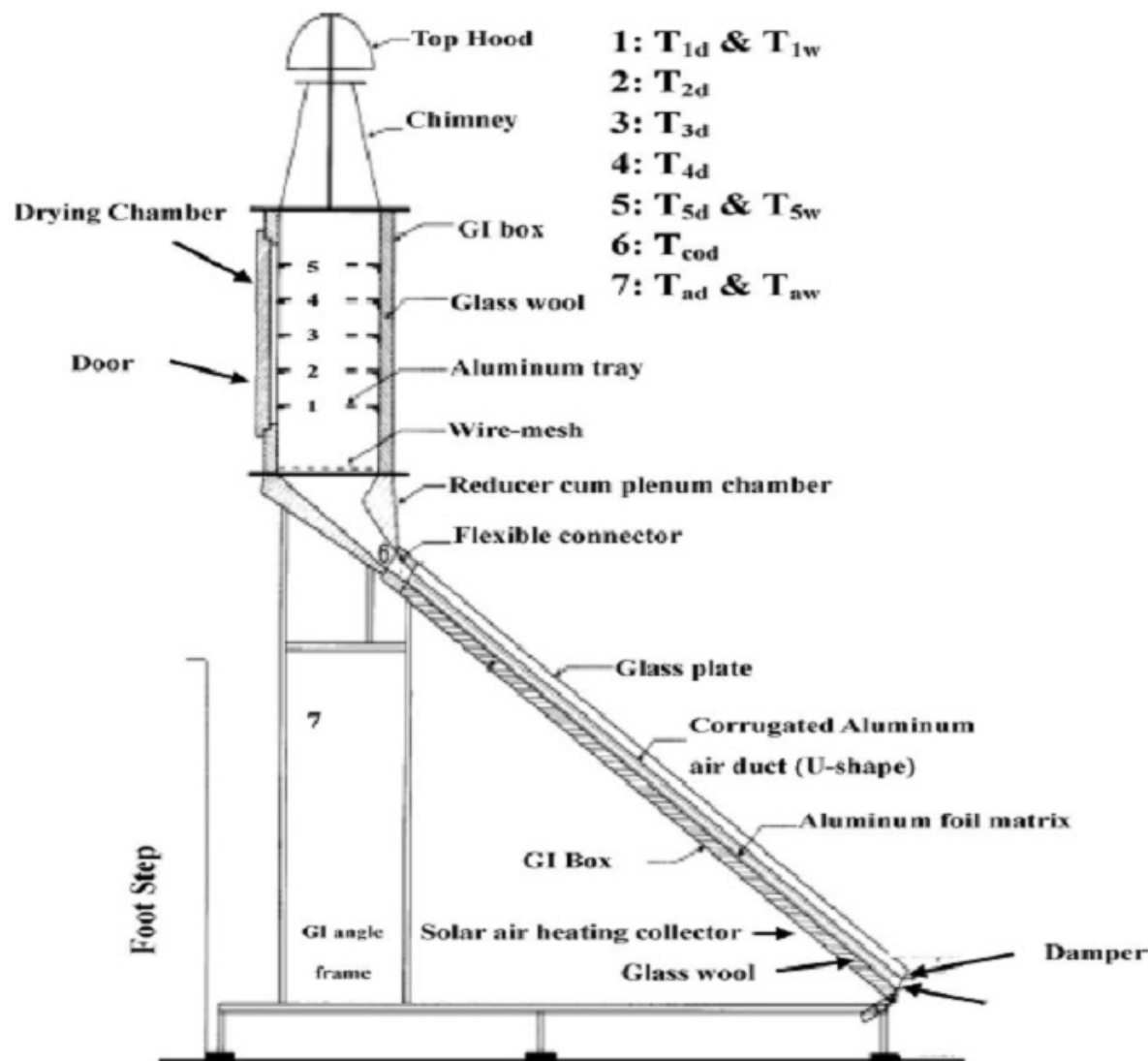


Figure 3-25. Cabinet dryer schematic [Reprinted with permission from Pangavhane et al., 2002 (Page 582, Figure 1).]

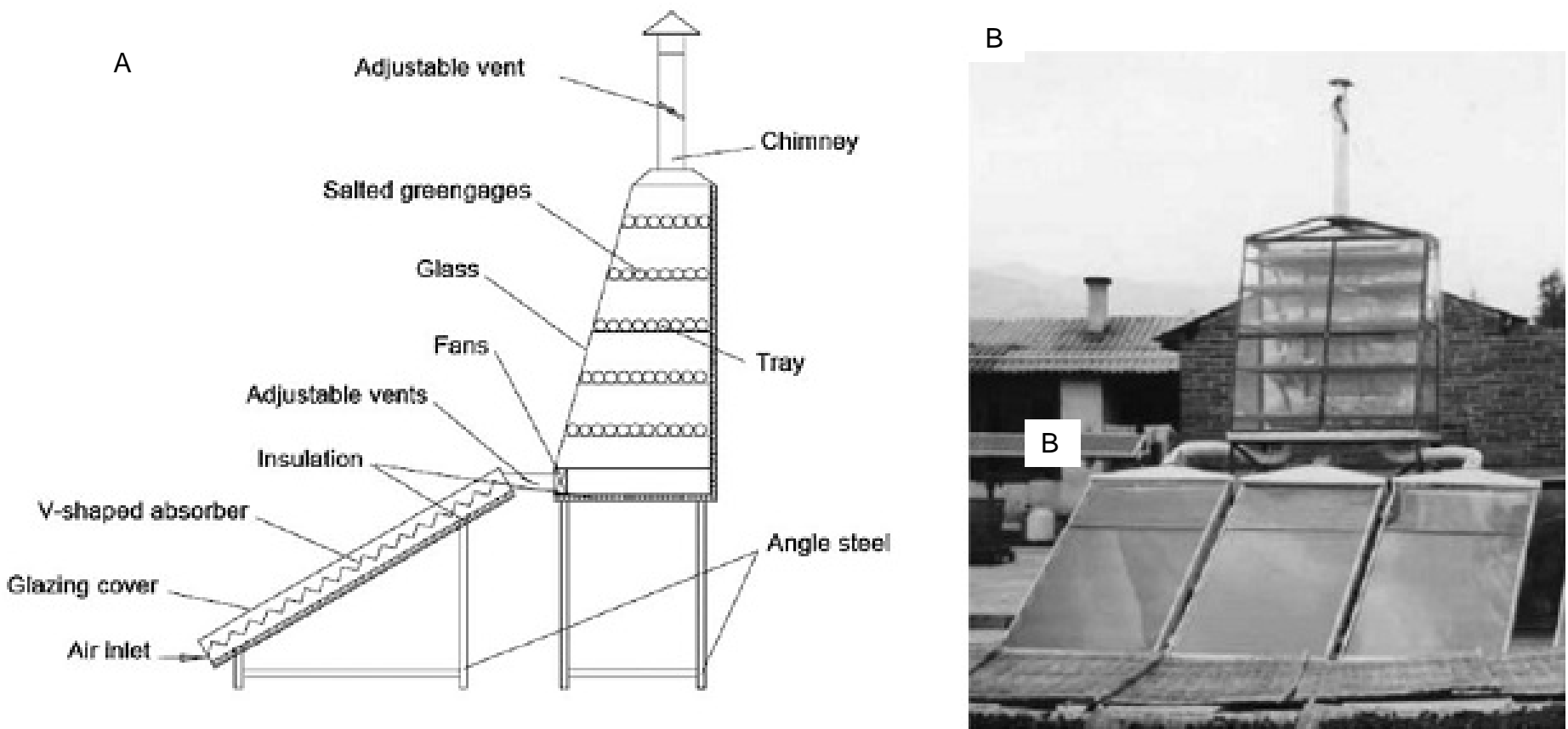


Figure 3-26. Cabinet dryer with multiple solar collectors. A) Cross-sectional schematic. B) Pictorial view. [Reprinted with permission from Li et al., 2006 (Page 839-840, Figure 1 and 2).]

C

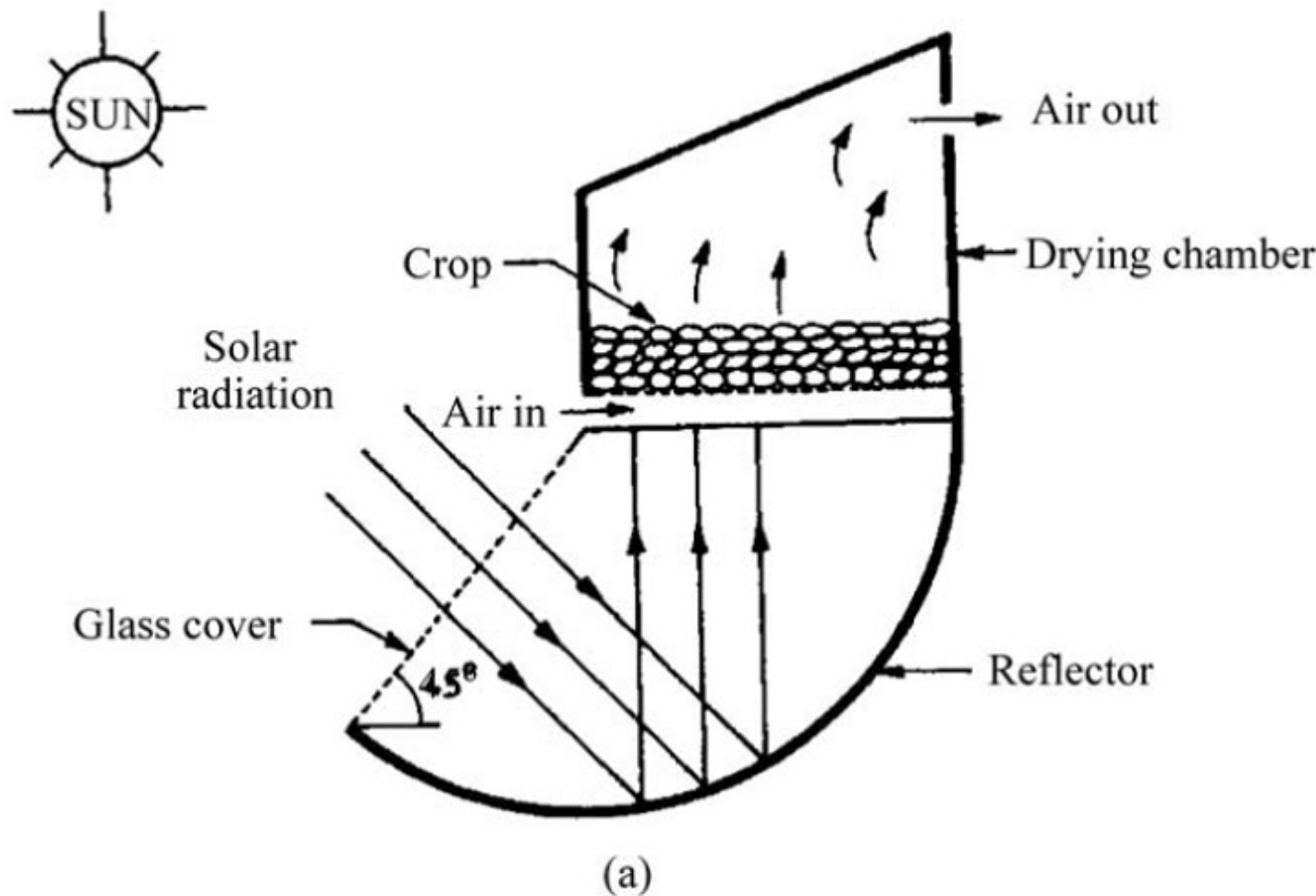
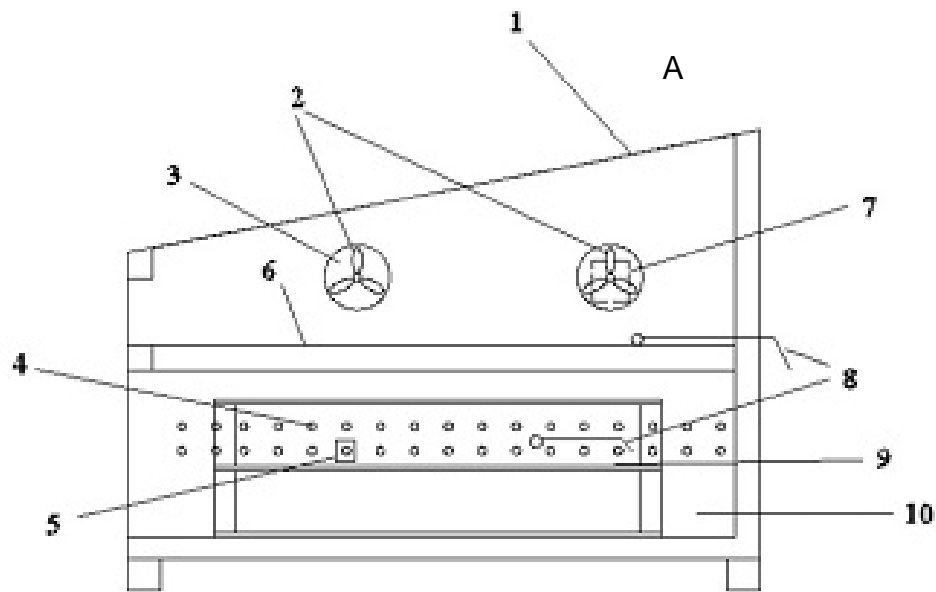


Figure 3-27. Reverse absorber cabinet dryer, RACD [Reprinted with permission from Goyal and Tiwari, 1999 (Page 387, Figure 1).]



1-Glazing; 2-Fans; 3-Air inlet; 4-Exit of air; 5-Humidity probe; 6-Drier absorber plate;  
7-Velocity probe; 8-Temperature sensors; 9-Perforated tray; 10-Drying cabinet

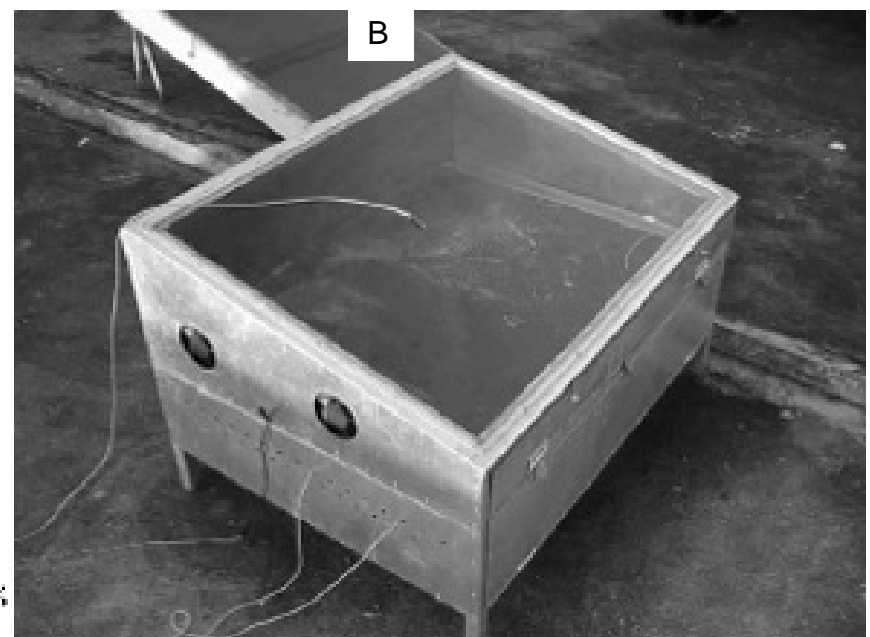


Figure 3-28. Cabinet dryer with top absorber. A) Side schematic. B) Photograph. [Reprinted with permission from Sreekumar et al., 2008 (Page 1389-1390, Figure 3 and 4).]

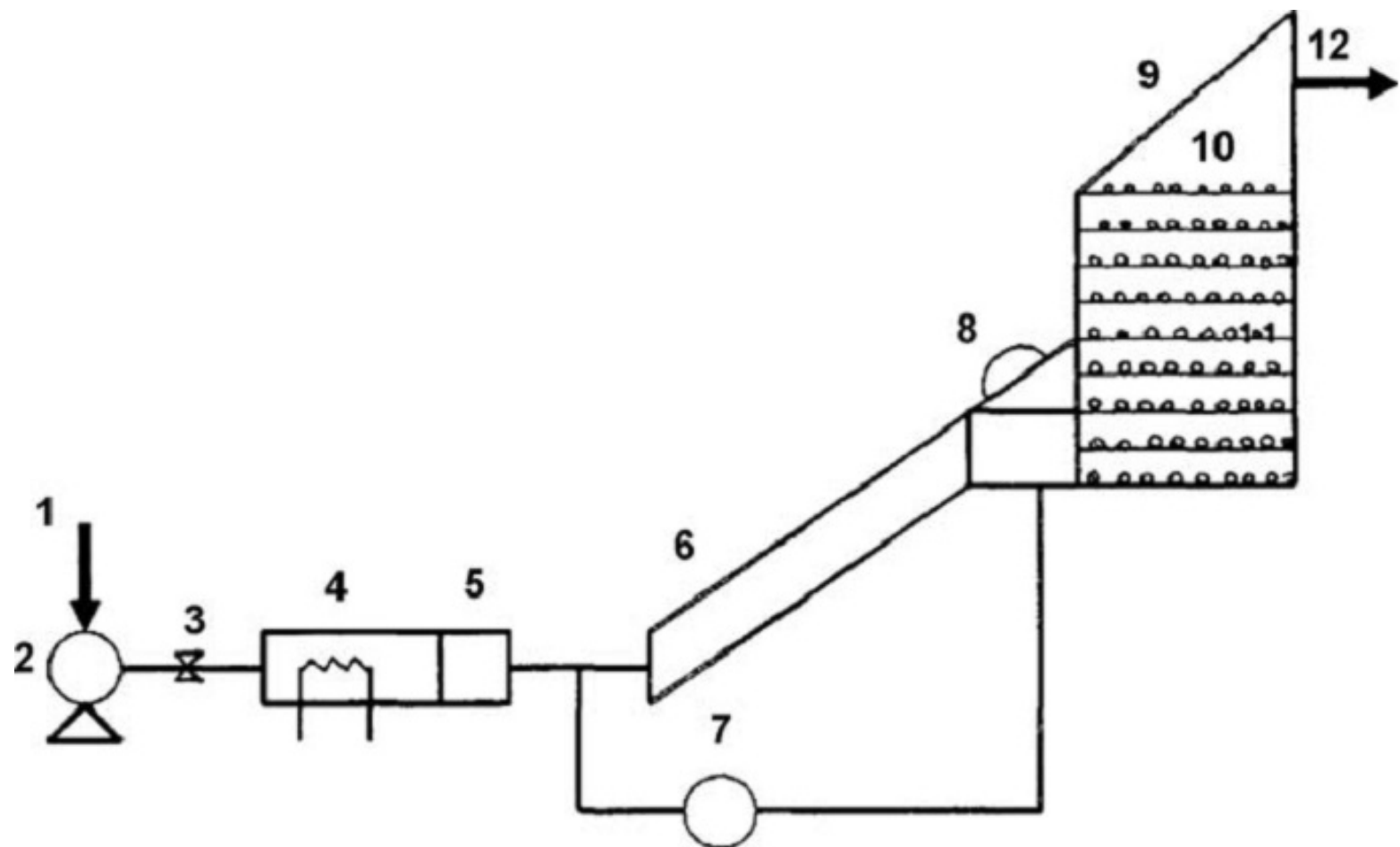


Figure 3-29. Simple active cabinet dryer, schematic [Reprinted with permission from Tiris et al., 1995 (Page 206, Figure 1).]

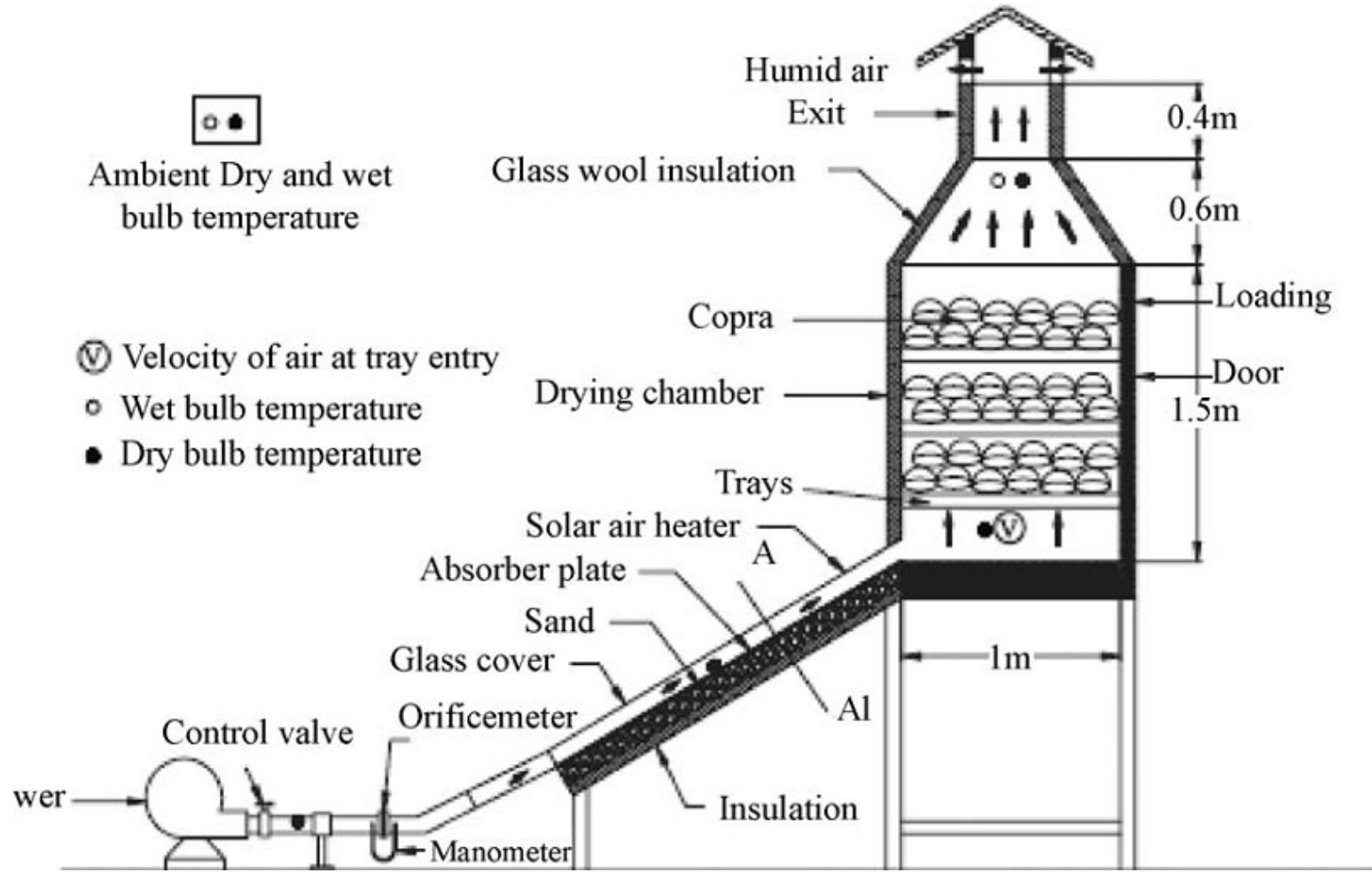


Figure 3-30. Active cabinet dryer, schematic [Reprinted with permission from Mohanraj and Chandrasekar, 2008 (Page 605, Figure 1).]

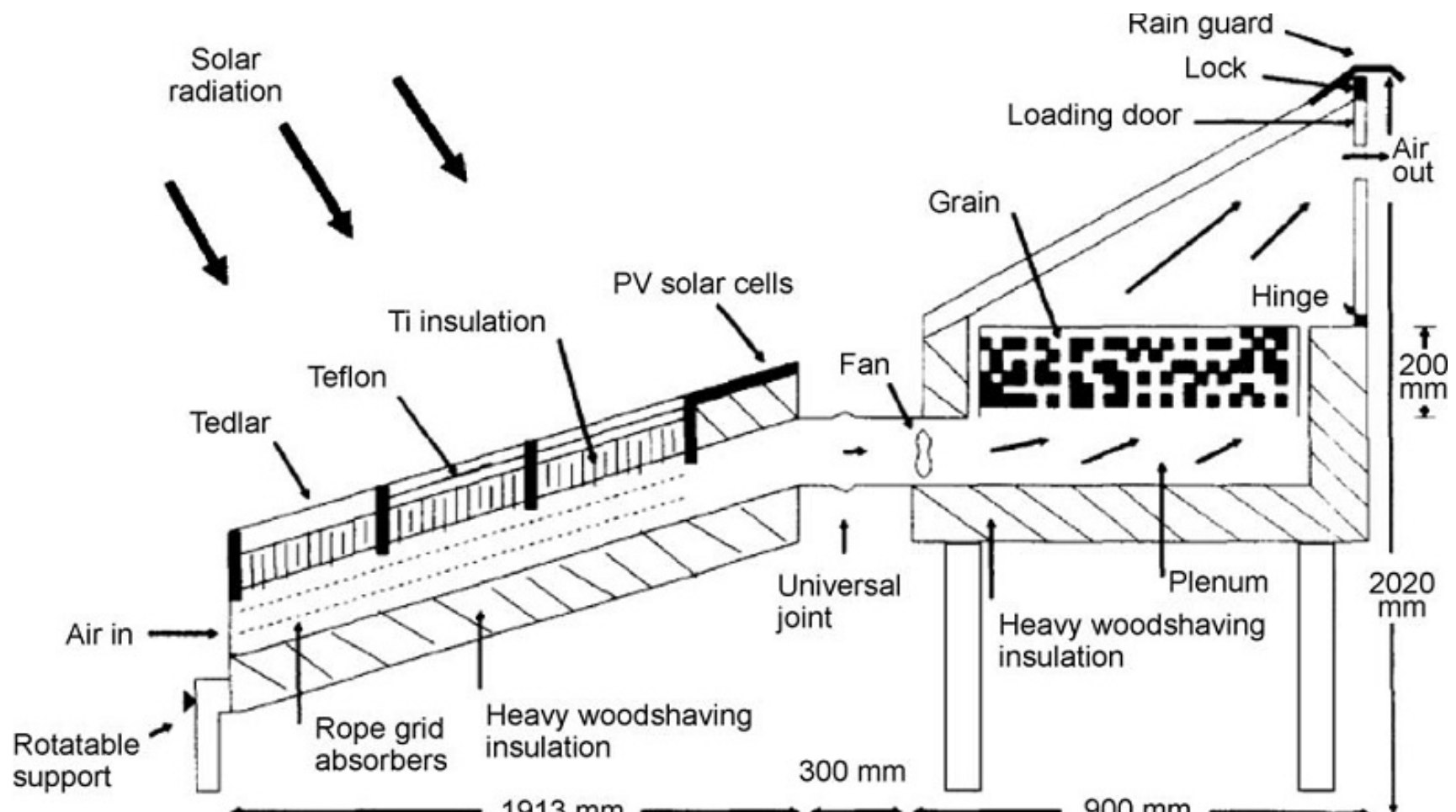


Figure 3-31. Active cabinet dryer with absorber mesh, schematic [Reprinted with permission from Mumba, 1996 (Page 616, Figure 1).]

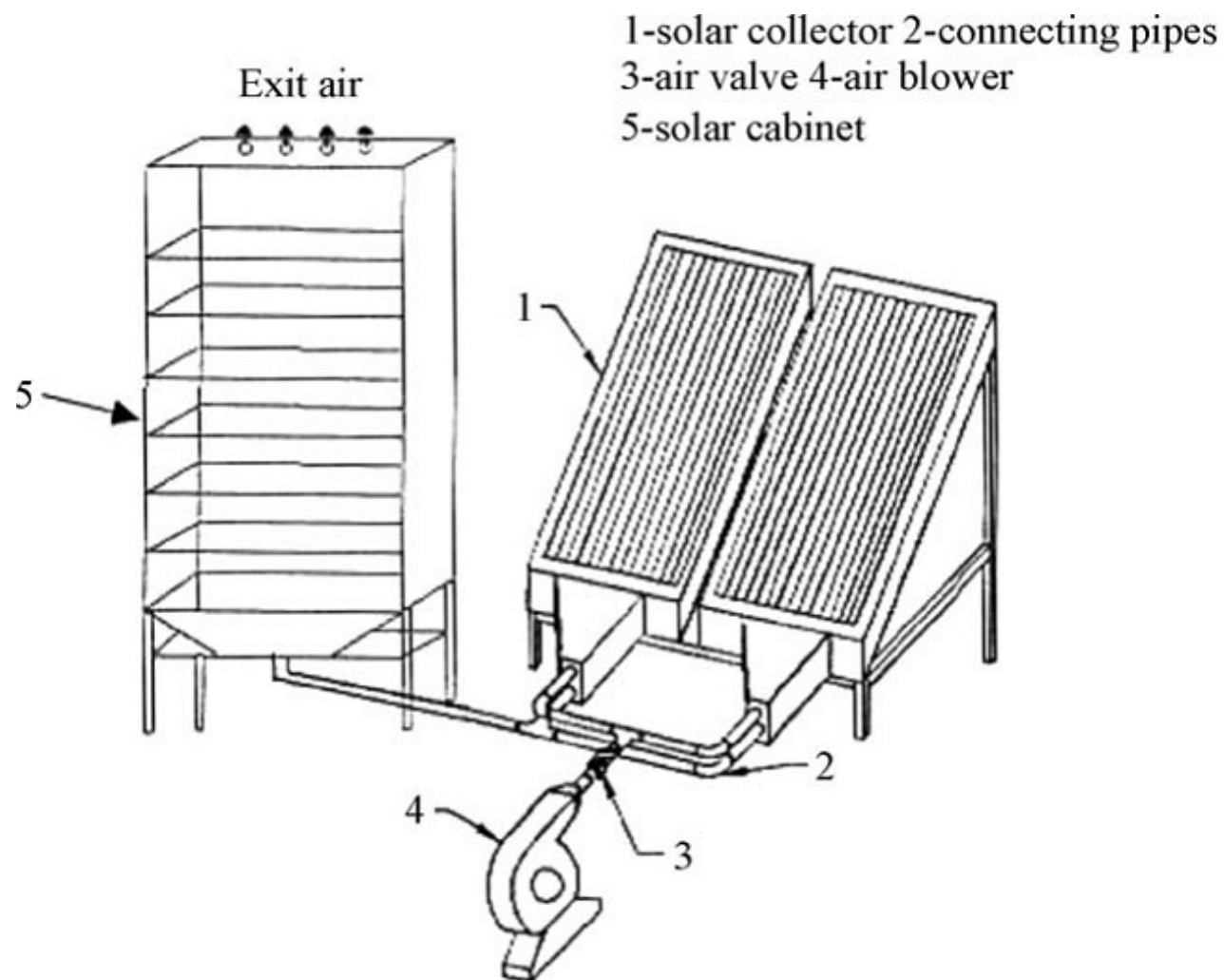


Figure 3-32. Active cabinet dryer with piping [Reprinted with permission from Al-Juamily et al., 2007 (Page 166, Figure 1).]

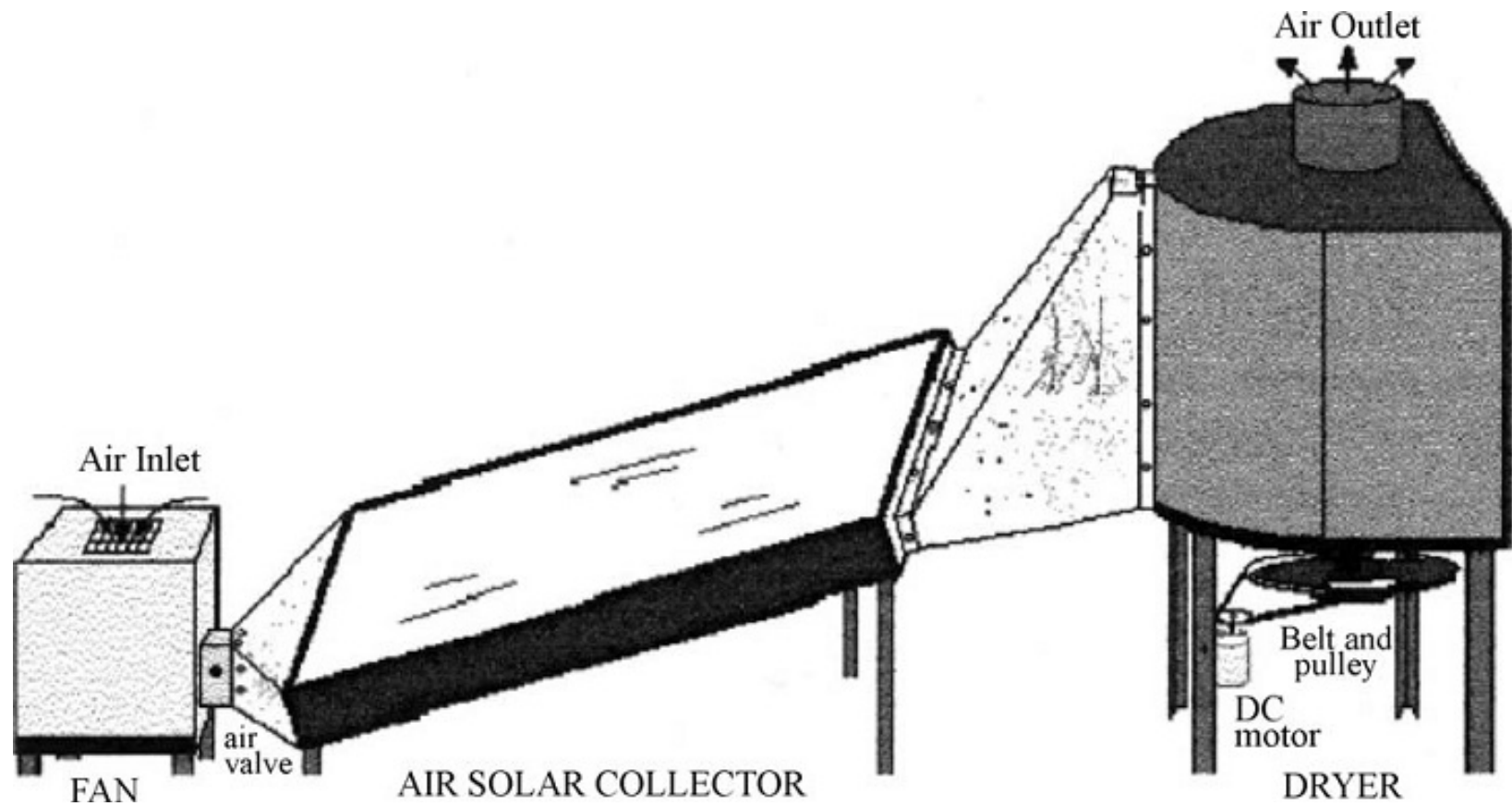


Figure 3-33. Rotary column cylindrical dryer, RCCD [Reprinted with permission from Sarsilmaz et al., 2000 (Page 119, Figure 1).]

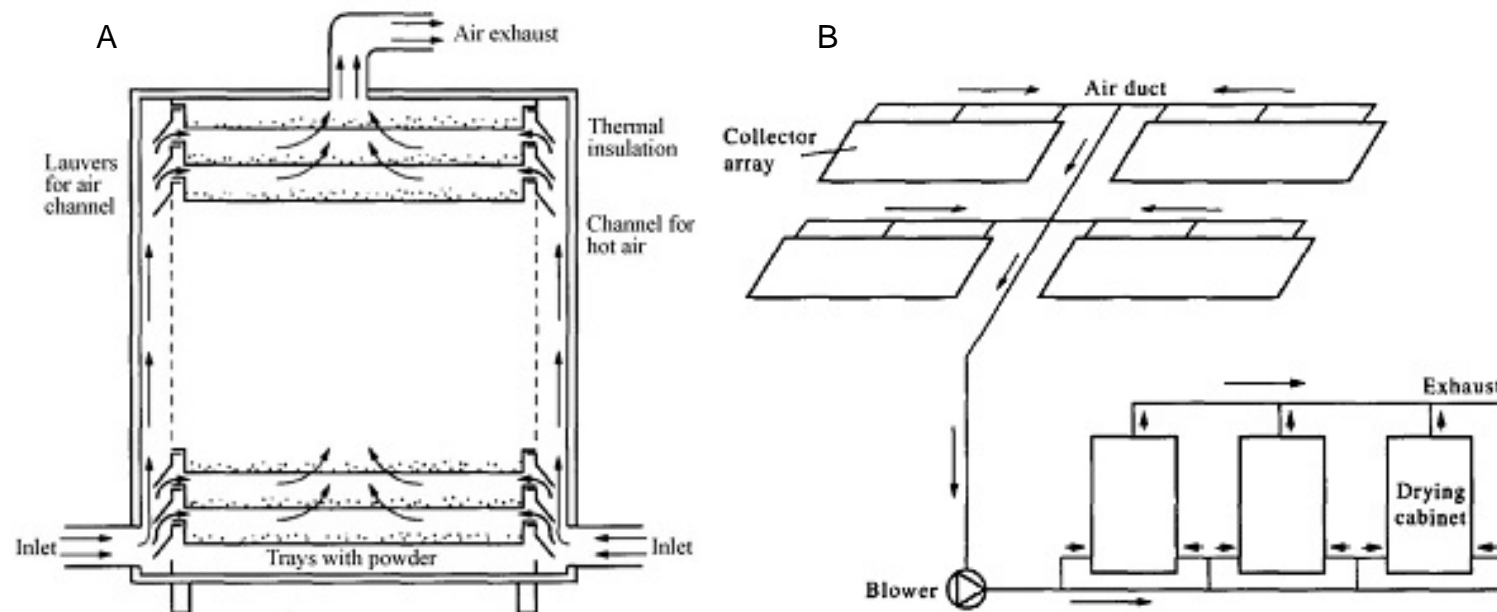


Figure 3-34. Large-scale cabinet dryer with heater array. A) Dryer schematic. B) Heater array. [Reprinted with permission from Pawar et al., 1995 (Page 1088-1090, Figure 2 and 5).]

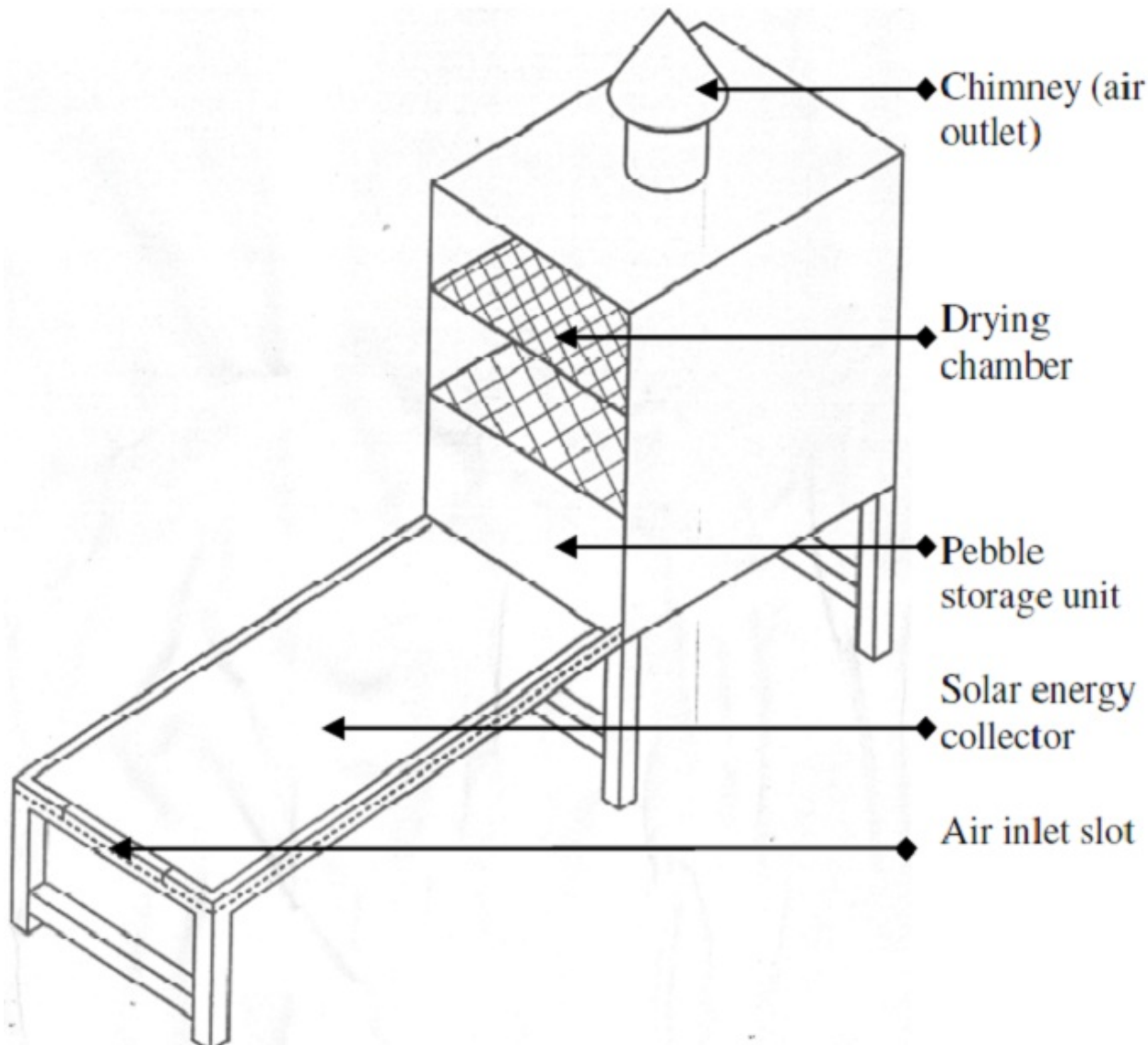


Figure 3-35. Cabinet dryer with thermal, gravel storage [Reprinted with permission from Adebayo and Irtwange, 2009 (Page 45, Figure 1).]

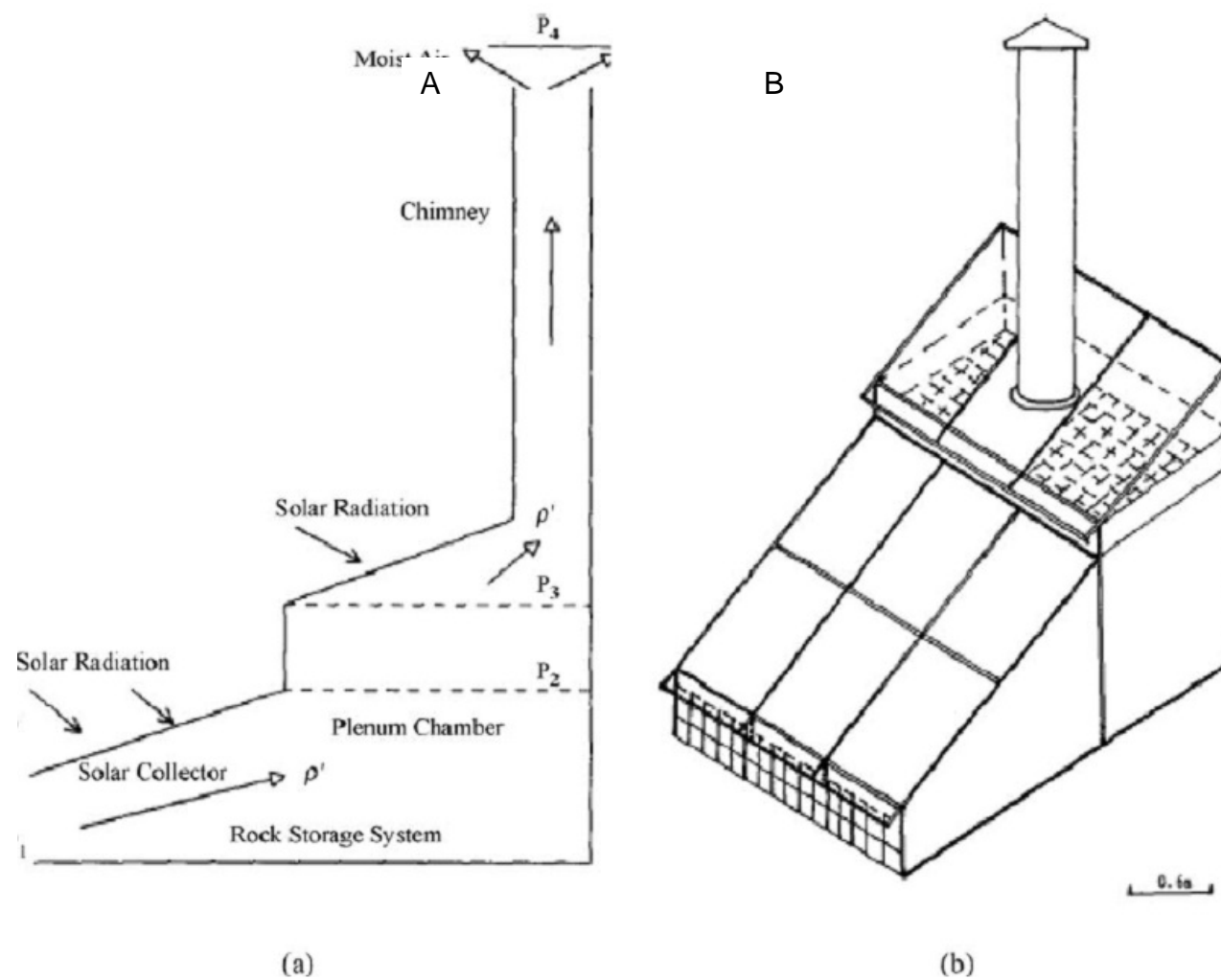


Figure 3-36. Cabinet dryer with thermal, rock storage. A) Mode of operation from side view. B) Schematic of dryer.  
[Reprinted with permission from Ayensu, 1997 (Page 123, Figure 2 and 3).]

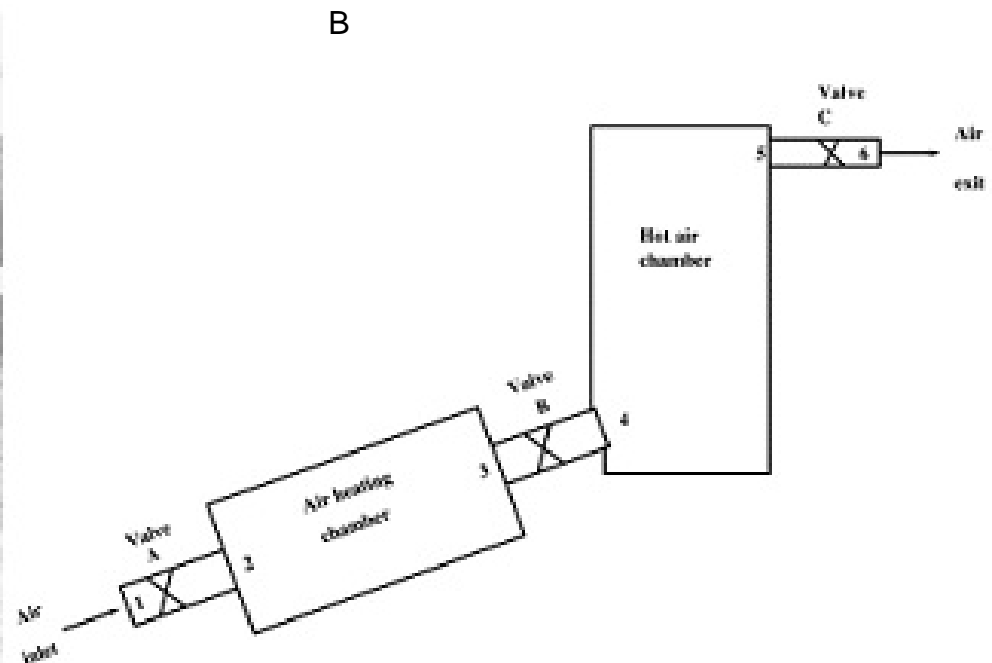
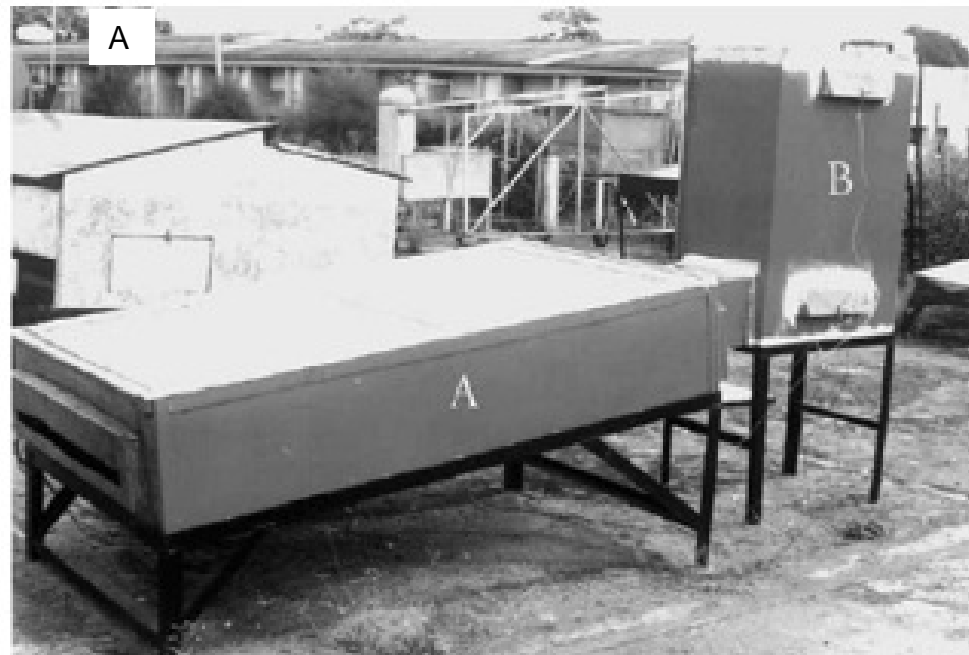


Figure 3-37. Cabinet dryer with thermal , PCM storage. A) Photograph of drying system. B) Schematic of drying system. [Reprinted with permission from Enibe, 1997 (Page 71-72, Figure 1 and 2).]

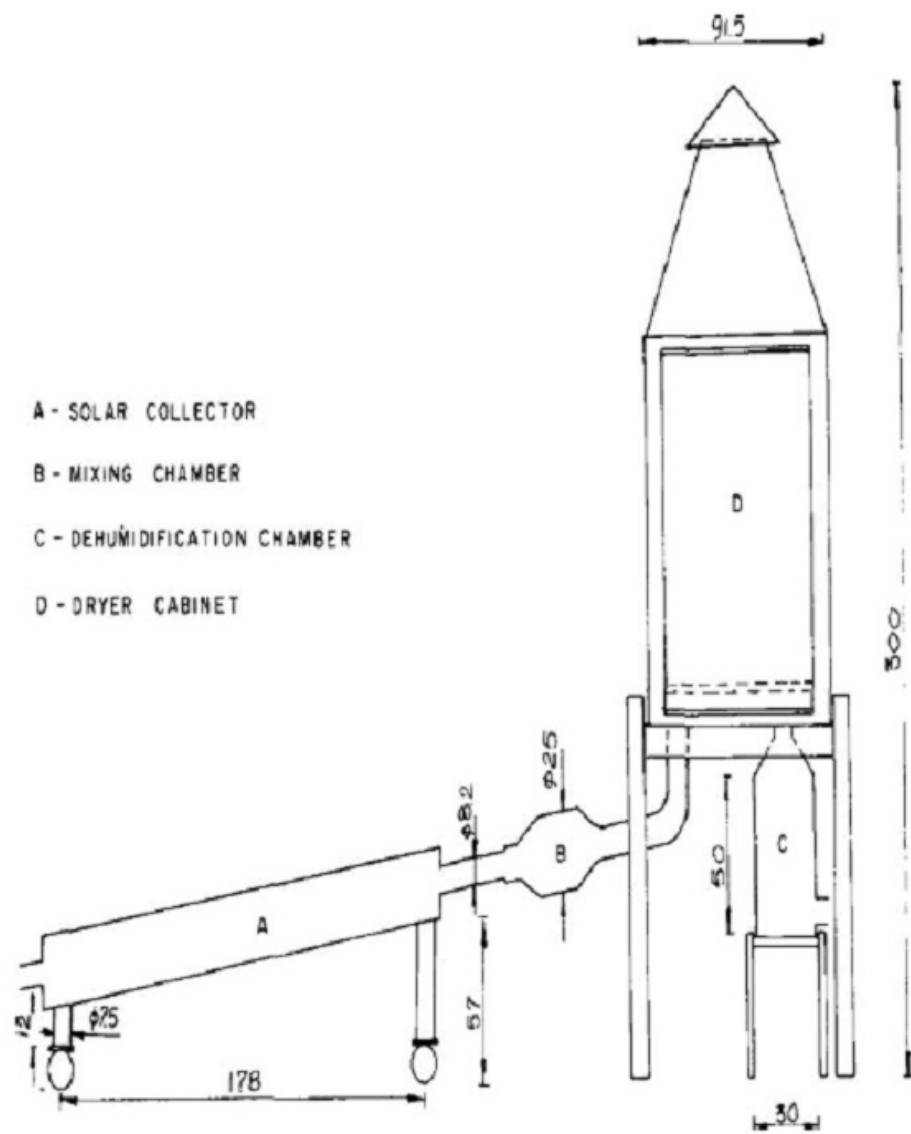


Figure 3-38. Cabinet dryer with thermal, silica gel storage [Reprinted with permission from Ezeike, 1986 (Page 3, Figure 1).]

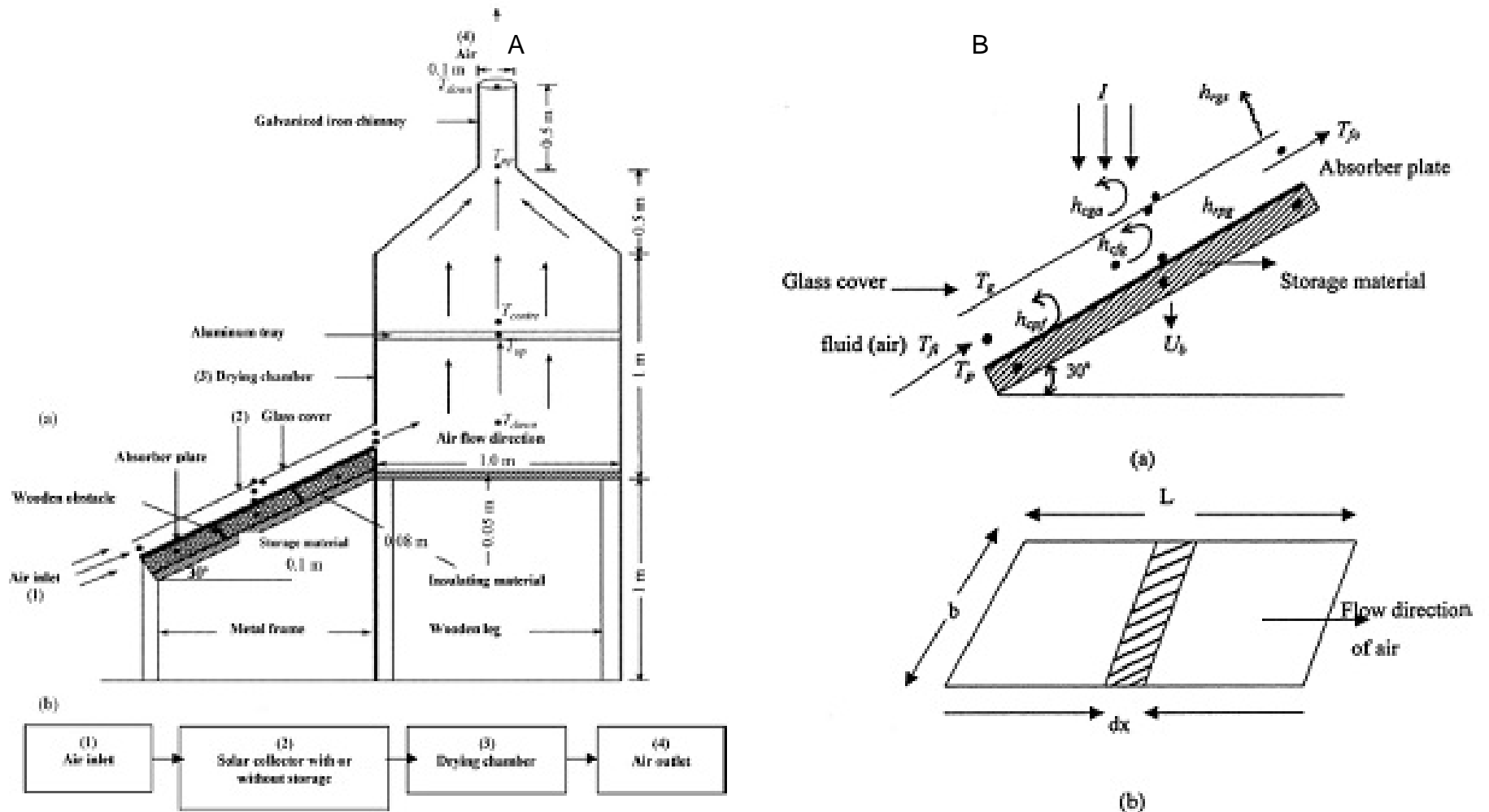
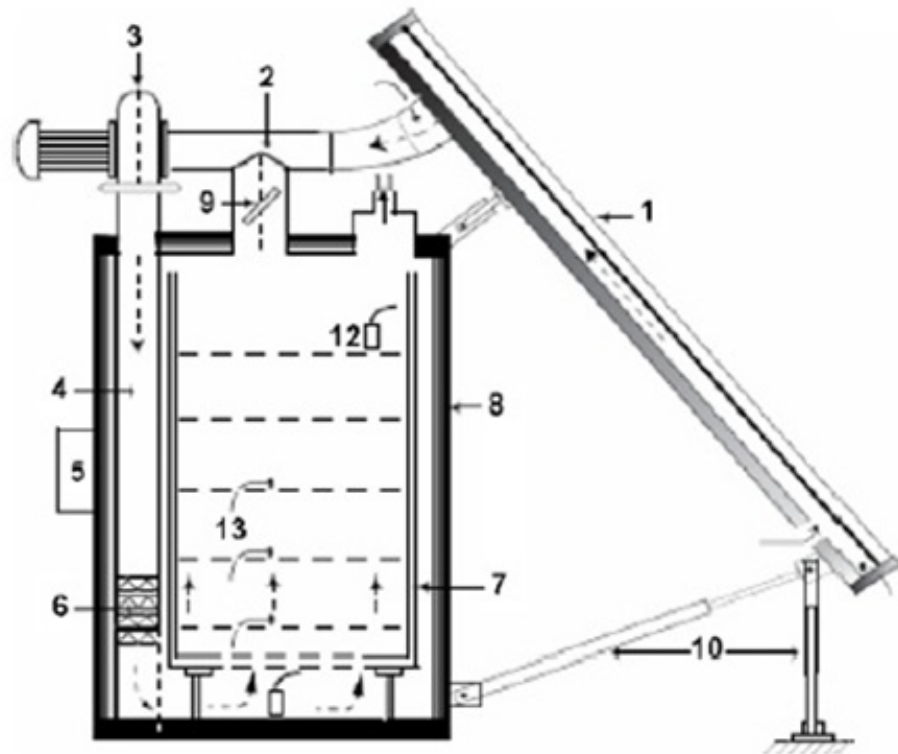


Figure 3-39. Cabinet dryer with interchangeable thermal, sand storage. A) Schematic of drying system. B) Cross section of solar collector. [Reprinted with permission from El-Sabaii et al., 2002 (Page 2254, Figure 1).]

A



B



- (1) solar collector; (2) circulation fan;(3) fan; (4) air flow direction; (5) control box; (6) auxiliary heating system; (7) shelves; (8) drying cabinet; (9) recycling air; (10) control foot; (11) exit of air; (12) humidity probes;(13) thermocouples

Figure 3-40. Cabinet dryer with auxiliary heater. A) Schematic. B) Photograph. [Reprinted with permission from Mohamed et al., 2008 (Page 942, Figure 1).]

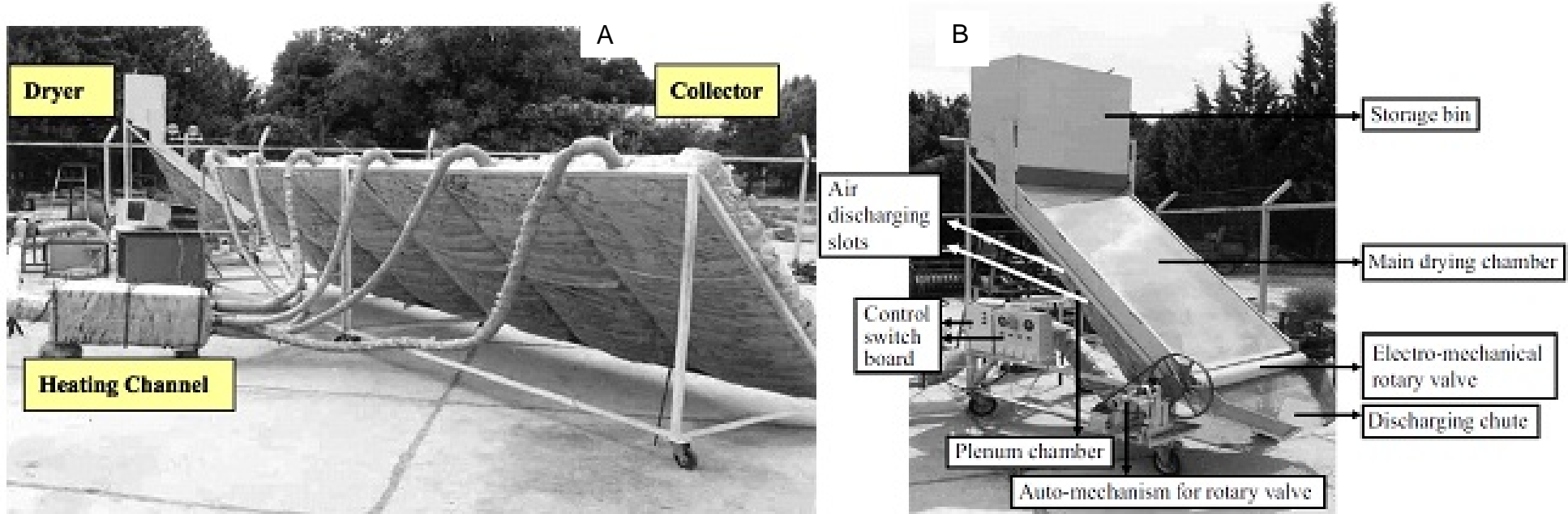


Figure 3-41. Cabinet dryer with auxiliary heating channel. A) Solar collector array. B) Drying system. [Reprinted with permission from Zomorodian, 2007 (Page 131-132, Figure 1 and 2).]

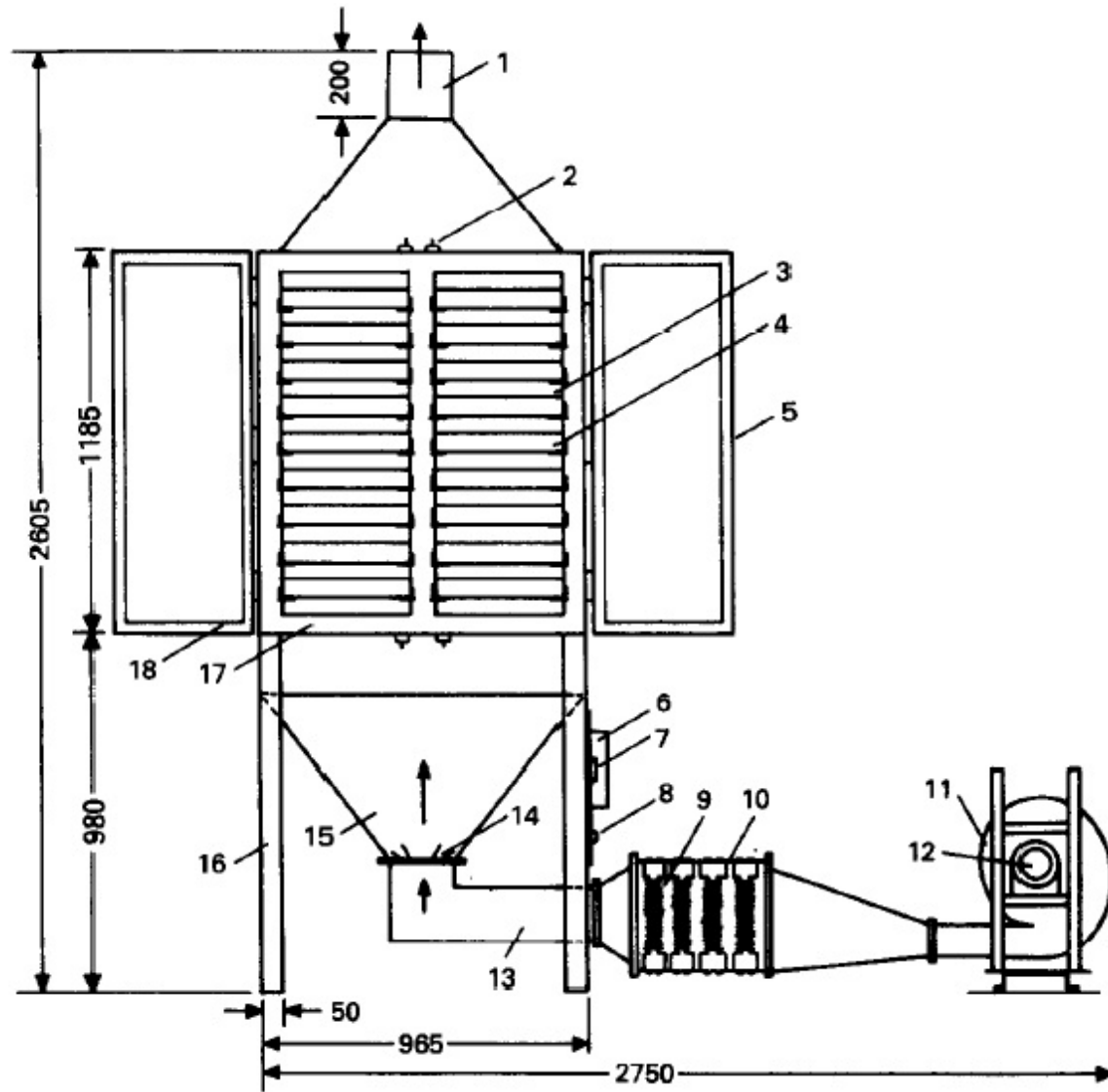


Figure 3-42. Cabinet dryer with heating elements, schematic [Reprinted with permission from Singh, 1994 (Page 21, Figure 1).]

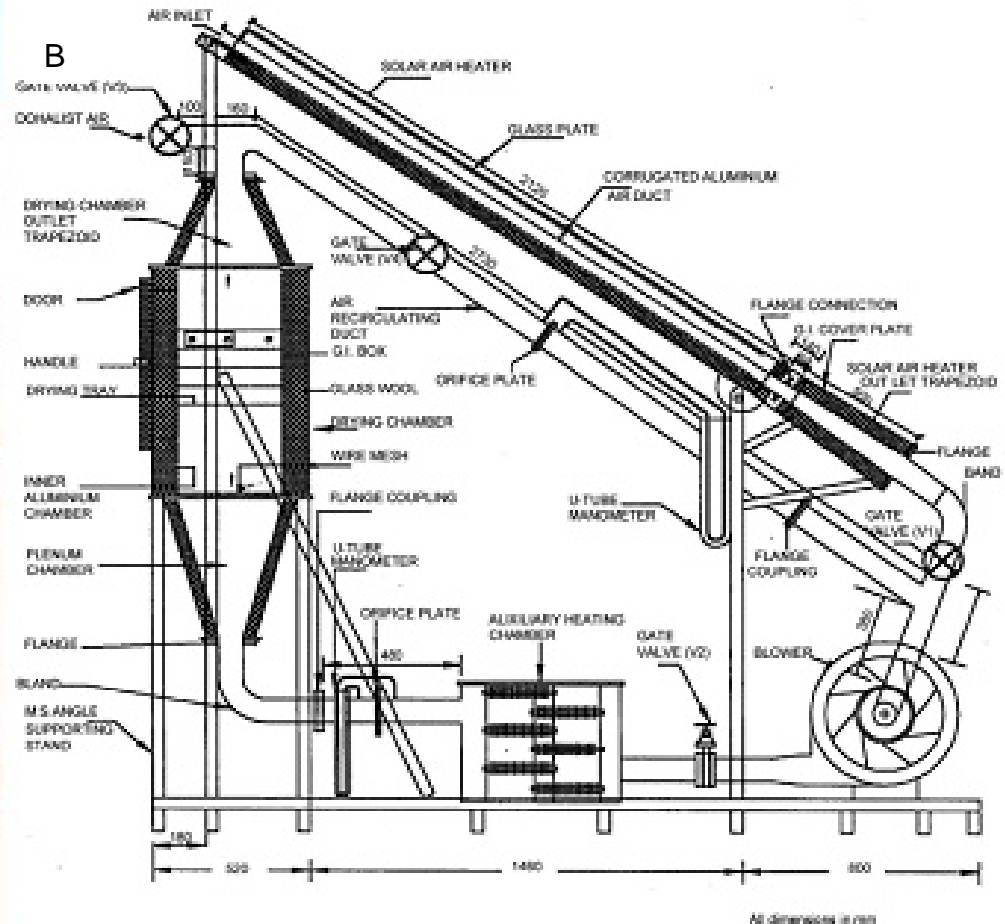


Figure 3-43. Cabinet dryer with exhaust recirculation. A) Pictorial. B) Schematic view. [Reprinted with permission from Sarsavadia, 2007 (Page 2532-2533, Figure 1 and 2).]

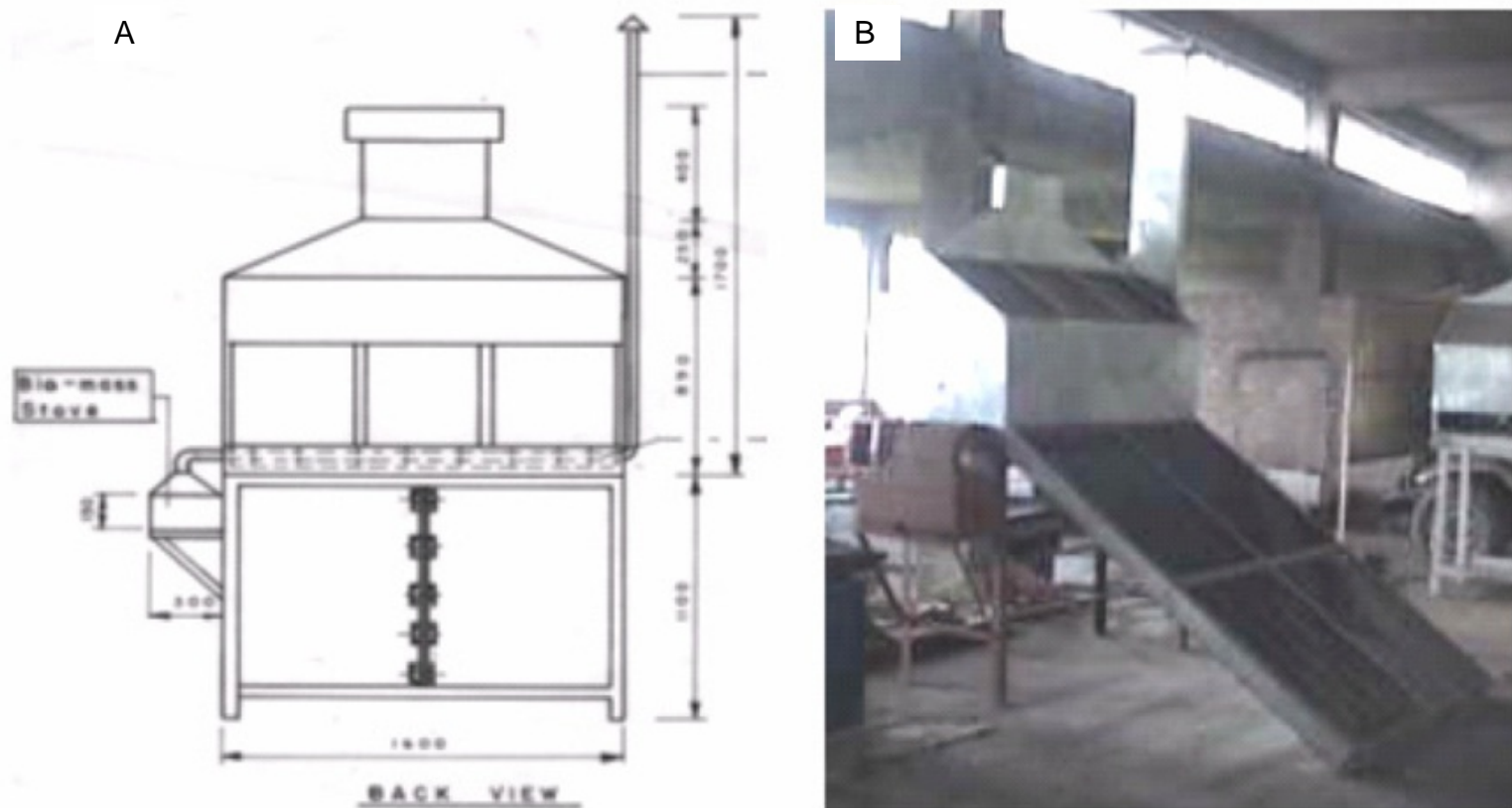


Figure 3-44. Indirect cabinet dryer with biomass burner. A) Schematic of dryer. B) Photograph of dryer. [Reprinted with permission from Bhandari et al., 2005 (Page 26-27, Figure 1 and 2).]

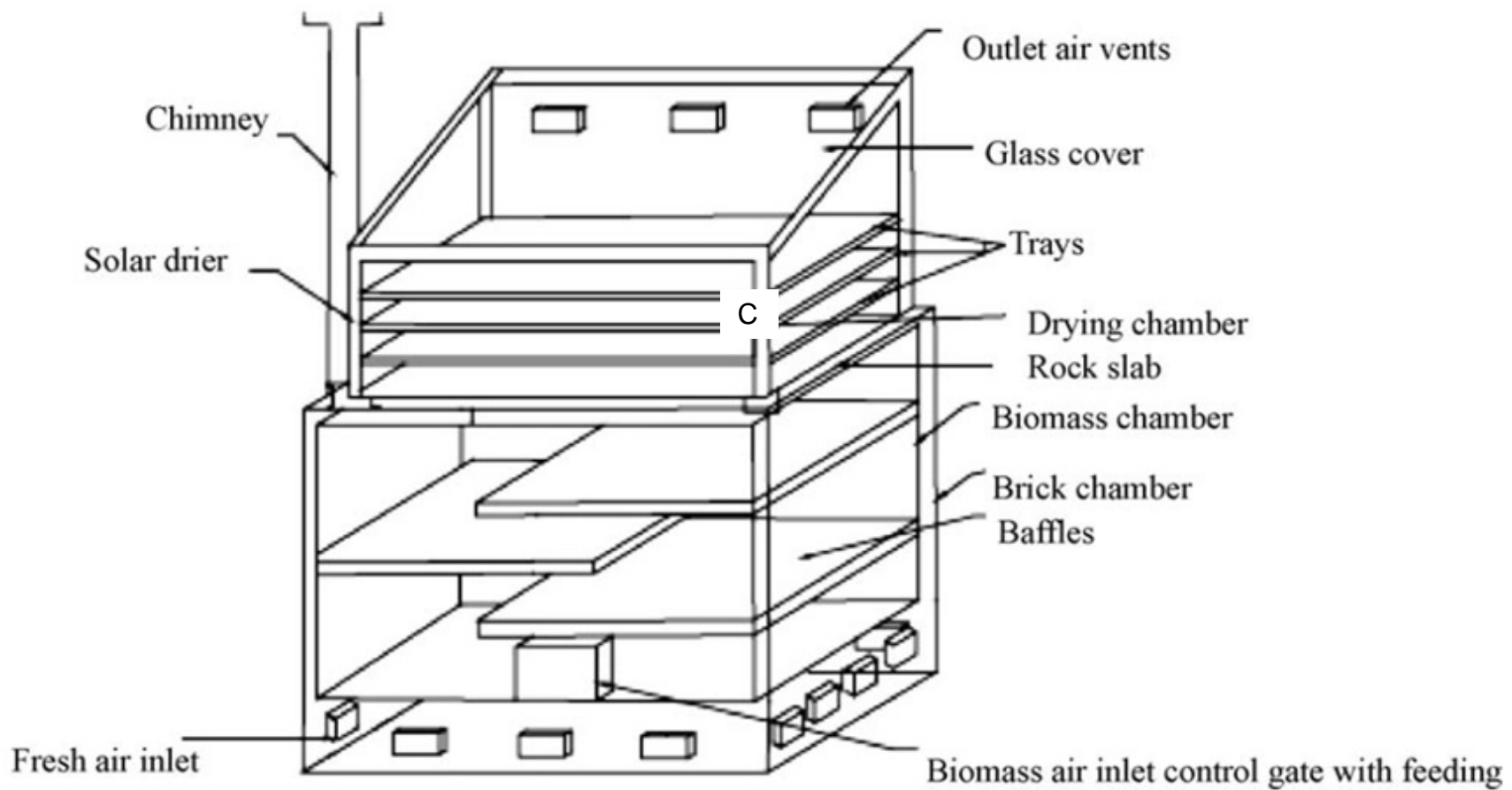


Figure 3-45. Direct cabinet dryer with biomass burner [Reprinted with permission from Prasad, 2006 (Page 498, Figure 1).]



B

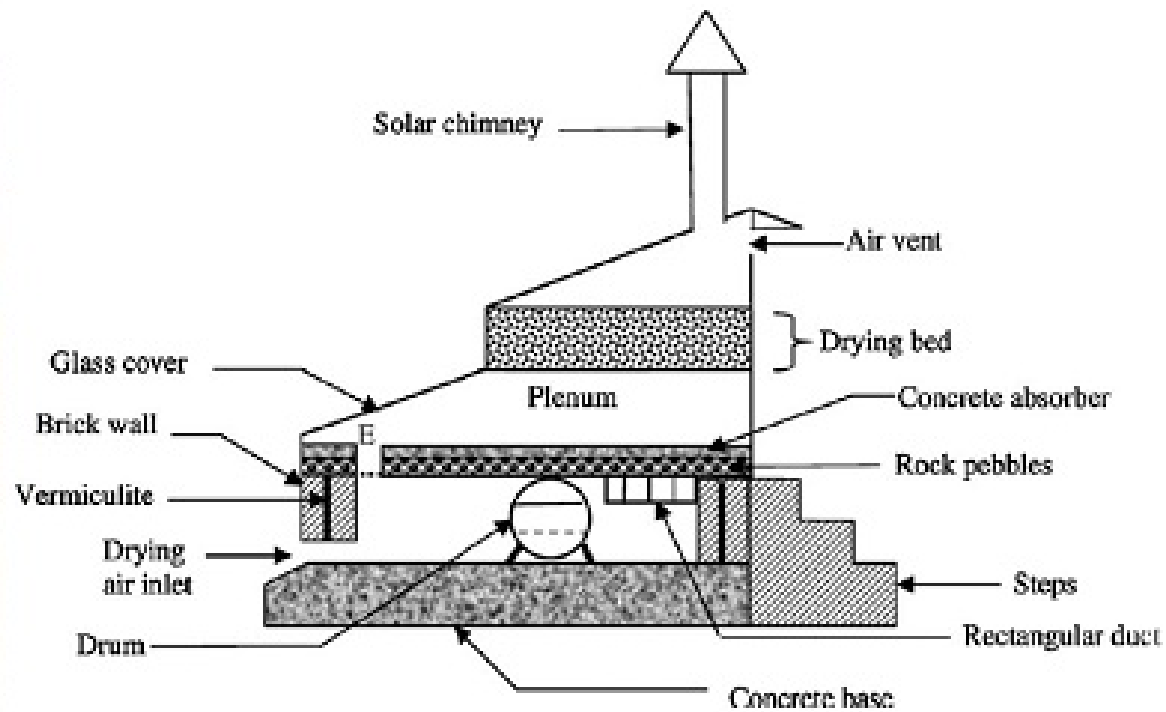


Figure 3-46. Cabinet dryer with biomass burner and thermal storage. A) Photograph of dryer. B) Schematic of dryer.  
[Reprinted with permission from Madhlopa and Ngwalo, 2007 (Page 451-453, Figure 1 and 3).]

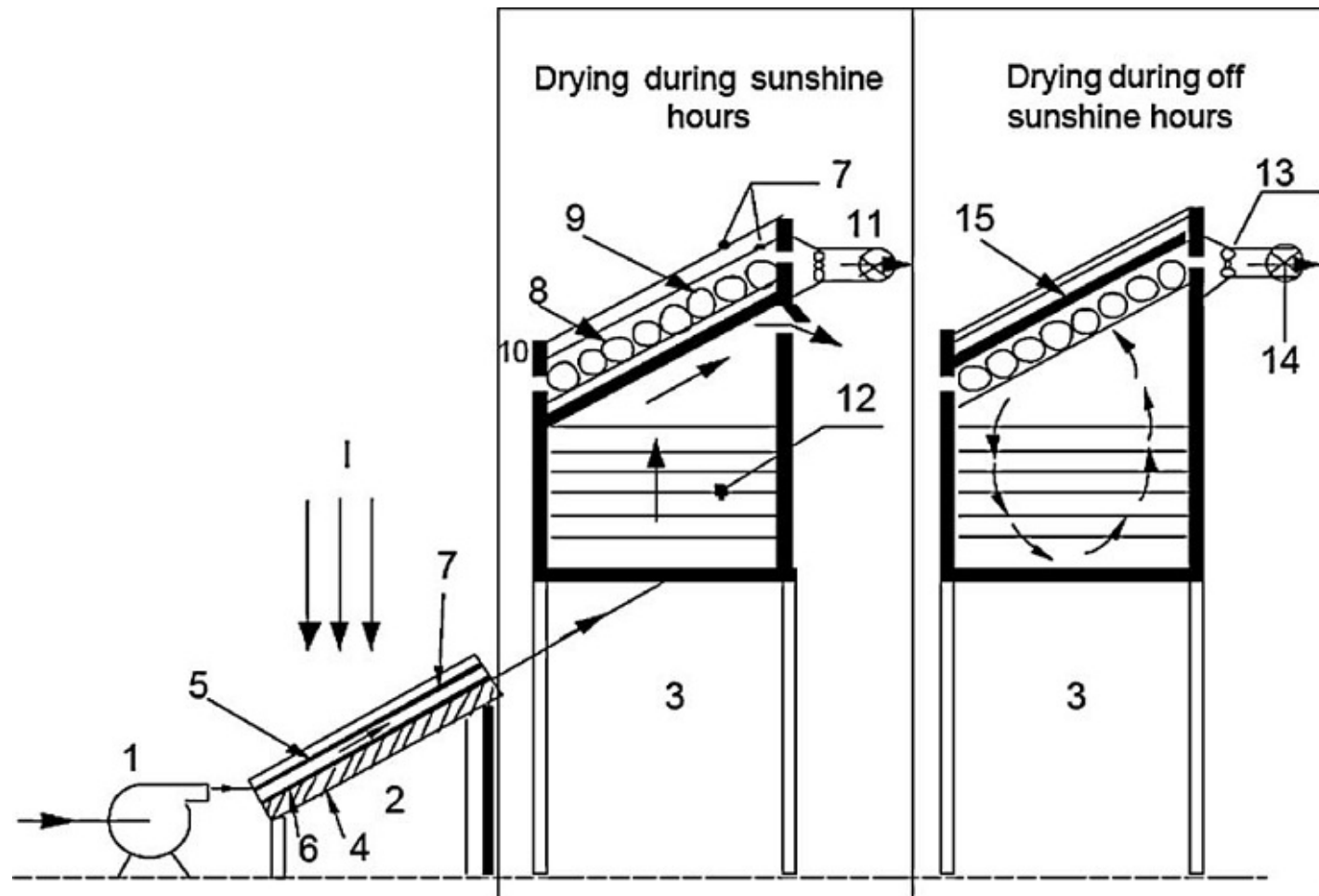


Figure 3-47. Forced cabinet dryer with integrated desiccant [Reprinted with permission from Shanmugam and Natarajan, 2006 (Page 1242, Figure 1).]

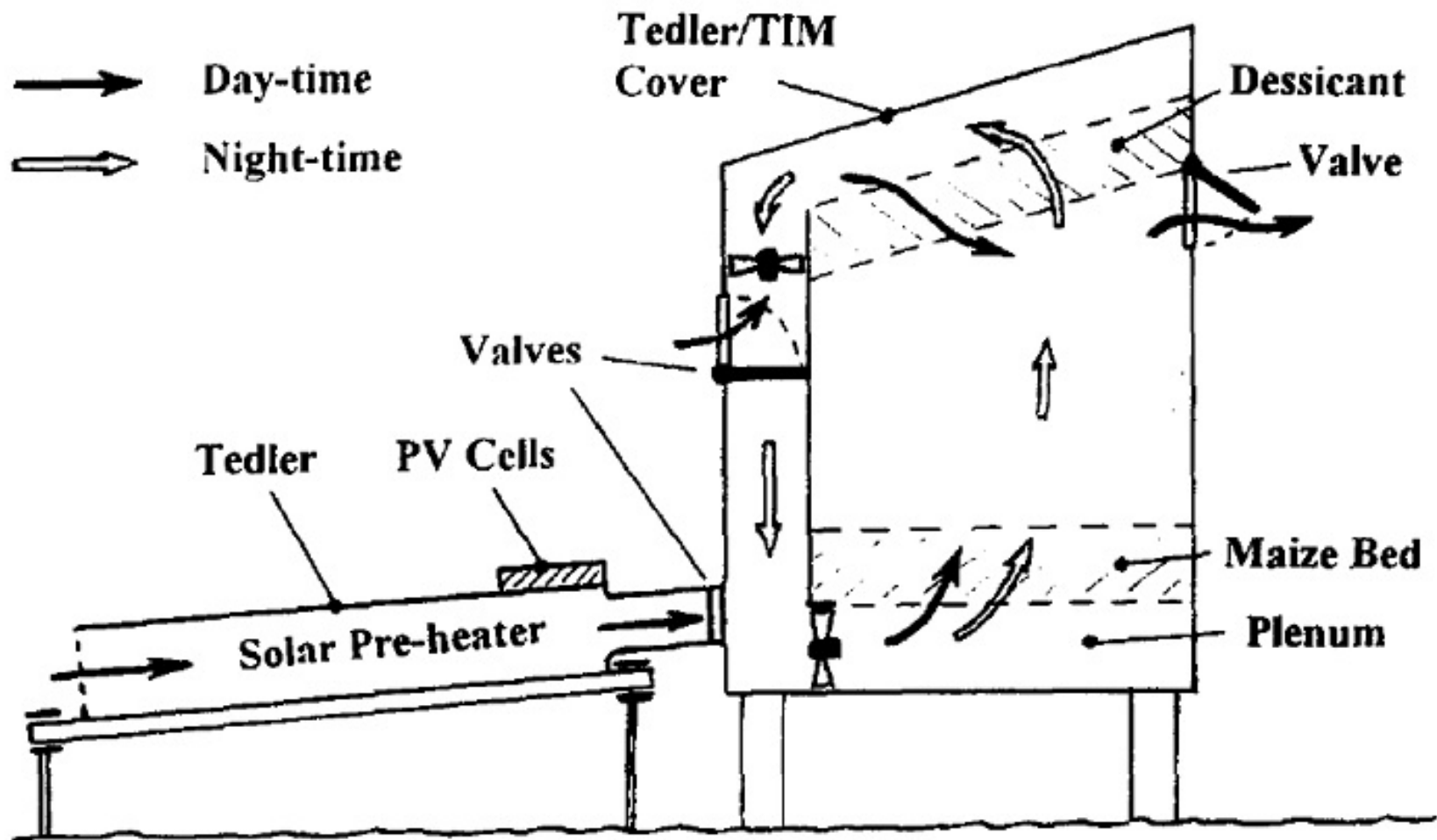


Figure 3-48. Cabinet dryer with integrated desiccant [Reprinted with permission from Thoruwa et al., 1996 (Page 688, Figure 1).]



B

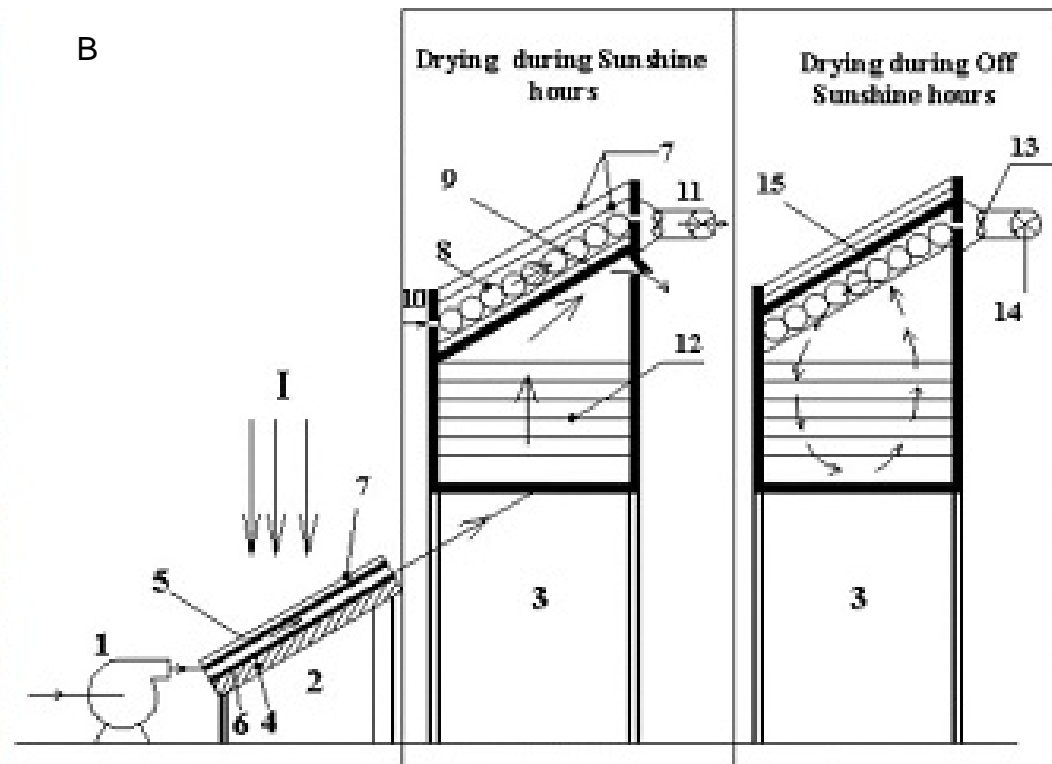


Figure 3-49. Cabinet dryer with integrated desiccant and mirror. A) Photograph of dryer. B) Schematic of dryer.  
[Reprinted with permission from Shanmugman and Natarajan, 2007 (Page 1545-1546, Figure 1 and 2).]

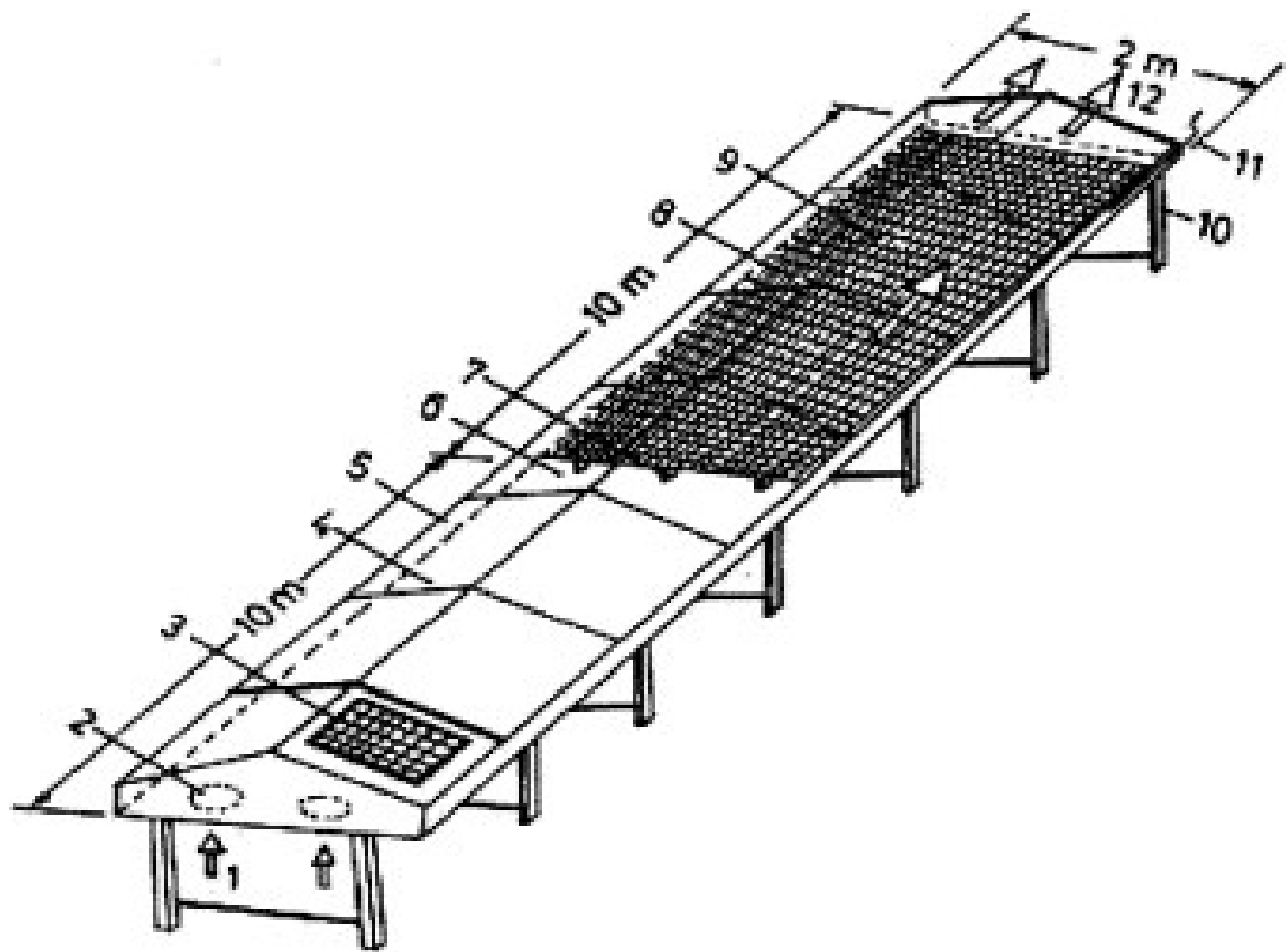


Figure 3-50. Simple tunnel dryer schematic [Reprinted with permission from Hossain and Bala, 2007 (Page 87, Figure 1).]

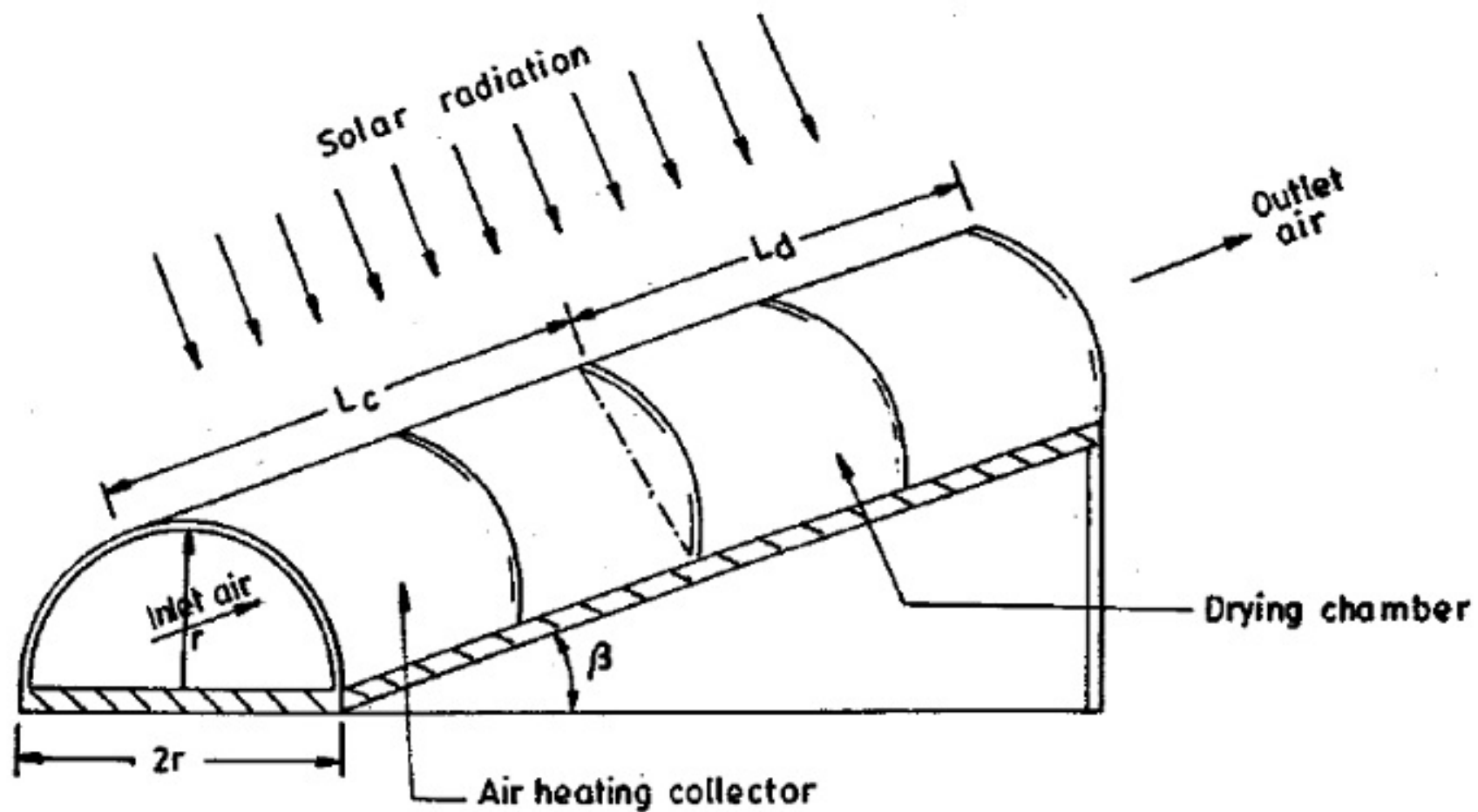


Figure 3-51. Tunnel dryer schematic [Reprinted with permission from Datta et al., 1998 (Page 1167, Figure 1).]

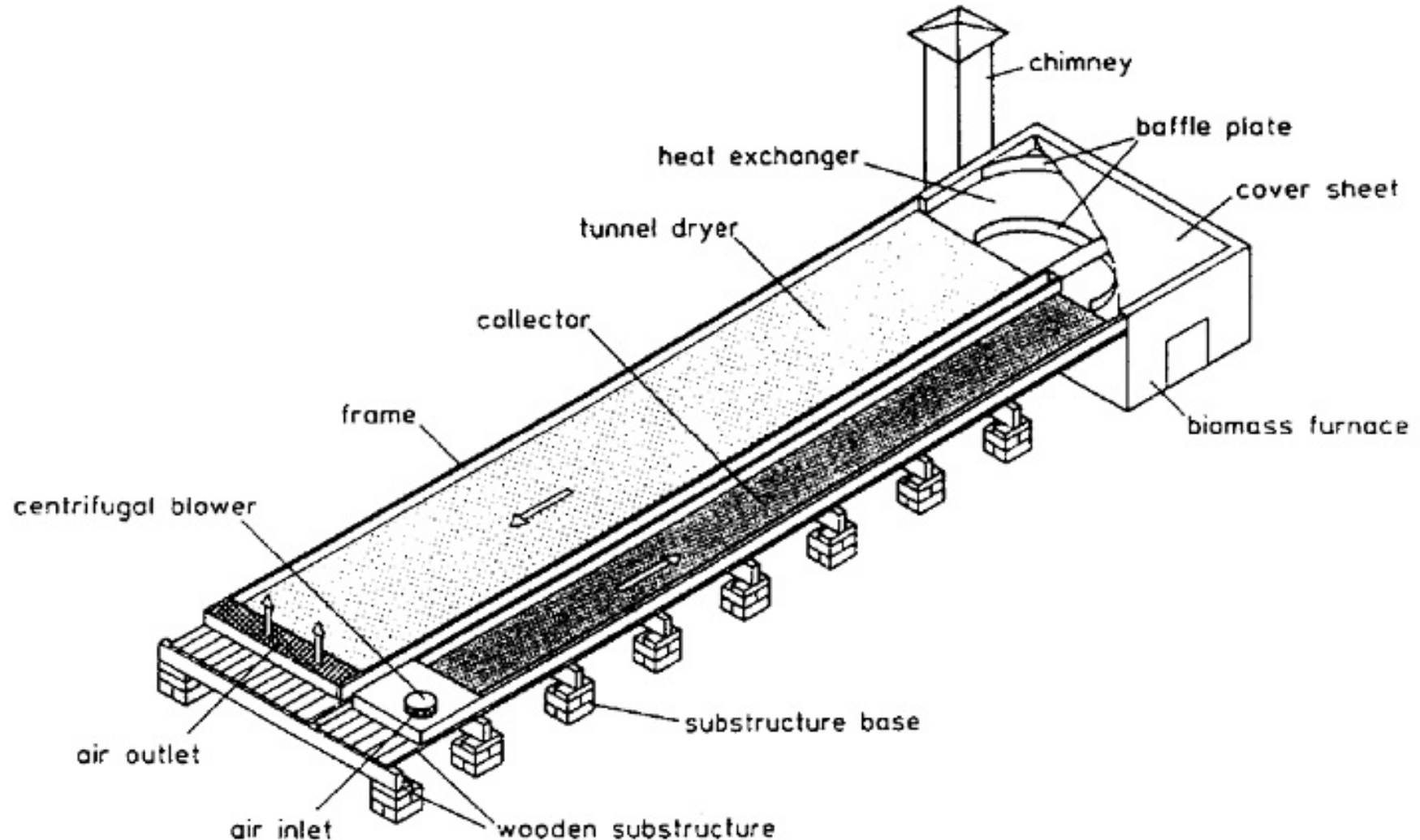


Figure 3-52. Tunnel dryer with biomass burner [Reprinted with permission from Amir et al., 1991 (Page 169, Figure 1).]

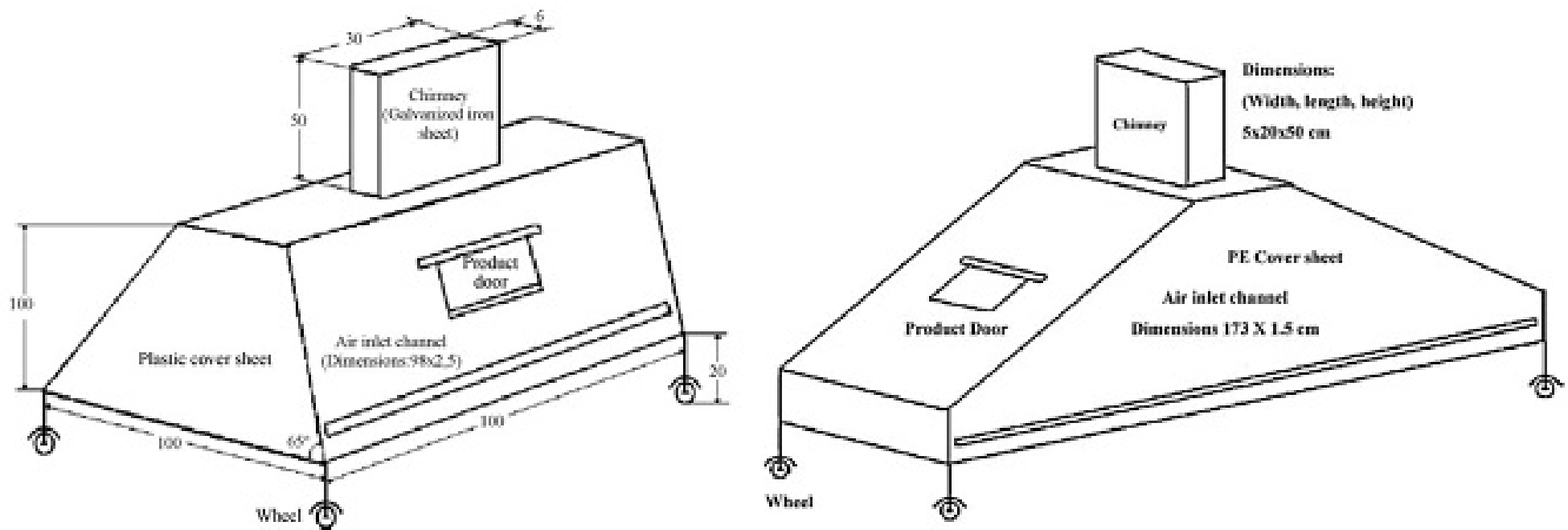
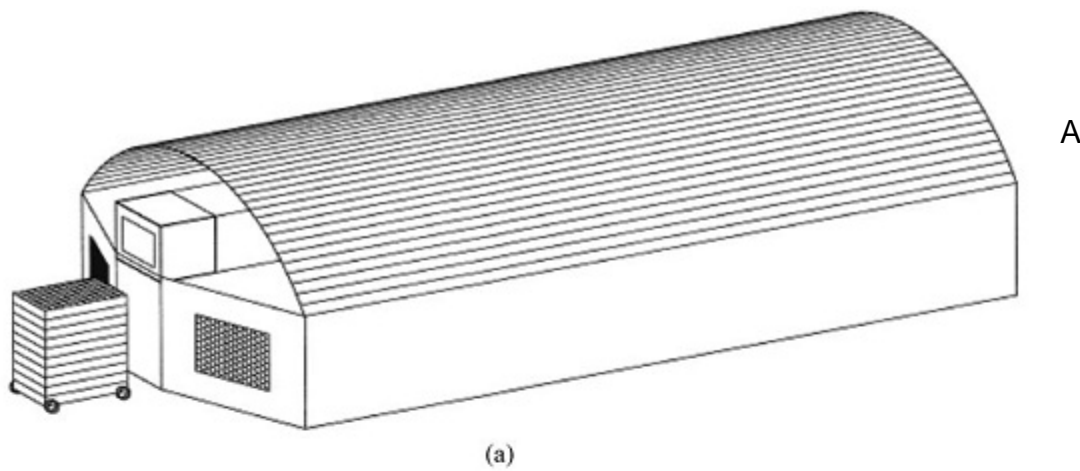
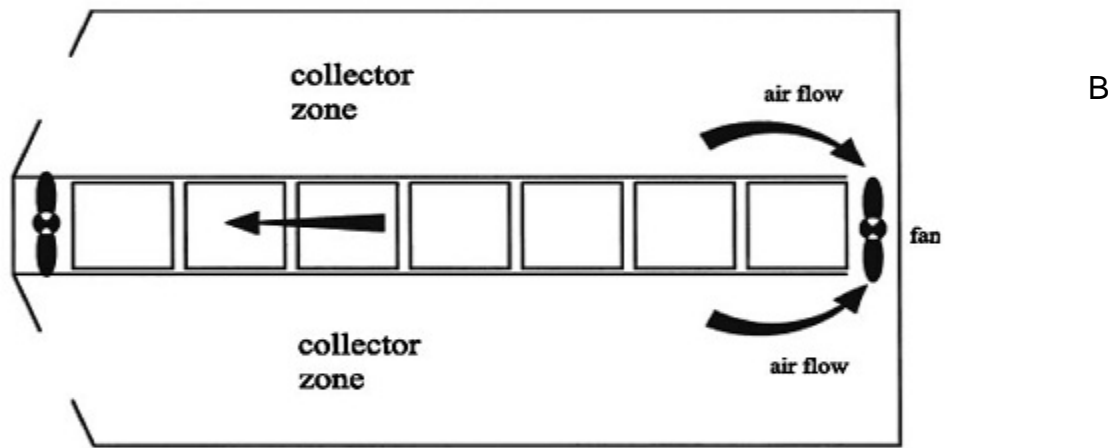


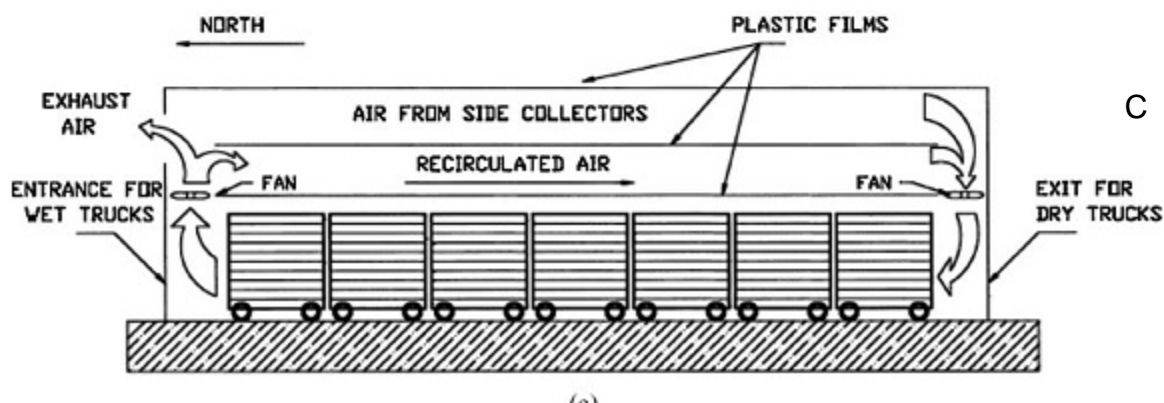
Figure 3-53. Greenhouse dryer schematics [Reprinted with permission from Koyuncu, 2006 (Page 1058-1059, Figure 2 and 4).]



(a)



(b)



(c)

Figure 3-54. Greenhouse dryer. A) Face view. B) Plant view. C) Side view. [Reprinted with permission from Condori et al., 2001 (Page 448-449, Figure 1-3).]

Table 3-3. Commonly used materials for solar dryers in developing countries

PART	OPTIONS
Support	Barrels, Concrete, Loam, Metal, Mortar, Slate, Stone
Frame	Concrete, Loam, Metal Sheet (aluminum, corrugated iron/steel, Galvanized Iron, Mild Steel), Slate, Stone, Wood (Plywood)
Insulation	Building Insulation, Coconut Fibers, Cork, Corrugated Cardboard, Expanded Polystyrene, Flax, Hay, Leaves, Palm Fibers, Mineral Wool (Rockwool, Glasswool), Polyurethane, Rice Husk, Sawdust, Straw, Styrofoam, Wood (Plywood), Wood Fiber, Wood Shavings
Glazing (cover)	Glass, FEP (Suntek), Plastic Sheets (LD-PE, LLD-PE, PTFE, PVC, PE-EVA, PMMA, Polycarbonate, Plexiglas), PET (Novolux), Polyester (Mylar), PVF (Tedlar)
Power Source	Diesel/Petroleum Generator, PV cells, Utility Power
Trays	Aluminum Frames, Bamboo Lattice, Fishing Nets, Mesh (Chicken Wire, Stainless Steel, Galvanized Steel, Nylon), Wire Netting
Absorber	Aluminum Sheet, Corrugated GI Sheet, Galvanized Iron/Steel, Black Polyester Fabric
Thermal Storage	Gravel, Phase Change Material (PCM), Rock, Sand, Silica Gel

Note: Materials listed here are summarized from previously reported studies as discussed in this literature review

Table 3-4. Optimum tilt angles for solar collectors

Latitude [degree]	Best collector tilt in:					
	June	Orientation	Sept./March	Orientation	December	Orientation
50 N	26.5	S	50	S	73.5	S
40 N	16.5	S	40	S	63.5	S
30 N	6.5	S	30	S	53.5	S
20 N	3.5	N	20	S	43.5	S
15 N	8.5	N	15	S	38.5	S
10 N	13.5	N	10	S	33.5	S
Equator = 0	23.5	N	0	-	23.5	S
10 S	33.5	N	10	N	13.5	S
15 S	38.5	N	15	N	8.5	S
20 S	43.5	N	20	N	3.5	S
30 S	53.5	N	30	N	6.5	N
40 S	63.5	N	40	N	16.5	N
50 S	73.5	N	50	N	26.5	N

Buchinger, J., & Weiss, W. (2002). Solar Drying. Austrian Development Cooperation: Institute for Sustainable Technologies.

## CHAPTER 4

### MATERIALS AND METHODS

#### **Task 1: Sorption Isotherm**

Since the production of dried mango slices is largely dependent on the properties of the fruit, analysis of fresh mango was necessary. Preliminary experiments were conducted with ripe mangoes to determine appropriate slice thickness and to develop a thermodynamic tool known as a sorption isotherm. The sorption isotherm helps to determine the extent of drying required to obtain a stable product and allows for estimation of moisture content if a sample's water activity is known.

Thus, work was undertaken in this task to gain an understanding of the moisture content and corresponding water activity of the fruit as both of these properties influence product quality, stability and susceptibility to microbial spoilage (Bolin, 1980). Moisture content is the quantity of water in the product while water activity is essentially the measure of the state of water in the mango. As such, water activity must be lowered indirectly by decreasing the moisture content through a drying process. Accomplishing this task helps to minimize microbial growth rates and prevent adverse chemical reactions from occurring within the fruit. The development of the sorption isotherm provided an understanding of the demand placed on the drying system to produce dried mango slices with increased shelf life and improved quality.

Commercially available, dried mango slices of an unknown variety were obtained from a local market, sealed to prevent significant moisture exchange with the environment, and analyzed shortly thereafter. The moisture content of these dried slices was determined by standard oven drying practices at 122°F (50°C) for 96 hours. The samples were weighed several times daily and equilibrium conditions were considered

to be reached after three consecutive readings were within  $\pm 1$ mg. Water activity was determined using an AquaLab water activity meter (Decagon Series 3) as this method provided a relatively quick assessment of the state of water. This information served as a reference and standard of the quality, moisture content and corresponding water activity that should be achieved in drying fresh mango with the solar dryer. Experiments were conducted in triplicate as recommended by Akanbi et al. (2006) and Falade et al. (2004).

Fresh, ripe mangoes of the Tommy Atkins variety were also obtained from a local market. The fruit was manually inspected to determine the general stage of ripeness. In this tactile assessment, the firmness of each fruit was manually inspected to ensure adequate ripeness. Fruit that was found to be exceptionally soft or overly firm were excluded from these experiments as the fruit was overly ripe or under-ripe, respectively.

The mangoes were first prepared to afford consistently uniform slices in an effort to determine adequate thickness for drying. Several unique thicknesses were evaluated to not only increase the drying rate, but also to improve product manageability, preserve compositional integrity and maintain sensory quality parameters such as texture and visual appearance. The thickness of dried mango slices has previously been evaluated and reported over a wide range from 3mm to 15mm, although inconsistent results are seen between studies (Brett et al., 1996; Madamba et al., 2002; Pott et al., 2005). Thus, slice thickness was measured with the use of a Vernier Caliper over this same range of values to identify an appropriate thickness for the mango slices. Drying of these variable

thickness slices was carried out with standard oven drying practices at 122°F (50°C) for 96 hours.

Fresh mango fruit was also washed, peeled and manually cut with sharp knives into thin, 3mm-thick slices. Care was taken in selecting fruit that was firm to the touch which indicated a sufficient stage and progression of ripeness while avoiding fruit that exhibited significantly soft flesh. Tactile assessments found that the softer fruits were indicative of overly ripe mango pulp which resulted in increased moisture content. In contrast, exceptionally firm fruit indicated under-ripe fruit with poor flavor and decreased moisture content. Thus, the data collected in this study was assumed to be reliable given the consistent methods of tactile assessment which provided a reasonable indication of the stage of ripeness. Furthermore, triplicate experiments contributed to the reliability of this data which was used to form the sorption isotherm. Evaluation of unripe or overly ripe fruit was avoided as the quality of these fruit was considered unsuitable and unnecessary for drying. Had experiments been conducted with these outlying ripeness fruits, the sorption isotherm would certainly be affected since the moisture content changed based on the stage of ripeness.

Isopiestic drying procedures, as detailed by Shyam et al. (2001), were used for measuring water activity by storing the sliced samples in closed chambers of known relative humidity. In this method, samples are allowed to reach equilibrium with the controlled atmosphere surrounding them, which is analogous to the water activity of the sample. Triplicate samples of fruit slices were placed on trays located in five distinct desiccating jars. Each jar contained a unique saturated salt solution that was selected to provide adequate screening of air relative humidity. The salts in each jar were dried and

calibrated prior to use. Equilibrium moisture contents were determined using MgCl<sub>2</sub> (32.8%), NaBr (57.6%), NaCl (75.3%), and KBr (81.8%). Several drops of formalin were added to cotton pads which were placed in each desiccator to prevent mold growth, particularly at high  $a_w$  as recommended by Falade and Aworh (2004).

The effect of ambient temperature variability on sorption isotherms is considered insignificant in most engineering work according to Henderson and Perry (1976). Therefore, the desiccators were left exposed to the ambient temperature of the lab which was approximately 71°F (22°C) for the duration of the experiment, despite the limited control over small temperature fluctuations. Potential shifts in the sorption isotherm resulting from these temperature deviations were considered negligible for the purpose of designing this solar dryer.

Triplet samples were also left exposed to and evaluated at the relative humidity of the lab. The temperature and relative humidity of the lab were monitored and recorded with an Onset® Temperature and Relative Humidity Data Logger (HOBO® H08-003-02) on an hourly basis. The average relative humidity of the lab was found to be 51% over the course of the experiment. Each sample was weighed once daily and equilibrium conditions were considered to be reached when three consecutive measurements gave identical readings within  $\pm 1\text{mg}$  as suggested by Mohamed et al. (2005). After reaching equilibrium conditions, samples were removed from the jars to undergo standard oven drying procedures for 96 hours at 122°F (50°C). The remaining moisture was removed from the fruit through this process which allowed for the determination of equilibrium moisture content. The results of this experiment were used

to form a graphical plot showing the relationship between moisture content and water activity.

The dry matter of analogous fresh fruit was concurrently obtained by oven drying at 122°F (50°C) until achieving constant weight after three consecutive measurements within  $\pm 1\text{mg}$ . This process allowed for the determination of the initial moisture content of the fresh mangoes. These experiments were also performed in triplicate.

Experimentally derived equilibrium moisture data were then fitted to both the BET and GAB sorption isotherm models that were detailed earlier in the literature review and are expressed in Equation 4-1 and Equation 4-2 respectively, as both have been reported to be suitable for high sugar content fruits (Falade & Aworh, 2004). While no isotherm model reported in literature is valid over the entire water activity range of 0 to 1, the GAB model is widely used with an approximate range of 0.10 up to 0.90, while the BET isotherm generally holds from 0.05 to 0.45 (Shyam et al., 2001). The parameters of the models were calculated using a developer's software package (Water Analyzer Series, Version 97.4) and the best fit model was determined using the least squares method.

$$M_{EQ} = \frac{a_w AB}{(1-a_w)(1+a_w(B-1))} \quad (4-1)$$

$$M_{EQ} = \frac{a_w ABC}{(1-Ca_w)(1-Ca_w+BCa_w)} \quad (4-2)$$

In Equation 4-1 and Equation 4-2, A is the monolayer moisture ( $M_0$ ), B is a surface heat constant, and C is a constant. Thus, the BET model is essentially a special case of the GAB model where the constant, C, is equal to a value of one.

The development of this signature physical property of the mangoes served to specify the moisture content needed in order to reach the target water activity of the

commercially-available, dried-mango reference. Using this information, the sorption isotherm helped determine the amount of moisture needed to be removed in the drying process. Thus, this tool served as an important parameter in determining the adequate and appropriate sizing and design of the solar drying system.

### **Task 2: Dryer Design**

The results of these experiments on mango fruit were used to aid in the design of a solar dryer based on procedures detailed in previously reported literature. Design criteria were identified and considered for implementation only after conducting an extensive literature review of solar dryers. The general design of this solar dryer was considered to be a natural-convection solar dryer with a thermal rock bed as described earlier in the literature review.

Specific design parameters were determined based on a series of engineering calculations that were modified from a procedure proposed by Ampratwum (1998) for natural-convection solar dryers. This adapted model takes into account a variety of factors including the physical properties of mangoes, the characteristics of previously reported solar systems in literature, Haitian environmental conditions, and the local production capabilities of small Haitian villages. These properties served as input for the proposed model and provided a preliminary standard for which the actual design was expected to meet and/or exceed in terms of efficiency. Specific characteristics of the solar dryer were then determined from the mathematical calculations and schematics were developed based on this information.

Fabrication of the solar dryer was then carried out based on the schematics. Consideration was given to construction materials that were inexpensive and potentially

available in developing communities. Of course, alternative materials are expected to replace the current design depending on material availability in specific Haitian communities. Experiments were then conducted to evaluate the performance of the solar dryer. These assessments were performed with and without loading of produce to evaluate the operation and efficiency of the dryer.

### **Design Features and Considerations**

The proposed dryer features an indirect, solar heating component and a separate drying chamber which houses five trays of product as shown in Figure 4-1. The justification for having two distinct components is that the product is spared from issues associated with direct exposure to solar radiation. Under such conditions, solar radiation is known to increase susceptibility to discoloration and case-hardening which results in declined product quality. While there is an extensive list of solar absorbers in the literature, this system was designed with simple and affordable fabrication practices in mind. Since building materials and skilled labor are often limited in developing countries, attempts were made to keep this design from becoming overly sophisticated.

### **Mathematical Procedure**

Specific design criteria were determined from engineering calculations after considering the general design of the dryer. Physical characteristics of the mango fruit were employed in these calculations as the design needed to meet the demands placed on it by the product. Weather conditions were also taken into account since the natural-convection principle employed in this solar dryer depends completely on weather for the creation of a driving force. Assumptions were also made in estimating feasible harvesting rates of small villages.

The actual performance of the newly developed dryer was expected to meet and/or exceed the model-estimated efficiency as the mathematical approach was considered to be rather conservative. A summary of the parameters considered in this analytical procedure are summarized in Table 4-1.

### **Mango Properties**

As detailed earlier in the report, the moisture content of mangoes was determined experimentally by gravimetric oven analysis. The initial moisture content of firm, ripe mangoes was found to range between 72.4% (wb) and 83.8% (wb). Thus, an average moisture content of 78.1% (wb) for fresh mangoes was assumed for this mathematical procedure. In contrast, the moisture content required in the final dried fruit was 11.9% (wb) as determined from measurements taken on commercially-available dried mangoes.

A range of thicknesses was evaluated with thinner slices (7mm or less) exhibiting both cracking and poor manageability throughout the drying process. This degraded product quality resulted in a loss of compositional integrity as the mango flesh was torn, and in some cases, dried product was too thin for handling and recovery. Thus, a thicker slice of 10mm was accepted as a reasonable thickness in terms of maintaining adequate drying rates and improving both the quality and manageability of the dried slices.

A single mango weighs approximately 1 lb (0.45 kg) and this assertion was confirmed by weighing whole, fresh mangoes. The maximum allowable temperature for high sugar content fruit was taken as 150°F (65.56°C) according to Sodha et al. (1987) and was substantiated by visual inspection of slices dried at several temperatures.

Temperatures in excess of 150°F (65.6°C) resulted in significant brown discoloration of the mango flesh.

Local production capabilities of Haitian villages were also considered such as the duration of the harvesting period. A reasonable estimate of the potential harvesting rate was also made. A five month harvesting season (Castañeda et al., 2011) was accounted for with a value of 30 fruit considered to be harvested, prepared and dried in each batch. This was assumed to be a reasonable estimate for small communities based on the use of a single solar drying system. A two-day period is assumed here as high moisture content fruit generally require extended time in excess of a single day to dry (Al-Juamily et al., 2007; Bhandari et al., 2008; Chen et al., 2007; Datta et al., 1998; Prasad et al., 2006). Extension of the drying time any further than this two day assumption was avoided as a slower drying process could allow for increased growth of microorganisms. The identification of these parameters allowed for the determination of a suitable loading density as well as other physical specifications of the dryer which were resolved by means of mathematical and thermodynamic calculations.

### **Dryer Parameters**

The loading density or batch size of the dryer was assumed by the weight difference between whole and sliced mango fruit. The results of this analysis found that approximately 19 lbs (8.62 kg) of whole, ripe mango yielded only 10 lbs (4.5kg) of sliced fruit. This difference in weight can be attributed to the large seed in each mango as well as the stem and peel that accounts for over 47% of the total weight. As a result, it was estimated that about 26.3 lb (11.9 kg) of freshly-sliced mangoes could be processed

with this system based on the assumption that 30 whole, ripe cull mangoes could be easily available from a single day's harvest.

It was also assumed in this model that the minimal temperatures ranging between 131-140°F (55-60°C) that are needed for drying high sugar-content fruit, as recorded by Sodha et al. (1987), could be attained by the proposed dryer. While temperatures in excess of 149°F (65°C) are shown to be effective in the initial stages of drying, Leon et al. (2002) recommends that this value be lowered later in drying to avoid quality degradation. For these reasons, a temperature of 140°F (60°C) was considered to be a reasonable and conservative estimate for this model. This assumption was further validated by inspection of the preserved quality of oven-dried slices at this temperature as well as numerous studies which demonstrate temperature gains in solar dryers of at least 54°F (30°C) above ambient conditions (Amir et al., 1991; Enebe & Ezekoye, 2006; Mumba, 1996; Mwithiga & Kigo, 2006; Prasad et al., 2006; Singh et al., 2004; Sreekumar et al., 2008; Zomorodian et al., 2007).

An estimate of 26% was also assumed for the collector efficiency which is an even more conservative estimate than the Ampratwum (1998) model. This proposed value is based on the lower limit of efficiency as reported in a review conducted by Jairaj et al. (2009). However, the actual efficiency of the collector was expected to exceed this conservative estimate.

The cross-sectional area of the drying chamber directly corresponds to the area of each tray. Although Buchinger and Weiss (2002) proposed a cross-sectional area with 10kg of product for every square meter of tray, a more conservative spatial arrangement of one-third of this estimate was assumed for application in the

mathematical procedure. The height of the thermal rock storage was determined by dividing the minimal volume of  $0.15 \text{ m}^3$ , as recommended by Goswami (1986) and detailed by Adebayo and Irtwange (2009), by the cross-sectional area. Furthermore, a vertical distance of three inches between the trays was maintained to allow clearance between the loaded trays and to permit easy access to each tray.

An overall design height was set as 6.56 ft (2 meters) as this height was expected to create enough density gradient to establish airflow within the dryer without creating a larger, unmanageable system. Of course, greater heights would increase this gradient, but this comes at the expense of additional material, labor and maintenance associated with a taller system. The number of trays also serves as an input to these mathematical calculations and as such, a total of five trays were proposed for this dryer in order to increase the product throughput. The vertical orientation of successive trays was expected to increase the pressure gradient as vertical height was extended accordingly. Establishing greater vertical height was thus given more consideration than simply enlarging the tray area to hold more product. It is assumed that negligible pressure resistance would result from the inhibited air flow through the trays.

## **Weather Conditions**

Environmental conditions such as ambient temperature, relative humidity, solar radiation, and solar inclination were also determined through climatic data or reasonable assumptions were made since these properties directly impact the sizing and design characteristics of the system (Enebe & Ezekoye, 2006). These data allowed for the determination of physical parameters of the dryer such as collector area, collector tilt and tray area among other attributes. This information was critical as the natural-

convection process depends completely on thermodynamic air properties which are established by weather conditions. While data for specific rural locations within Haiti were unavailable, weather data were taken primarily from the capital, Port-au-Prince for the purpose of this study.

The average monthly temperature of Port-au-Prince, Haiti was gathered from AccuWeather© Statistical Weather Data for the harvesting period spanning five months from April to August (Castañeda et al., 2011). The average daily temperature was found to be 82.9°F (28.3°C) and the density of air was referenced at this temperature. Similarly, the average monthly relative humidity was found to be 48%, the average monthly sunlight hours per day was determined as 8.71 hours, and the average monthly wind speed was found to be  $3\text{m}\cdot\text{s}^{-1}$ . The average, annual solar radiation level of Port-Au-Prince, Haiti was adopted from the Solar and Wind Energy Resource Assessment program (SWERA, Direct Normal Solar Radiation) as  $6 \text{ kWh}\cdot\text{m}^{-2}/\text{day}$  while the solar inclination ( $\beta$ ) of Saut-d'Eau, Haiti was taken as  $18^\circ 49' 0''$  N.

### **Engineering and Thermodynamic Calculations**

The initial humidity ratio and enthalpy values were determined with psychrometrics from ambient air temperature and the ambient relative humidity. The final enthalpy was then determined from the initial humidity ratio and the maximum allowable temperature. Equilibrium relative humidity was determined from the final moisture content using the isotherm model developed from isopiestic drying techniques of fresh mango slices. The final humidity ratio was determined from psychrometrics using the final relative humidity and enthalpy.

The mass of water to be evaporated,  $m_w$ , was determined by Equation 4-3 (Ampratwum, 1998).

$$m_w = \frac{m_p (M_i - M_f)}{100 - M_f} \quad (4-3)$$

The variable  $m_p$  is the loading density of sliced fruit,  $M_i$  is the initial moisture content, and  $M_f$  is the final moisture content. It is important to note that  $m_p$  refers to the mass of the sliced fruit which is significantly lower than the weight of whole fruit. This reduction in mass is expected to be a result of deseeding and peeling of the fruit.

The average drying rate,  $m_{dr}$ , was determined by Equation 4-4.

$$m_{dr} = \frac{m_w}{t_d} \quad (4-4)$$

The variable  $t_d$  is the drying time assuming a two day period of sunlight exposure.

The mass airflow rate,  $m_a$ , was determined from Equation 4-5 (Sodha et al., 1987).

$$m_a = \frac{m_{dr}}{W_f - W_i} \quad (4-5)$$

The variables  $W_f$  and  $W_i$  are the final and initial humidity ratios, respectively.

The volumetric airflow rate,  $V_a$ , was estimated using Equation 4-6.

$$V_a = \frac{m_a}{\rho_{air}} \quad (4-6)$$

The variable  $\rho_{air}$  is the density of air.

Total useful energy,  $E$ , was calculated by Equation 4-7 (Sodha et al., 1987).

$$E = m_a (h_f - h_i) t_d \quad (4-7)$$

The variable  $h_{final}$  is the enthalpy of drying air while  $h_{initial}$  is the enthalpy of ambient air.

The solar collection area,  $A_c$ , of the absorber was calculated with Equation 4-8 (Sodha et al., 1987).

$$A_c = \frac{E}{I\eta} \quad (4-8)$$

The variable  $I$  is the incident solar radiation and  $\eta$  is the collector efficiency.

The difference in air pressure,  $\Delta P$ , across the bed was estimated by Equation 4-9 given by Jindal and Gunasekaran (1982).

$$\Delta P = C(P_i - P_{ATM})gh = 0.00308g(T_i - T_{atm})H \quad (4-9)$$

The variable  $g$  is the acceleration due from gravity,  $T_{da}$  is the assumed temperature of drying air,  $T_{atm}$  is the ambient atmospheric temperature and  $H$  is the assumed height of the dryer system.

## **Construction**

Suitable materials were selected and specified for fabrication of this solar dryer with consideration given to affordable and readily available materials specifically in rural Haitian communities. The solar dryer was comprised of two primary components; a solar absorber and a drying cabinet. The two components were designed to be detachable for easier maintenance and mobility as needed. A single, hinged door was installed on the rear of the cabinet to provide access to the trays.

## **Absorber**

The framework of the absorber was constructed primarily from half-inch plywood with a corrugated aluminum sheet serving as a solar absorbing component.. A rigid layer of rock wool, mineral slab insulates the bottom layer of the absorbing panel to effectively maintain elevated temperatures within the absorber system. An air gap of approximately one inch was left above the insulation material and was sandwiched on

the top by the suspended aluminum sheet. Another air gap was formed between this metal absorber and the upmost layer of polycarbonate glazing. Thus, the absorber was designed to allow flow on both sides of the metal panel as shown in Figure 4-2. The corrugated aluminum was oriented to allow airflow through the channels formed by the corrugation.

The translucent glazing material made of thin wall polycarbonate allows radiation to enter the absorber system where opaque surfaces convert the radiation into low-grade heat. All interior and exterior surfaces of the absorber were painted matte black in order to improve heat collection. Additionally, the suspended, corrugated-aluminum sheet was oriented parallel to the airflow in order to enhance the heat gain while taking care to minimize airflow inhibition or pressure reduction. A screen was placed over the inlet of the absorber to prevent intrusion of insects and other debris.

The solar absorber was inclined at an approximate angle of 28° which is 10° more than the local geographical latitude of Saut-d'Eau, Haiti as recommended by Bolaji and Olalusi (2008). This angle was suggested to allow for maximum absorption of solar radiation with a fixed or stationary absorber. This same angle was employed during evaluation of the solar dryer in Gainesville, Florida despite the differences in latitude. The integration of solar tracking and tilting mechanisms was avoided as these designs were expected to increase design sophistication and would consequently increase investment cost. Besides, solar tracking systems have shown negligible improvements over stationary designs particularly in tropical communities as discussed by Mwithiga and Kigo (2006).

## Cabinet

The 2x2 ft<sup>2</sup> (0.61x0.61m<sup>2</sup>) cabinet, which was constructed primarily of plywood, houses five wire mesh trays in which mango slices are intended to be spread on. Each tray is constructed of a wooden frame encompassing a steel, expanded metal grating. Although steel is known to rust, particularly in moist environments, it was selected here to reduce investment and material costs. The trays are designed to be removable for easier cleaning and loading potential. Additionally, the trays can be rotated and exchanged with other positions to ensure uniform drying between each tray. The front end of each tray is designed with a wider frame to assist in the distribution of incoming heated air.

The chimney, which was designed to extend 26 inches above the cabinet, allows for a greater pressure gradient to be established through the dryer as the warm air rises and exits through the top of the system. A simple shutter was built into the chimney to provide some control of internal cabinet temperatures and wind speed. The shutter is essentially a rigid, steel panel which slides into the chimney to restrict the airflow. In the closed position, elevated temperatures were expected as airflow was cut-off.

Additionally, a thermal rock storage component was installed in the plenum area at the base of the cabinet and was sized according to the lower volume limit of 5.3 ft<sup>3</sup> (0.15 m<sup>3</sup>) as recommended by Goswami (1986) and detailed by Adebayo and Irtwange (2009). This storage area was designed to collect heat during sunlight exposure and subsequently dissipate heat at night, during cloud cover or in inclement weather. The expectation was to prevent rewetting of the mango fruit by providing a continuous heat source. A latch was installed to provide access to the thermal rock bed. The drying

cabinet, trays, chimney and thermal rock bed were all painted matte black to help maintain elevated temperatures within the dryer.

## Dryer Operation

### General Overview

The operation of the newly developed solar dryer was evaluated in Gainesville, FL during the summer months of July and August. The system was installed on University of Florida grounds, adjacent to a weather station operated by the Agricultural and Biological Engineering department. The local weather conditions were expected to closely resemble those seen during the harvesting season of Haiti. To investigate the thermal performance of the dryer, preliminary tests were conducted with no load in the cabinet. Further experiments were conducted while loaded with mango slices. Dryer operation was evaluated with respect to both the condition of the drying air and the dried mangoes. Figure 4-3 is a photograph of the solar dryer in operation, situated on the experimental site.

### No Load

Evaluation of the solar dryer was first carried out with no product loaded in the cabinet. Triplicate experiments were conducted with the shutter half-closed and with the shutter fully open to evaluate operation with and without shutter restriction. These experiments were carried out for two full sunlight days (39 hours) starting at 6:00am on the first day and ending at 9:00PM on the second day.

Ambient air conditions were recorded from the adjacent weather station since the weather is known to directly influence the dryer performance. Solar radiation, temperature, relative humidity, wind speed and wind direction were all recorded from

this weather station every 15 minutes. Temperatures within the solar dryer were measured with T-type, polyvinyl thermocouples and recorded to a data-logger with an accuracy of  $\pm 1.8^{\circ}\text{F}$  ( $1.0^{\circ}\text{C}$ ) every five minutes as recommended by Leon et al. (2002). The thermocouples were installed at the air inlet, exit, thermal rock bed and at each tray level inside the dryer. Relative humidity was recorded at the chimney exhaust every five minutes with an Onset® Temperature and Relative Humidity Data Logger (HOBO® H08-003-02). Wind speed was manually recorded at the chimney exhaust on an hourly basis using a Reed Thermo-Anemometer (LM-8000).

## **Load**

Fresh, ripe mangoes, of the Tommy Atkins variety, were obtained from a local market and were briefly cleaned in a bath containing 15ppm bleach. The fruit was manually inspected to determine the general stage of ripeness. In this tactile assessment, the firmness of each fruit was manually inspected to ensure adequate ripeness. Fruit that was found to be exceptionally soft or overly firm were excluded from these experiments as the fruit was overly ripe or under-ripe, respectively.

The mangoes were manually cut and peeled to afford thin slices of fruit with an approximate range of 5 to 10mm thick. To prevent discoloration, 0.1% citric acid was used as an antioxidant. This preservative helps to prevent adverse color changes resulting from enzymatic reactions. In this process, fruit slices were dipped in the citric acid solution for approximately 3 minutes. Alternatively, the use of lemon juice is proposed where commercially-available preservatives are unavailable. The total weight of product was then recorded prior to loading. Random, analogous samples were selected to determine the initial moisture content by standard oven drying procedures.

An average of 4.2 lbs (1.9 kg) of sliced mango was distributed and spread evenly to each tray as shown in Figure 4-4. Special care was given to avoid overlapping of fruit slices in an effort to achieve uniform drying of all slices. Loading of the drying cabinet was carried out at 6:00am and experiments were conducted for two full sunlight days (39hours). Based on preliminary investigations, uneven drying was observed between product loaded on upper trays compared with product on lower trays. As was expected, the drying air became saturated with evaporated moisture from the lower trays, thus preventing adequate drying at the upper trays. Localized temperatures within the drying cabinet were also observed to drop as a result of evaporative cooling. As moisture was evaporated from the mango slices, heat energy was lost to the water vapor in the local vicinity of the mango slices.

For this reason, a continuous mode of operation was also evaluated in the operation of this solar dryer. In this process, the lowest tray was removed when the product was found to be adequately dry. The remaining trays were shifted downward in the cabinet and fresh product was added to the highest tray position. This allowed for continuous operation of the dryer rather than processing as a single batch.

Trays of product were considered adequately dry by examining random samples which were selected and marked for ongoing evaluation of moisture content. Four tagged fruit slices were distributed to each tray and were removed hourly as suggested by Ranganna (1986) for weight readings. The moisture content of these slices was determined from the weight measurements. Product spread on the same tray was considered adequately dry when the moisture content of the tagged samples dropped below 11.9% (wb). Alternatively, tactile assessments or visual inspections can be

performed on the fruits slices to determine the stage of drying. While manual evaluation of the product texture can easily be assessed for adequate dryness, softness and flexibility; color evaluation is slightly more involved. As the mango slices dry, some color change is observed from yellow to orange. Therefore, a standard color chart must be created or comparison must be made to similar dried product in order to assess the stage of drying based on color.

## Evaluation

The efficiency of the solar dryer was evaluated in terms of collector efficiency, pick-up efficiency and drying efficiency as recommended by Leon et al. (2002). Collector efficiency is the measure of how effectively the energy available in the solar radiation is transferred to the flowing air within the system (Tiris et al., 1995). This parameter was determined by assuming steady state conditions using Equation 4-10 (Ahmad et al., 1996).

$$\eta_{COLLECTOR} = \frac{GC_p\Delta T}{I} = \frac{GC_p(T_o - T_i)}{I} \quad (4-10)$$

The variable G is the mass flow rate of air per unit collector area,  $C_p$  is the specific heat of air evaluated at the average temperature within the solar collector,  $T_o$  is the temperature of air at the outlet of the absorber,  $T_i$  is the temperature at the absorber inlet, and I is the total solar energy incident upon the plane of the collector per unit time per unit area.

Pick-up efficiency is a practical evaluation of the amount of moisture evaporated from the product. This parameter essentially measures the effectiveness of the heated air to absorb the evaporated moisture. Thus a comparison is made between the actual absorbance of moisture to the capacity of moisture absorbance by the heated air.

Equation 4-11 was used to evaluate the pick-up efficiency according to Tiris et al. (1995).

$$\eta_{\text{PICK-UP}} = \frac{h_o - h_i}{h_{as} - h_i} = \frac{W}{\rho V t (h_{as} - h_i)} \quad (4-11)$$

The variables  $h_o$ ,  $h_i$  and  $h_{as}$  are the absolute humidities of air leaving the drying chamber, entering the drying chamber and entering the dryer at the point of adiabatic saturation, respectively.  $W$  is defined as the weight of water evaporated from the product,  $\rho$  is the density of air evaluated at the average temperature of air within the dryer and  $V$  is the volumetric air flow rate.

The system efficiency of a solar dryer is the measure of how effectively the solar energy input is used in drying the product (Leon et al., 2002). This term is defined by Equation 4-12.

$$\eta_{\text{SYSTEM}} = \frac{WL}{IA} \quad (4-12)$$

The variable  $L$  is the latent heat of vaporization of water at the exit air temperature and  $A$  is the aperture area of the solar collector.

The water activity of the solar-dried mangoes was determined using an AquaLab water activity meter (Decagon Series 3) and verified with the newly developed sorption isotherm. In this manner, the quality of the solar-dried mango was compared with the commercially-available, dried mangoes. Sensory quality parameters of the solar-dried mango slices were visually evaluated in terms of color and appearance to determine if quality standards were achieved in comparison to commercially available product.

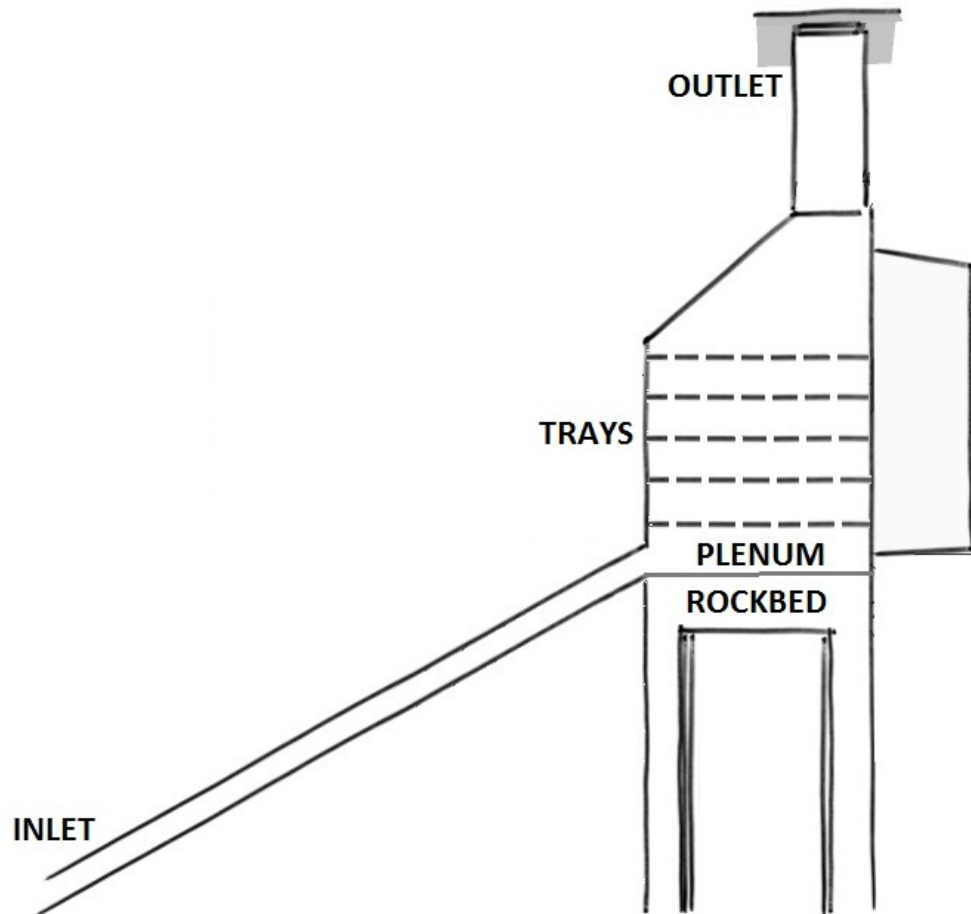


Figure 4-1. Natural-convection solar dryer featuring a solar collector and separate drying cabinet with five trays

Table 4-1. Design parameter input for natural-convection solar dryer

		SI		IP	
Mango Properties	Symbol	Value	Units	Value	Units
Number of Fresh Fruit	N <sub>fruit</sub>	30	-	30	-
Weight of Fresh Fruit	m <sub>fruit</sub>	13.61	kg	30	lb
Weight of Sliced Fruit	m <sub>p</sub>	7.16	kg	15.79	lb
Slice Thickness	d	10	mm	0.39	in
Initial Moisture Content (WB)	M <sub>i</sub>	78.1	%	78.1	%
Final Moisture Content (WB)	M <sub>f</sub>	11.9	%	11.9	%
Maximum Allowable Temp	T <sub>max</sub>	65.6	°C	150	°F
Dryer Parameters	Symbol	Value	Units	Value	Units
Number of Trays	N <sub>trays</sub>	5	-	5	-
Vertical Distance Btw Trays	h	7.63	cm	3.00	in
Height (head)	H	2.00	m	6.56	ft
Cross-sectional Area	A <sub>cs</sub>	0.14	m <sup>2</sup>	1.54	ft <sup>2</sup>
Depth of Thermal Storage	h <sub>thermal</sub>	26.77	cm	8.78	in
Temp of Drying Air	T <sub>da</sub>	60	°C	140	°F
Collector Efficiency	η	26	%	26	%
Weather/Climate	Symbol	Value	Units	Value	Units
Collector Angle	β	29	°	29	°
Ambient Air Temperature	T <sub>atm</sub>	28.3	°C	83	°F
Ambient Relative Humidity	φ <sub>atm</sub>	48.0	%	48	%
Drying Time (sunshine hours)	t <sub>d</sub>	8.7	hours	8.7	hours
Wind Speed	v <sub>wind</sub>	3	m/s	9.8	ft/s
Incident Solar Radiation	I	6	kWh/m <sup>2</sup> day	1902	Btu/ft <sup>2</sup> day
Air Density (@ T <sub>atm</sub> )	p <sub>air</sub>	1.17	kg/m <sup>3</sup>	0.07	lb/ft <sup>3</sup>

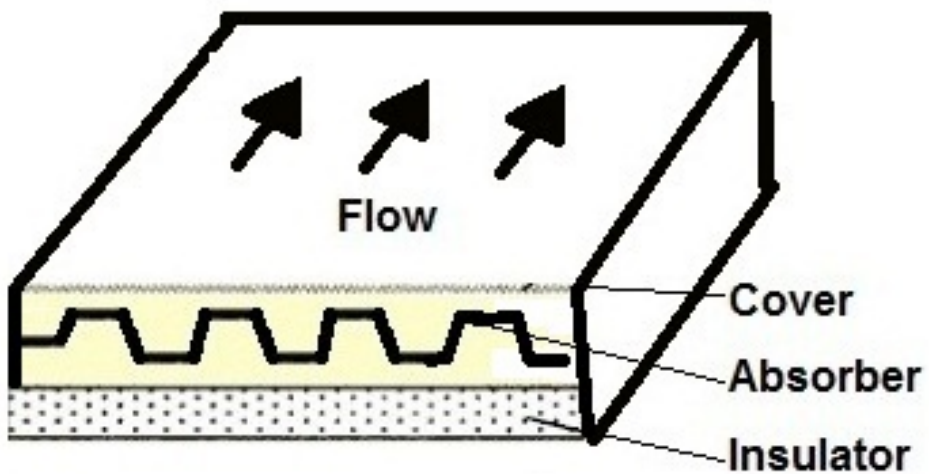


Figure 4-2. Schematic of solar collector, cross section



Figure 4-3. Solar convection dryer on UF campus in Gainesville, FL



Figure 4-4. Trays loaded within the cabinet section of the solar convection dryer

## CHAPTER 5

### RESULTS AND DISCUSSION

#### Sorption Isotherm

Sorption data were fitted into both the GAB and BET isotherm models. The parameters of both models are shown in Table 5-1. The GAB model provided the best fit by exhibiting the highest correlation coefficient of 0.995. This sorption isotherm model is shown in Figure 5-1 with the associated data as determined by isopiestic drying experiments. The water activity of commercially-available, dried-mango slices was found to be 0.56 with an initial moisture content of 11.9% (wb) which lies considerably close to the isotherm curve. The average temperature in the lab in which these experiments were conducted was determined to be 71 °F (22°C) with an average deviation of  $\pm 0.7^{\circ}\text{F}$  (0.4°C). These minimal temperature fluctuations were considered negligible.

While the general shape of sorption isotherms is sigmoidal for most agricultural products (De Jung et al., 1996) this isotherm exhibits a type III isotherm pattern (Labuza and Altunakar, 2008) as is common with high sugar content fruit (Ayrancı and Dogantancı, 1990; Falade and Aworh, 2004; Tsami et al., 1990). This shape is due to changes in constitution, dimensions and phase transformation of sugars which occur as the mango slices experience moisture loss from within the fruit (Falade and Aworh, 2004). This isotherm pattern is similar to a previously developed model (Rangel-Marrón et al., 2011) which was conducted with liquefied mango pulp at several temperatures ranging from 59°F (15°C) to 95°F (35°C). However, the current model, which was evaluated at an intermediate temperature, exhibits a small shift to the left of this previously reported model. This shift results in slightly higher values for moisture

content in the current model than the values based on the previously reported model. Minor inconsistencies between the current model and the previously reported model may be attributed to the different physical states of mango fruit in which the studies were conducted.

### **Solar Dryer Design**

The results of the engineering calculations are shown in Table 5-2 along with references corresponding to the applied methodology as discussed earlier in this report. The absorber was designed to have a surface area of  $18.4 \text{ ft}^2$  ( $1.71\text{m}^2$ ) as determined from the calculations and shown in Figure 5-2. The  $2\times 2 \text{ ft}^2$ , cross-sectional cabinet which houses five wire-mesh trays is shown in Figure 5-3.

### **Dryer Operation**

#### **No-Load**

The incident solar radiation, as recorded from the weather station, is shown in Figure 5-4 for two full days of sunlight exposure. Triplicate experiments were conducted for each procedure to provide the average radiation levels as shown. The solar radiation levels were generally similar amongst separate trials except during experiments conducted with the shutter in place. During this experiment with shutter-restricted airflow, the observed solar radiation was considerably lower particularly on the first day of testing. Since the operation of this drying system is completely dependent on solar energy, the reduced level of radiation seen in this trial certainly had effects on the outcome of the study as discussed further in this report. Daily solar radiation levels generally ranged from 50 up to  $800 \frac{W}{m^2}$  with an average of  $319.7 \frac{W}{m^2}$  during sunlight hours. Peak solar radiation occurred between 11:30am and 2:30pm each day with

values of 893.0, 831.0 and  $870.5 \frac{W}{m^2}$  for shutter-restricted, un-restricted and loaded experiments, respectively.

Temperatures, as recorded without product loaded in the cabinet, are shown in Figure 5-5. As seen in both cases, with and without air flow restriction, the temperatures within the solar dryer were significantly elevated from the environmental temperature. For the case with unrestricted airflow, the plenum temperature reached an optimum of 156.3°F (69.0°C) which is 62.5°F (34.7°C) in excess of environmental conditions which had a high of 93.8°F (34.3°C). In the experiments conducted with shutter restriction, temperatures were able to reach a high of 162.9°F (72.7°C) on the second day which is approximately 72.1°F (40.0°C) in excess of the environmental temperature of 90.8°F (32.7°C). However, the temperatures on the first day of this experiment were substantially lower as the solar radiation observed on the first day was drastically reduced by cloud cover. This indicates the strong correlation of solar radiation to the attainable temperatures within the solar dryer.

The plenum temperatures were generally the highest as the plenum area directly follows the solar absorber. As heated air flowed through the cabinet there was some heat loss resulting in temperature reductions further in the cabinet. This is evident from the slightly decreased temperatures recorded at each tray level as well as the exhaust/outlet. The rock bed exhibited the lowest recorded temperatures; however, this thermal storage unit maintained temperatures elevated above the ambient levels until 7:00am on the second day. This indicated effective heat storage and dissipation through the night, although it generally took 6 to 7 hours for the rock bed to reach the heated temperature each morning which is a somewhat slower temperature rise than other

regions within the dryer. This delayed warming is a result of the slower heat adsorption into the rocks.

The temperatures recorded at all five tray levels were averaged together to provide general, internal cabinet temperatures as shown in Figure 5-6. Contrary to what was expected, the case with unrestricted airflow exhibited the highest temperatures within the cabinet while the shutter-restricted case was considerably lower, particularly on the first day. The average cabinet temperatures were found to be 98.9 °F (37.1 °C) and 110 °F (43.7 °C) for the case of with and without shutter-restriction during sunlight hours, respectively. Again this was due to the relatively low solar radiation observed during experiments that were conducted with restricted airflow. The temperatures for the case with a loaded solar dryer were also significantly lower from the no-load experiments. This was due to the heat lost to the mango slices which corresponded to lower temperatures in the cabinet.

Relative humidity, as recorded near the chimney exhaust, is shown in Figure 5-7. As was expected, the shutter trapped the moisture inside the cabinet which resulted in elevated relative humidity. In the case with no shutter to restrict the airflow, the moisture was able to escape from the cabinet resulting in lower relative humidity within the dryer. In fact, without the shutter, relative humidity was lowered to an average of 35.1% during sunlight hours. This is much lower than the average relative humidity of 46.2% resulting from shutter-restricted experiments. However, both with and without the shutter, relative humidity was effectively decreased from ambient relative humidity by at least 18.8% during sunlight hours. These results indicate effective transport and exhaust of moisture from within the dryer.

The exhaust air velocity recorded at the chimney exhaust is shown in Figure 5-8.

As was expected, the exhaust air velocity was slightly reduced with the shutter somewhat closed. Removing the shutter allowed for increased airflow exhausting from the chimney. Average, unrestricted air flow velocity was determined to be 1.4 mph during sunlight hours, while restricted air flow velocity was only 1.0 mph on average during sunlight hours. The exhausted air velocity in loaded experiments was found to be 1.1 mph on average during sunlight hours. Although unexpected, this preserved rate of exhaust indicates negligible airflow restriction through the loaded trays.

### **Load Experiments**

The temperatures, as recorded while the cabinet was loaded with product, are shown in Figure 5-9. The plenum temperature was elevated to an optimum of 151.8°F (66.6°C) which is still 58.3°F (32.5°C) in excess of the environmental temperature which had a high of 93.5°F (34.1°C). The internal cabinet temperatures were somewhat lower which is expected from the heat loss to the cabinet as well as the mango slices. The average cabinet temperature during sunlight hours was determined to be 98.5 °F (37.0 °C).

Figure 5-10 shows the plenum and rock bed temperatures for the cases of loaded cabinet and no-load experiments. As both the plenum and rock bed are upstream from the cabinet, the attainable temperatures were unaffected by the presence of mango slices in the cabinet. The temperatures in these two regions directly correspond to the efficiency of the absorber which does not change based on the loading of the dryer with product.

Figure 15-11 shows the temperatures recorded at the exhaust outlet for the instances of no loading and loaded with mango slices. The temperature in the exhaust was greatly reduced by loading product into the cabinet particularly on the first day. This reduction in temperature is due to the heat lost to the mango slices. The larger discrepancy during Day 1 is a consequence of the increased level of relative humidity observed during the initial stages of drying. In general, exhaust temperatures were reduced by approximately 30°F (16.7°C) as compared with the incoming heated air delivered into the plenum area.

The relative humidity, as recorded in the exhaust of the loaded cabinet, is shown in Figure 5-12. The moisture from the mango slices placed additional loading on the dryer resulting in increased relative humidity than what was observed in the non-loaded experiments. In fact, the average relative humidity recorded in the loaded experiments was found to be 61.6% during sunlight hours. This is at least 15.4% higher than the average relative humidities recorded in non-loaded experiments. This additional moisture from the product prohibited significant removal of relative humidity from within the cabinet. It is also noted that the relative humidity on the second day of the loaded experiment was slightly reduced from the first day as a consequence of the excess moisture that was present on the product surface on Day 1.

Figure 5-13 shows the moisture content for mango slices when the dryer was operated in the batch mode. The initial moisture content of the slices was approximately 84% (wb) which was slightly elevated as a result of the citric acid solution which added some moisture to the product. A total weight of 21.4 lb (9.71 kg) of sliced mango was distributed among the five trays and the product was dried over a two-day period.

Drying rates were somewhat slow at the initial stages of drying as solar radiation was low in the morning and the mango slices had to be heated before water began to evaporate. It would be expected that preheating of the mango slices would improve the initial drying rate of the product. The bottom tray exhibited the fastest drying rate as expected since evaporated moisture from this tray accumulated on the upper trays. Thus, the upper trays exhibited slower drying rates as they were exposed to the evaporated moisture from below.

By the end of the second day, product on all trays had reached a moisture content of approximately 9.4% (wb) on average, with a range of as low as 6.4% (wb) on the bottom tray and up to 11.1% (wb) on the top tray. These values of moisture content are rather low even compared with the commercially available, dried-mango reference which was generally 11.9% (wb). By bringing the moisture content down to such low levels, heat energy was essentially wasted as the product does not require drying to this extent. Furthermore, product quality was degraded as the mango slices lost significant amounts of moisture. The final weight of dried slices was determined to be 3.4 lbs (1.53 kg) which is somewhat lower than the expected value due to partially unrecoverable product on the trays. This corresponds to a total of 18.0 lbs (8.18 kg) of water removed from the mango slices.

Experiments conducted with continuous loading of the solar dryer were carried out by replacing finished product with fresh product as needed. The results for moisture content, under the continuous mode of operation, are shown in Figure 5-14. The initial moisture content of the slices was found to be approximately 85% (wb) after citric acid treatment. A total of 21.9 lb (9.95 kg) of sliced mango was initially distributed among the

five trays with an average of 4.4 lb (1.99 kg) per tray. When the product on a single tray reached approximately 12% (wb), it was removed. Fresh product was then added to sustain a continuous drying process. By noon on the second day, the first tray had reached a moisture content of 11.1% (wb) which demonstrated the improved drying rate of the bottom tray compared with the upper trays.. This tray was removed and fresh product was rotated into the cabinet.

In this manner, three additional trays were able to begin drying on the second day. The moisture content of these new trays was lowered by up to 20% (wb) before sunset. The final weight of the initially loaded product was determined to be 3.5 lbs (1.61 kg) which is somewhat lower than the expected value due to partially unrecoverable product on the trays. This corresponds to a total of 18.4 lbs (8.34 kg) of water removed from the initial load of mango slices.

Continuous loading allowed for drying of more product than what was accomplished with batch loading. In fact, the weekly productivity of the solar dryer was determined to be 83.2 lbs (37.7kg) of fresh mango for the continuous mode of operation while only 74.9 lbs (34.0 kg) of fresh mango could be dried with batch mode of operation. This corresponds to a weekly production of 24.5 lbs (11.1 kg) of dried slices with continuous mode of operation while only 23.8 lbs (10.8 kg) are produced with batch mode of operation.

In both the batch and continuous modes of operation, initial rates of drying progressed rapidly. This is a result of the rapid evaporation of excess moisture on the product surface as well as the high temperatures reached within the cabinet. Subsequent drying of the mango slices was dependent on the rate at which internal

water migrated to the product surface via diffusion (Chen et al., 2009). Furthermore, as solar radiation levels dropped at nightfall, the drying rate slowed where it generally remained constant through the night. Although slight increases in moisture content were observed for the bottom tray through the night, the small rise of approximately 7.4% (wb) was considered negligible. Drying rates improved once again early on the second day.

## Evaluation

### Dryer Efficiency

The performance of the solar dryer was evaluated in terms of several efficiency parameters as described earlier using the thermodynamic properties shown in Table 5-3. The efficiency of the solar collector was determined to be 29.5% which is significantly improved over the assumption that was made during mathematical analysis and development of this solar dryer. This improvement was evidenced by the fact that temperatures in excess of the analytical-estimated values were achieved in the actual experiments. The pick-up efficiency was found to be only 10.8% which indicates a slightly diminished effectiveness of moisture absorbance by the heated air. However, the drying efficiency was found to be 33.9% which indicates a rather effective use of solar radiation in drying the product.

### Product Quality

The average moisture content of the solar-dried mangoes between batch and continuous modes of operation was found to be 10.25% (wb) using standard oven drying procedure. This moisture content corresponds to a water activity of approximately 0.56 as determined by analysis using the sorption isotherm. This water

activity was verified with an AquaLab water activity meter (Decagon Series 3) as 0.55 which is lower than the water activity of the commercially available, dried-mango slices. Color and appearance were also preserved in the solar dried slices as determined by visual inspection of the fruit. Figure 5-15 shows a photograph of the solar-dried mango slices compared to commercially available mango slices.

The solar dryer was able to dry at least 21.4 lbs (9.71kg) of fresh mango slices every two days. This drying rate is significantly increased from the estimated loading capacity of 15.8lbs (7.16kg) used in the mathematical design calculations. This corresponds to a 135% increase in processing capacity. Thus, the actual performance of the solar dryer exceeded the conservative analytical model that was used to design the system. Considering this improved performance over the mathematical design, the actual weather conditions should also be noted in relation to the design parameters.

The environmental conditions observed during solar drying experiments were generally downgraded compared to the values assumed in the mathematical design calculations. While the average environmental temperature of 81.3 °F (27.4 °C) during sunlight hours was relatively close to the temperature input used in the mathematical calculations, the actual relative humidity was increased. The average relative humidity observed during field operations was 22% higher than the estimated value of 43% which placed a much larger strain on the dryer. Additionally, solar radiation was decreased from the estimated value by about 28.2% as the dryer was designed for the higher solar radiation levels typical of tropical regions such as Haiti. It was concluded that the conservative, mathematical calculations used in the design and development of this solar dryer were effective.

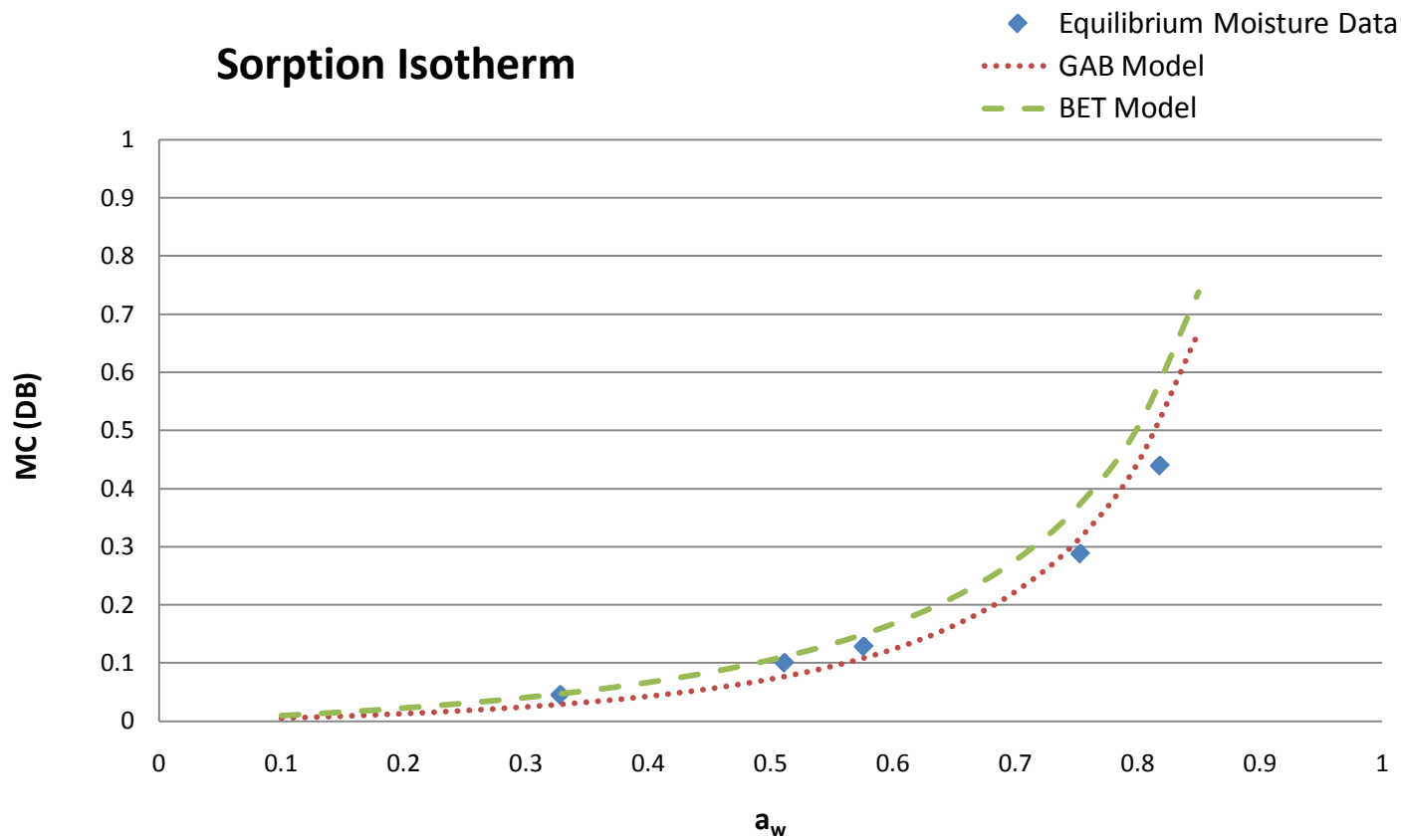


Figure 5-1. Sorption isotherm for mango at 71°F (22°C)

Table 5-1. Estimated parameters of sorption isotherm models of mango slices

Parameters	BET Model	GAB Model
A	0.1448	0.4203
B	0.5732	0.1117
C	1.000	0.945
R <sup>2</sup>	0.949	0.995

Table 5-2. Design parameter output for natural-convection solar dryer

Parameter	Symbol	Value	Units	Value	Units
Initial Humidity Ratio	W <sub>i</sub>	0.01	kg <sub>w</sub> /kg <sub>da</sub>	0.01	lb <sub>w</sub> /lb <sub>da</sub>
Initial Enthalpy	h <sub>initial</sub>	58.07	kJ/kg <sub>da</sub>	32.62	Btu/lb <sub>da</sub>
Final Enthalpy	h <sub>final</sub>	96.31	kJ/kg <sub>da</sub>	49.05	Btu/lb <sub>da</sub>
Equilibrium RH	φ <sub>f</sub>	51.00	%	51.00	%
Final Humidity Ratio	W <sub>f</sub>	0.02	kg <sub>w</sub> /kg <sub>da</sub>	0.02	lb <sub>w</sub> /lb <sub>da</sub>
Mass H <sub>2</sub> O to Evaporate	m <sub>w</sub>	5.38	kg	11.86	lb
Average Drying Rate	m <sub>dr</sub>	0.31	kg <sub>w</sub> /hr	0.68	lb <sub>w</sub> /hr
Airflow Rate	m <sub>a</sub>	28.80	kg <sub>da</sub> /hr	63.45	lb <sub>da</sub> /hr
Volumetric Airflow Rate	V <sub>a</sub>	24.65	m <sup>3</sup> /hr	869.85	ft <sup>3</sup> /hr
Total Useful Energy	E	9595	kJ	9078	Btu
Solar Collector Area	A <sub>c</sub>	1.71	m <sup>2</sup>	18.36	ft <sup>2</sup>
Air Pressure Difference	ΔP	1.91	Pa	37.09	psi

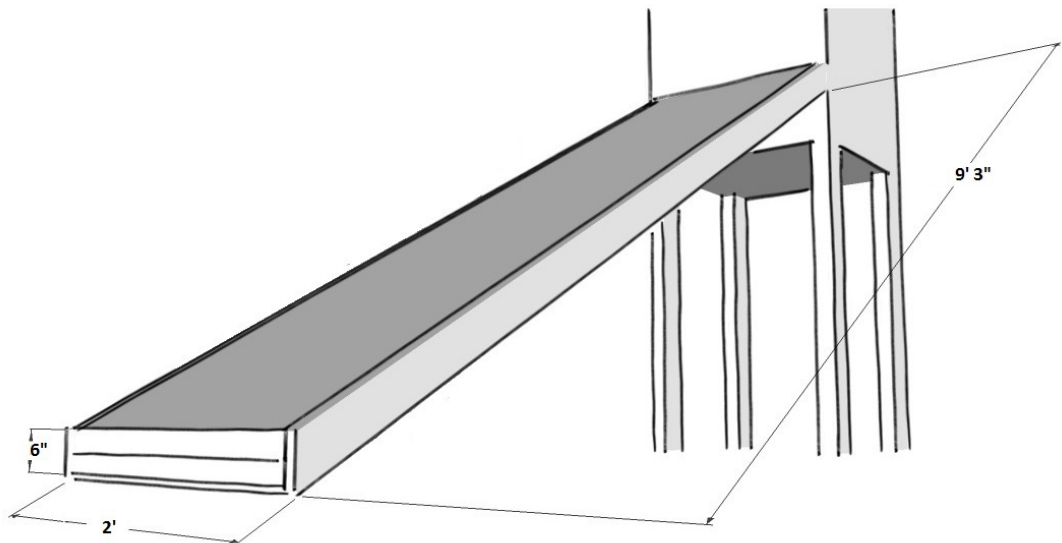


Figure 5-2. Solar collector schematic

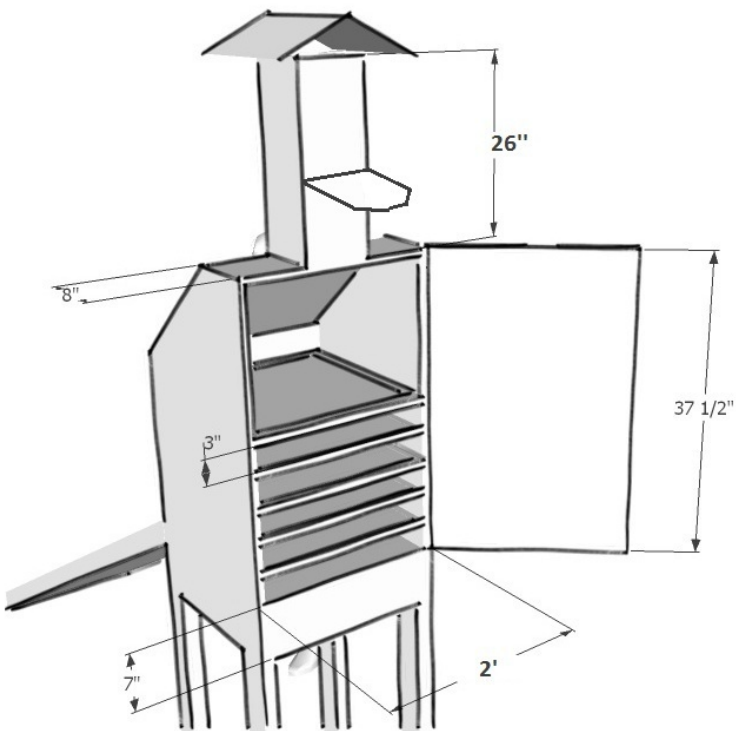


Figure 5-3. Drying cabinet with chimney, shutter and trays (schematic)

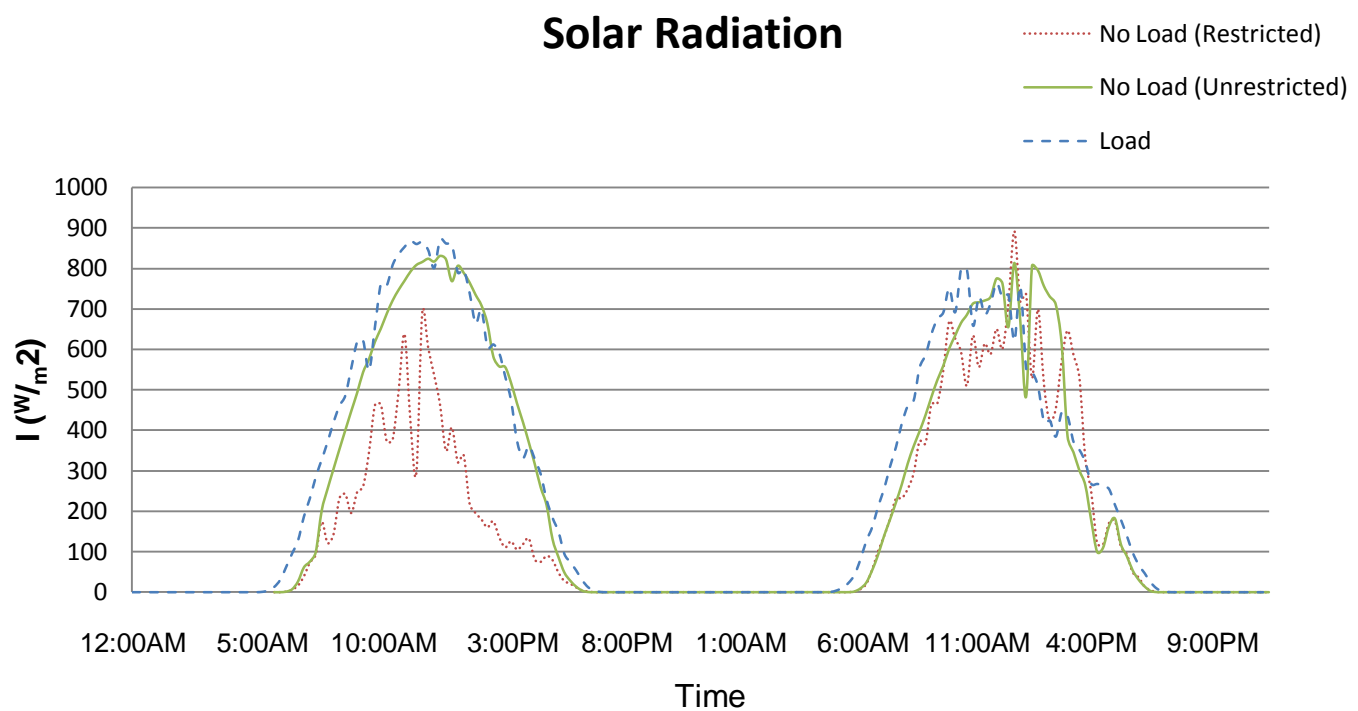
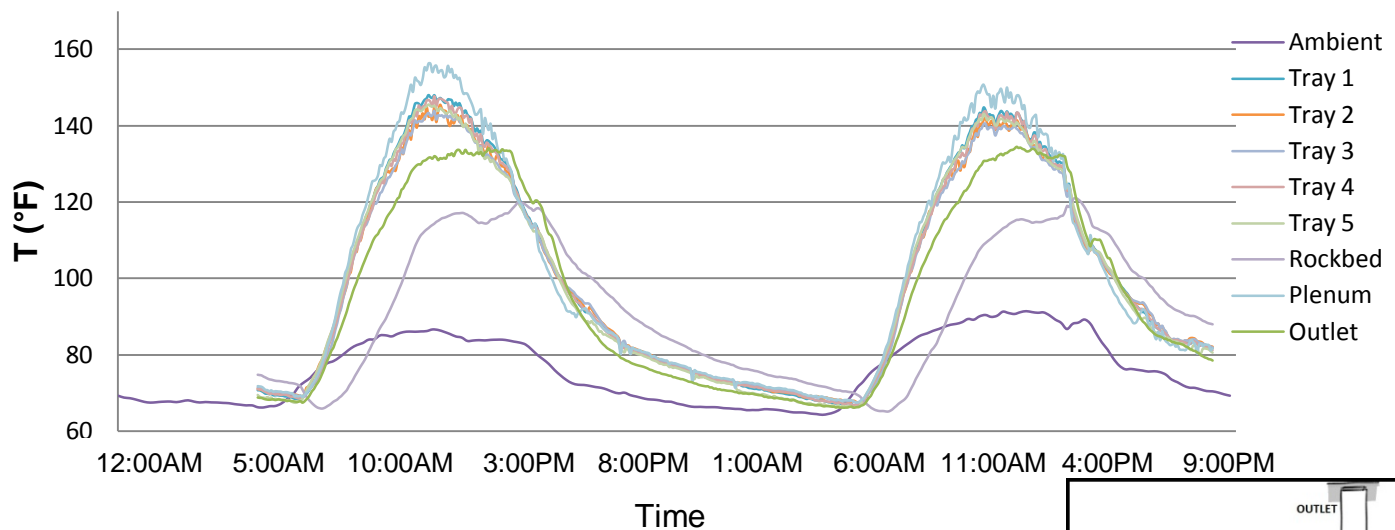


Figure 5-4. Incident solar radiation recorded at weather station

**A**

## Temperatures (No Shutter)

**B**

## Temperatures (Shutter)

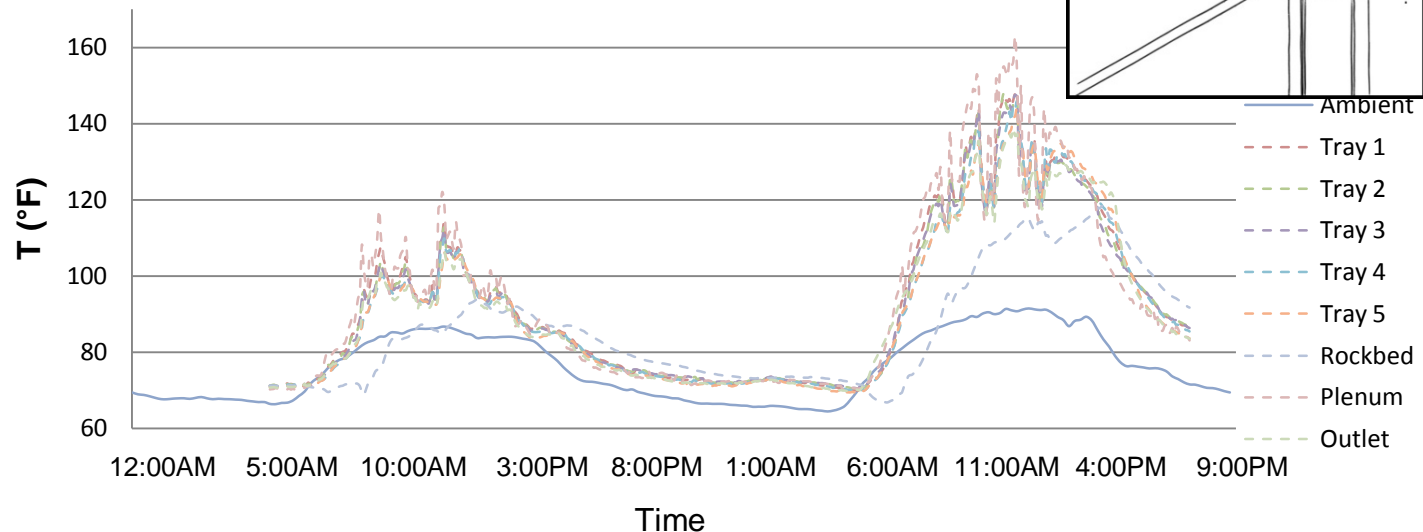


Figure 5-5. Temperatures recorded within the solar dryer. A) With no shutter. B) With Shutter.

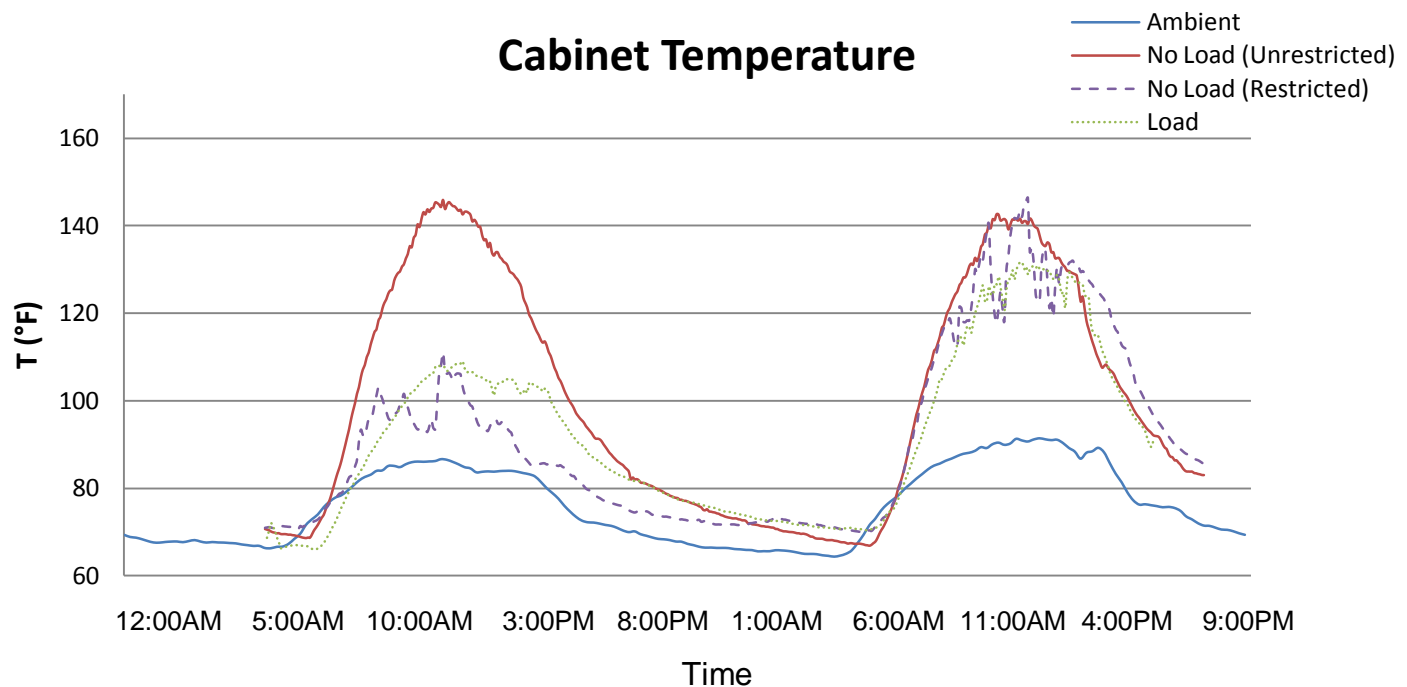


Figure 5-6. Cabinet temperatures based on average temperatures between all trays

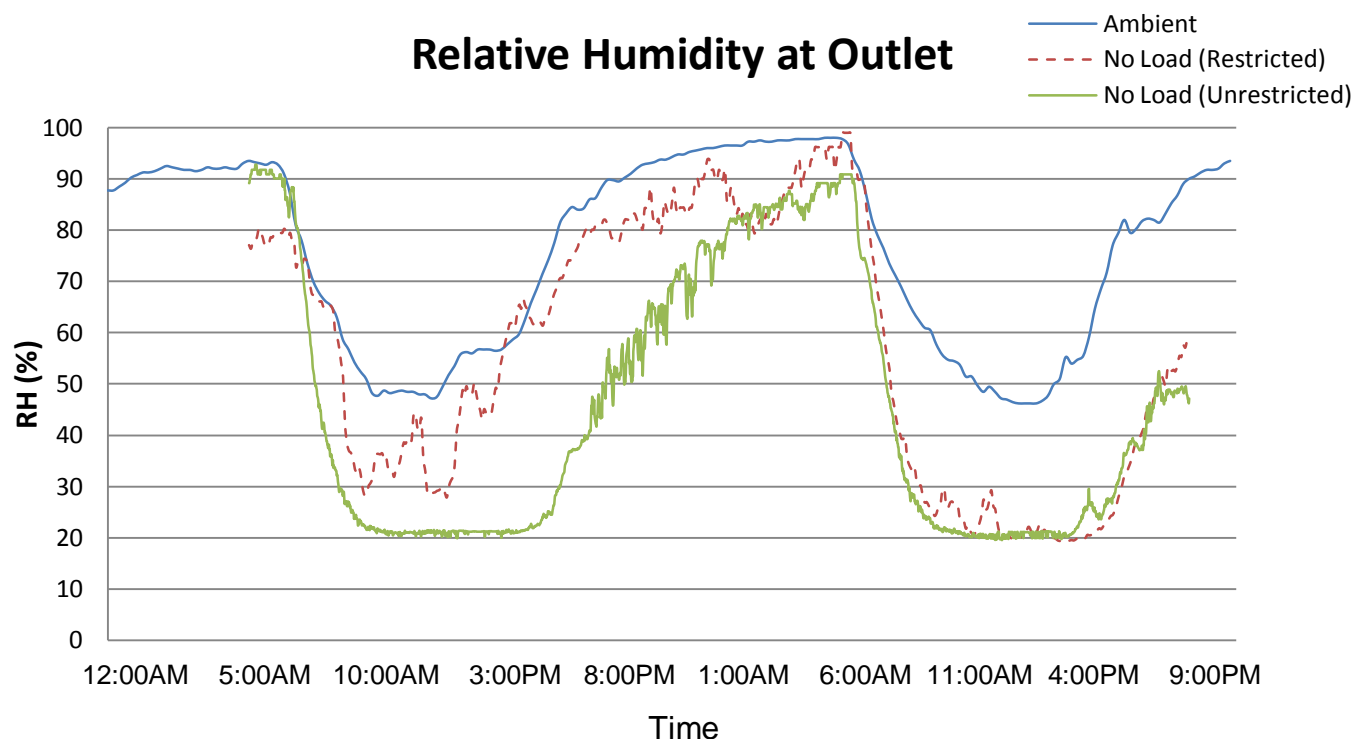


Figure 5-7. Relative humidity as recorded near chimney exhaust

## Exhaust Air Velocity at Outlet

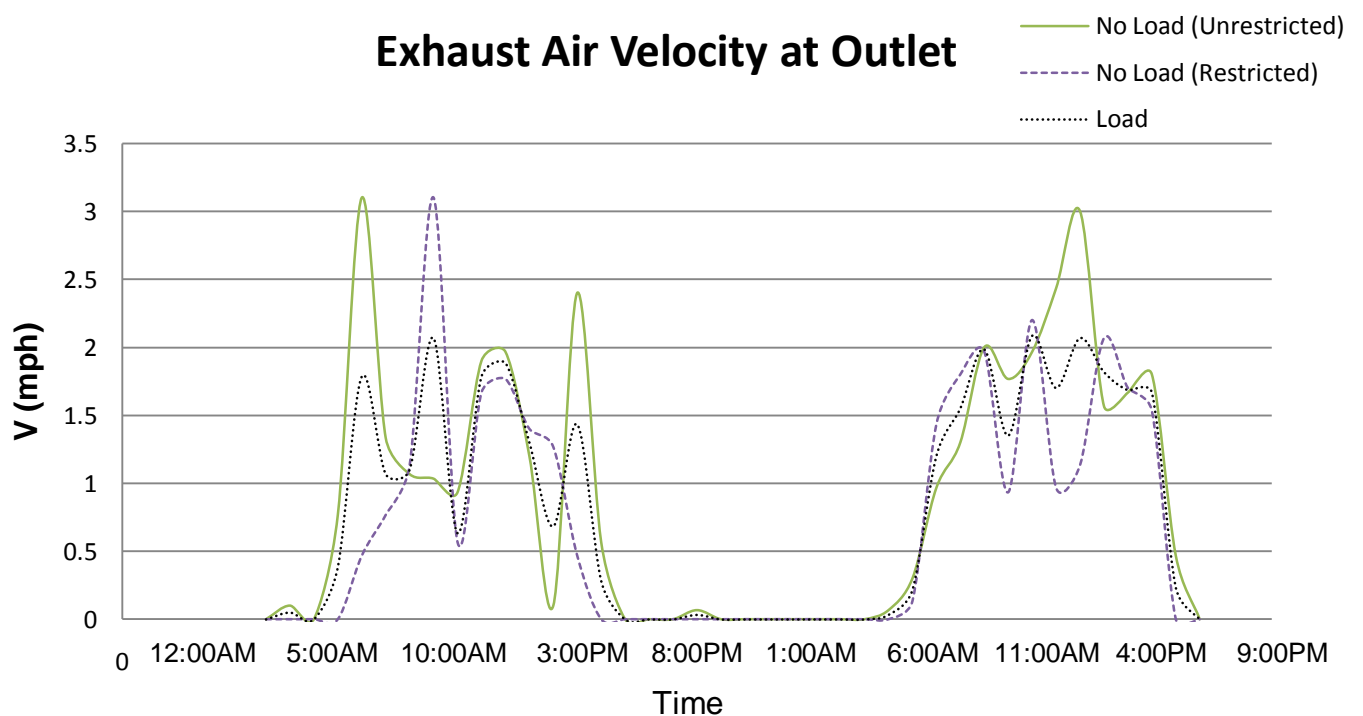


Figure 5-8. Exhaust air velocity recorded at chimney exhaust

## Temperatures (Loaded)

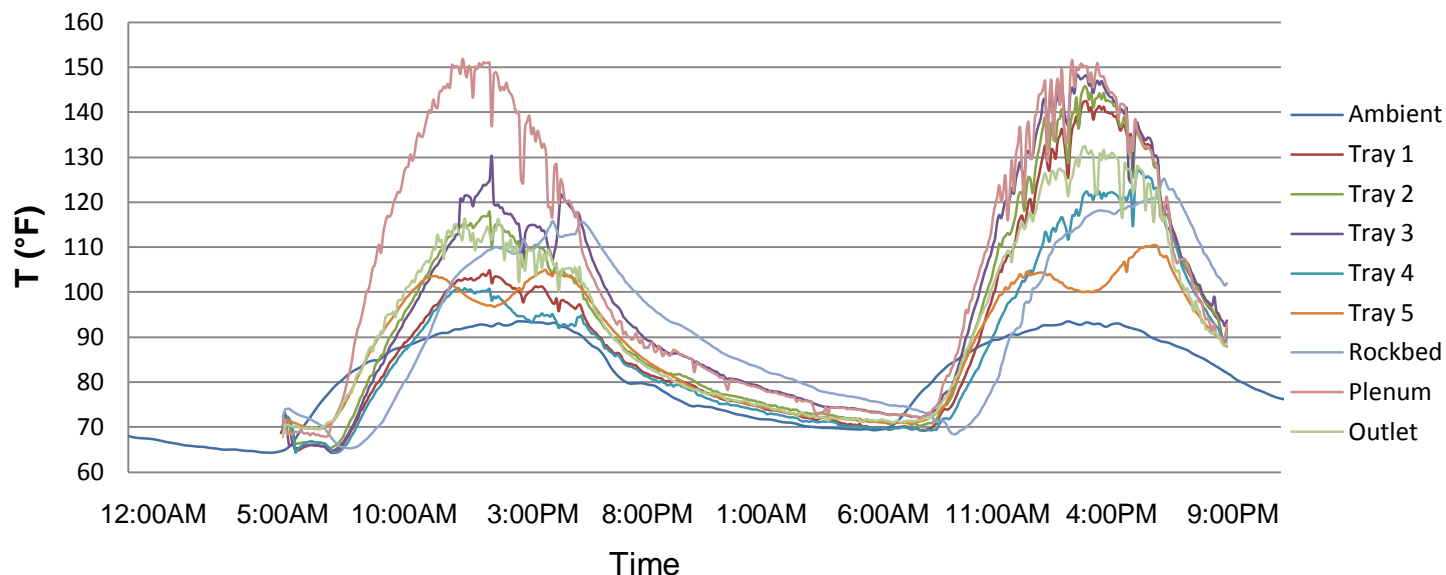


Figure 5-9. Temperatures within the solar dryer at various locations

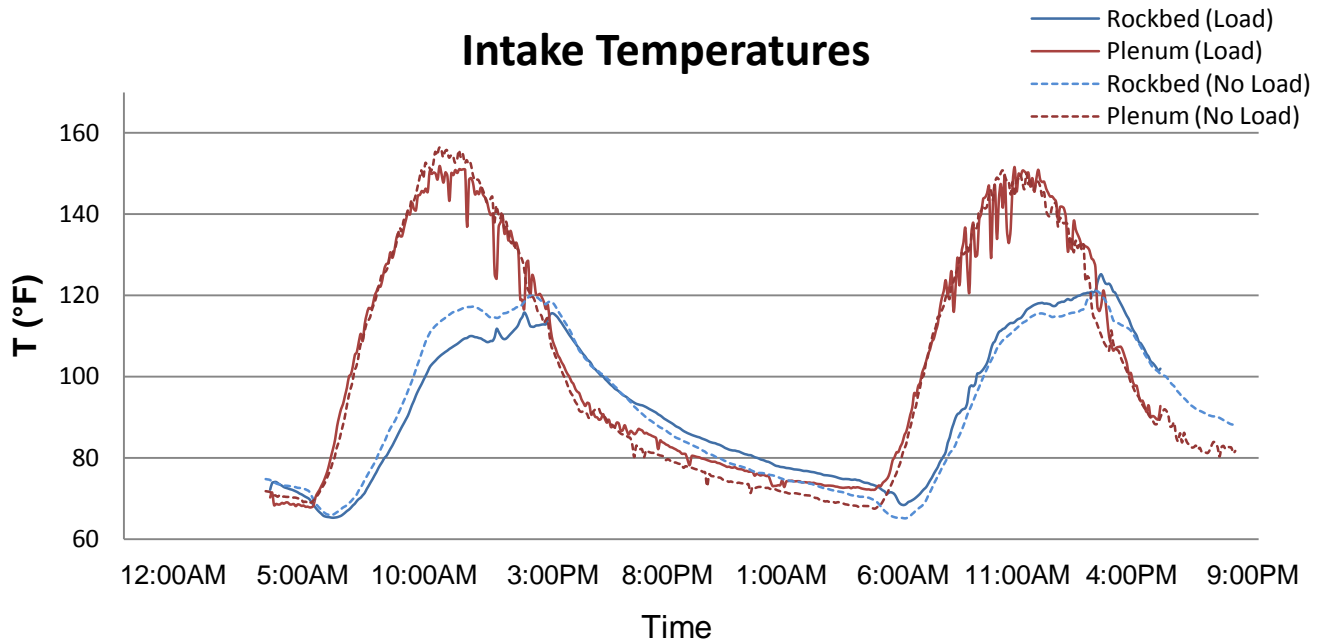


Figure 5-10. Temperatures of incoming air in the plenum and rock bed

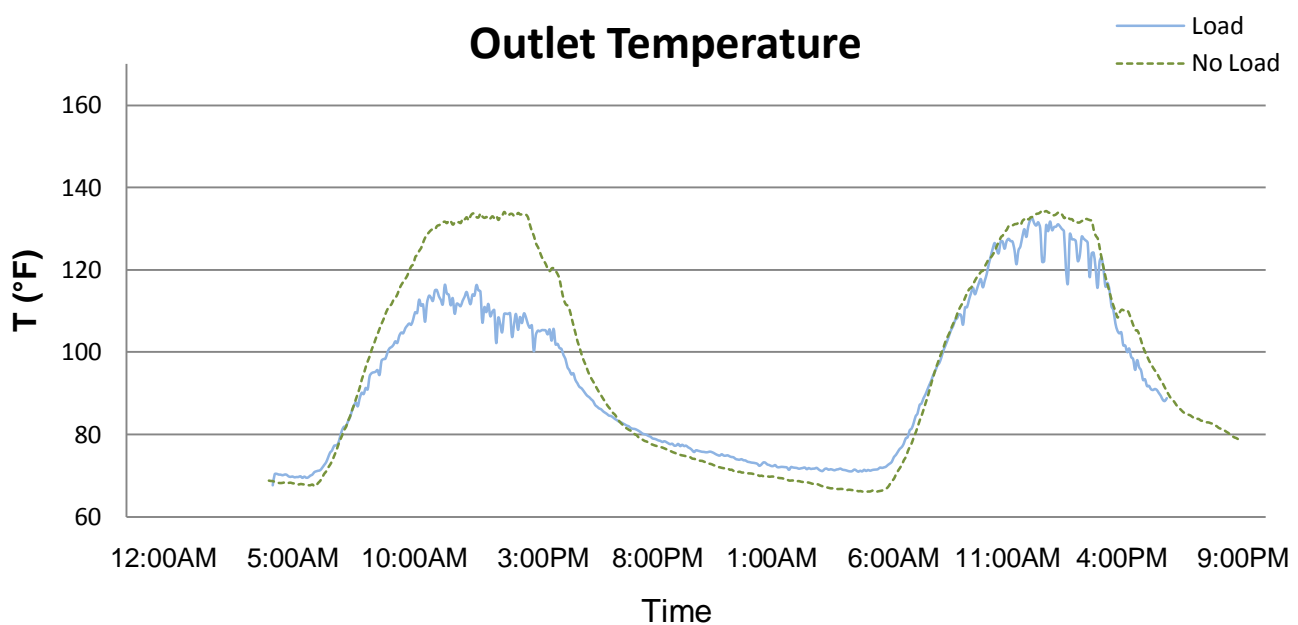


Figure 5-11. Temperatures recorded at the exhaust outlet

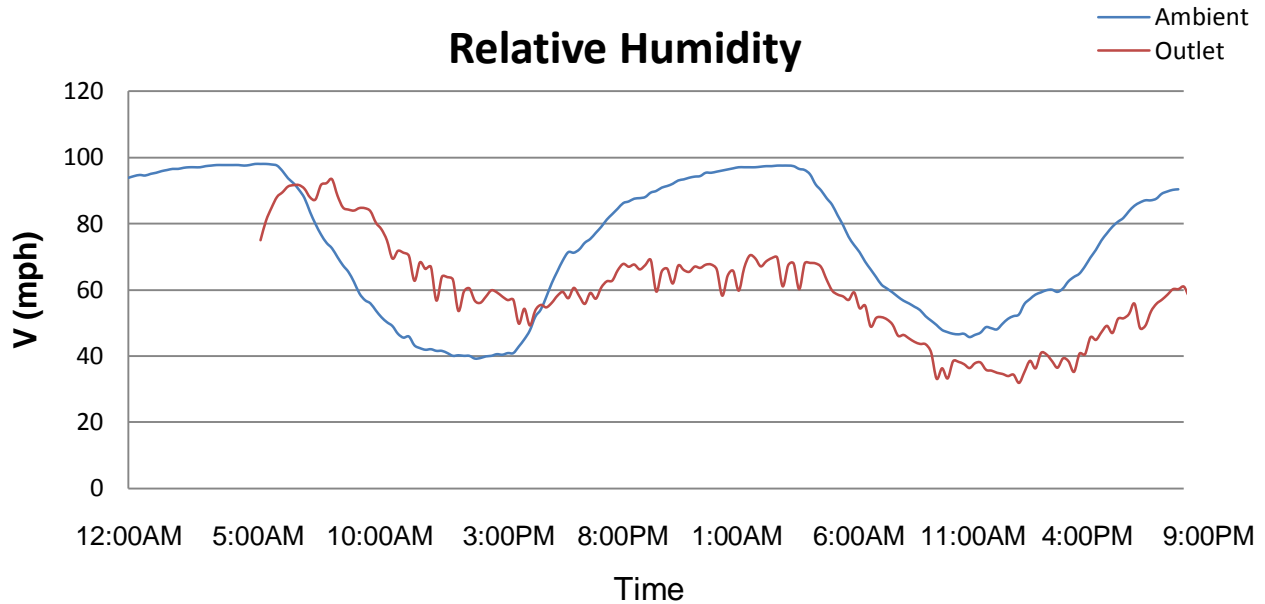


Figure 5-12. Relative humidity of ambient air as recorded at weather station and in chimney/exhaust

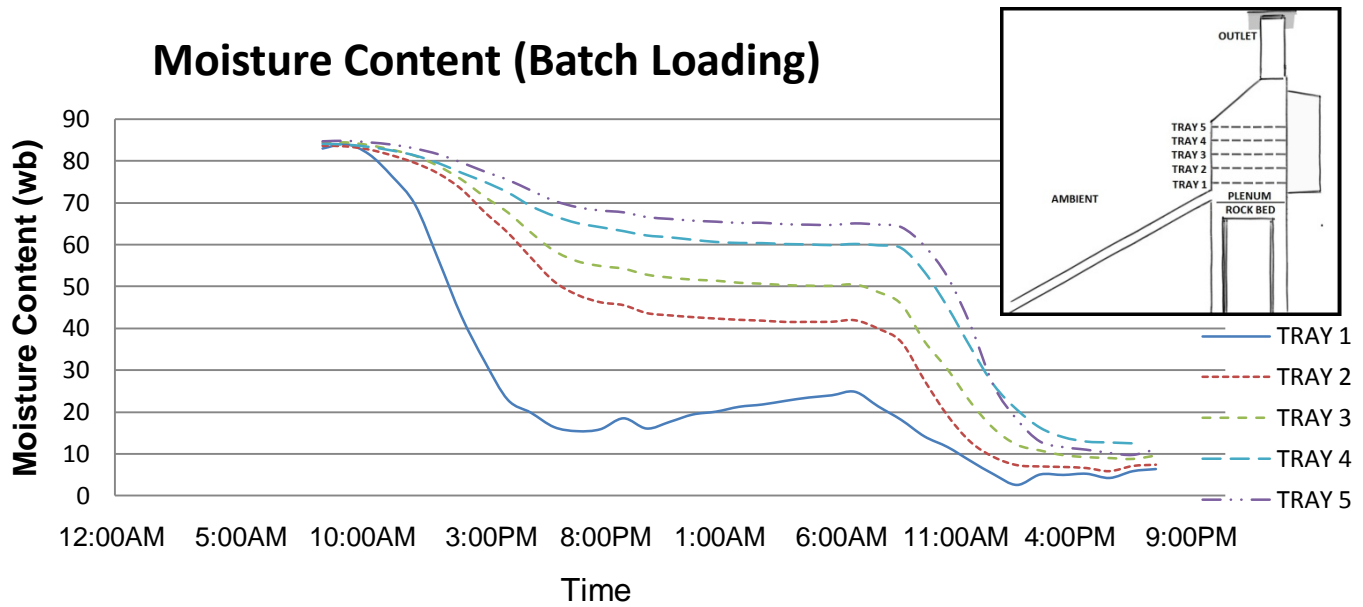


Figure 5-13. Moisture content of mango slices in solar dryer over 2 full days of sunlight with batch mode of operation

## Moisture Content (Continuous Loading)

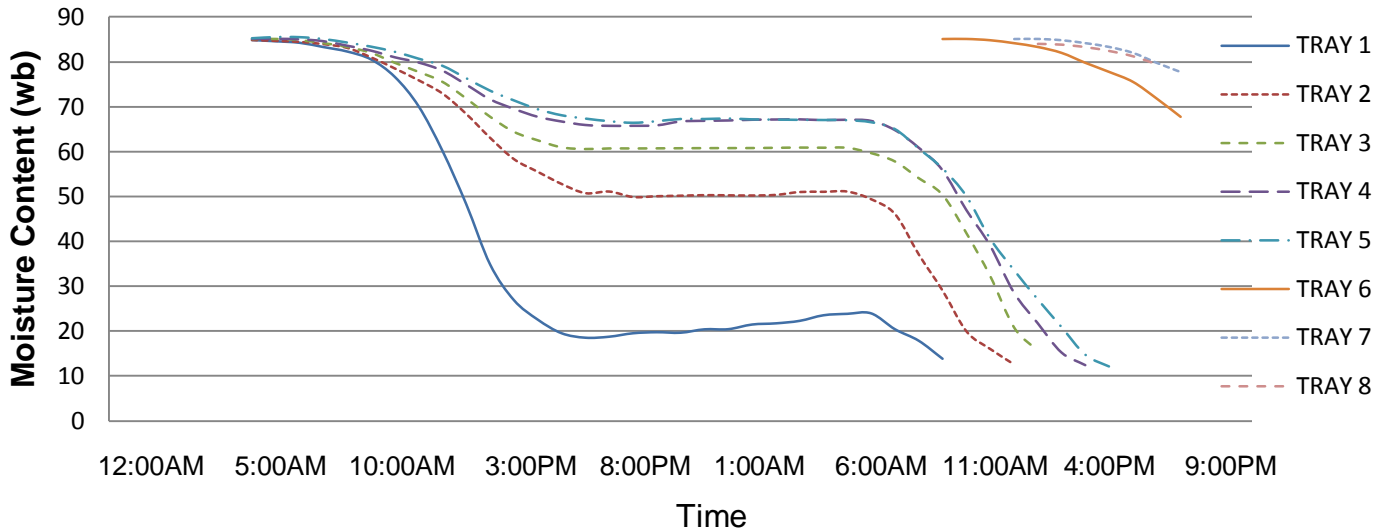


Figure 5-14. Moisture content of mango slices in solar dryer over 2 full days of sunlight with continuous mode of operation

Table 5-3: Efficiency parameters

VARIABLE	DEFINITION	VALUE	UNITS
G	Mass flow rate of air per unit collector area	0.720	$\frac{\text{kg}}{\text{m}^2\text{s}}$
$C_p$	Specific heat of air (@ $T_{AVG}$ )	1.005	$\frac{\text{kJ}}{\text{kgK}}$
$T_o$	Absorber Outlet Temperature	40.41	$^{\circ}\text{C}$
$T_i$	Inlet Temperature (Average Ambient Temp)	27.40	$^{\circ}\text{C}$
$T_{AVG}$	Average Temperature between $T_o$ and $T_i$	33.91	$^{\circ}\text{C}$
I	Total solar energy incident upon plane of collector per unit time per unit area	319.73	$\frac{\text{W}}{\text{m}^2}$
W	Weight of water evaporated from the product	8.26	$\frac{\text{kg}}{\text{kg}}$
$\rho$	Density of air (@ $T_{AVG}$ )	1.151	$\frac{\text{kg}}{\text{m}^3}$
V	Volumetric Air Flow Rate	0.026	$\frac{\text{m}^3}{\text{s}}$
t	Drying Time	43020	$\text{s}$
$h_{as}$	absolute humidity of the air entering the dryer at the point of adiabatic saturation	0.022	%
$h_i$	absolute humidity of air entering the drying chamber	0.082	%
L	Latent heat of vaporization of water at exit air temperature	2257	$\frac{\text{kJ}}{\text{kg}}$
A	Aperture Area of the Dryer	1.719	$\frac{\text{m}^2}{\text{m}^2}$

The averaged values in this table were taken for sunlight hours only, thus omitting nighttime



Figure 5-15. Photograph of solar dried mangoes compared with commercially-available mango slices

## CHAPTER 6 CONCLUSION

An inexpensive, natural-convection solar dryer capable of producing dried mango slices has been developed to reduce spoilage of fresh fruit in rural communities of Haiti. Experiments conducted with fresh mango fruit found the average initial moisture content to be 78.1% (wb) while commercially-available dried mango was 11.9% (wb). Sorption isotherms of mango slices followed a type III isotherm, which is characteristic of high sugar content products. Of both models tested, the GAB model resulted in the best fit of experimental data with a correlation coefficient of 0.995. A conservative analytical procedure was used in the design and development of this indirect-mode solar dryer. From this mathematical procedure, a 2.2 ft (0.67 m) high chimney was designed for exhaust of moist air with a solar absorber designed to be 18.36ft<sup>2</sup> (1.71m<sup>2</sup>) at a 28° inclination for maximum absorption of solar radiation in Haiti.

Evaluation of the solar dryer showed that under no-load conditions optimum temperatures of 162.9°F (72.7°C) and 156.3°F (69.0°C) were attained for trials with and without airflow-restriction respectively. The shutter demonstrated effective control of internal cabinet temperatures and relative humidity within the dryer. Tests performed with batch and continuous modes of operation, found that an average of 21.6 lbs (9.80 kg) of mango slices could be dried from approximately 84% (wb) down to an average of 10.25% (wb) in only 39 hours with optimum temperatures of 151.8°F (66.6°C). From these experiments, the collector, drying and system efficiency were determined to be 29.46%, 10.77% and 33.93% respectively. Furthermore, the thermal rock bed was found to effectively store and dissipate heat during periods of limited solar radiation.

Solar dried mango slices were found to have an average water activity of 0.56

using the newly developed isotherm model. This indicates an effective level of preservation as compared with commercially-available dried mangoes. Furthermore, color and texture were also preserved in these solar dried mango slices. Thus, this inexpensive dryer was found to be efficient and technically feasible for producing dried mango slices with the utilization of a widely available natural energy resource. Additionally, it stands to uplift socio-economy through potential employment opportunities and income generation by producing the highest value mango product while minimizing postharvest loss associated with fungal and bacterial infestation and wastage.

## CHAPTER 7 FUTURE DEVELOPMENTS

Several suggestions for the improvement of the current solar dryer design are noted here. These potential developments are detailed and discussed in this document in order to provide a basis for continuing the improvement of the current prototype. These proposed modifications are intended to improve the system in terms of the drying effectiveness, efficiency and throughput.

Through evaluation of the solar dryer, it was determined that an average of 21.6 lbs (9.80 kg) of mango slices could be dried in only 39 hours. A primary method of increasing the throughput is by scale-up of the current prototype. In this way, a larger system can be developed to process more fruit in the same time period. It is also expected that the drying time could be reduced by angling the drying trays. This would potentially allow more surface area contact with the drying air resulting in improved drying rates. Of course the drying rate can also be improved with the introduction of forced air, but this comes at the expense of a fan, a photovoltaic power source and other necessary electrical components.

The solar collector can also be modified to evaluate more effective designs. For instance, mesh can be incorporated to absorb additional heat or different material compositions can be explored to achieve improved solar collection. Additionally, the use of a supplemental heat component can be investigated. One option to explore is a biomass burner which could be fueled partially with mango peels. Although this option would require additional construction material to create an organic combustion area and a system to capture the heat, it does make use of mango peels which seem to have little use in the rural communities intended for the implementation of this solar dryer.

Further use of the mango peel byproduct can also be investigated to determine any uses such as oil extraction. Furthermore, the use of a desiccant can be explored to determine the feasibility of removing excess moisture from the air. The solar dryer can also be modified to incorporate a direct radiation component in the top portion of the drying cabinet. This could be beneficial particularly if the solar dryer is used with different products which are able tolerate direct radiation.

## APPENDIX A

### DRYING PARAMETERS

Table A-1. Mango drying parameters and storage conditions

<b>Initial Moisture Content:</b>	80-85 %	
<b>Final Moisture Content:</b>	12-18 %	
<b>Energy Required (MJ/kg):</b>	1.564	
<b>Maximum Temperature:</b>	70 °C	
<b>Storage</b>	Oval bundles and hung Larger amounts stored in millet granaries Fruit bars are wrapped in cellophane Leather is wrapped in polypropylene	
<b>Drying Methods</b>	<b>Low Temperature</b> 1. sun or solar (decentral small-scale batch system at farm) 2. tunnel 3. vacuum-drying 4. forced air dehydrator for leather	<b>High Temperature</b> 5. osmotically (8000 ppm SO <sub>2</sub> ) 6. sun and mechanical (fruit bars)
<b>Required drying time</b>	1. 1-2 weeks 2. – 3. – 4. 2 hours	5. – 6. 10 hours solar plus 16 hours electric or steam power
<b>Required drying temperature</b>	1. 70 °C; 55 °C in last stage of drying	6. 55 °C at beginning to a high of 70°C

Buchinger, J., & Weiss, W. (2002). Solar Drying. Austrian Development Cooperation: Institute for Sustainable Technologies.

## APPENDIX B STANDARD OPERATING PROCEDURES

### **Product Preparation**

Care should be taken in selecting fresh mango fruit which is moderately firm to the touch indicating a sufficient stage of ripening. Significantly soft fruit should be avoided as this is indicative of overly ripe fruit while excessively firm fruit indicates fruit that is not fully ripe. The whole mangoes should be thoroughly washed, peeled and cut into thin slices of approximately 5 to 10 mm. If any internal browning, bruising or other adverse quality characteristics are observed, the use of that fruit is not recommended. The mango slices should be dipped in warm water containing 0.1ppm citric acid or lemon juice for 3 minutes. Allow fresh mango slices to drain for several minutes before spreading on trays.

### **Dryer Operation**

Product should be spread evenly on the trays while ensuring no overlapping of fruit. For initial operation of the solar dryer, all trays are to be added at sunrise (7:00am) as indicated in the schedule presented further in this document. Proper operation of the solar dryer should allow the bottom tray to be completed midway (2:00pm) through the first day. The bottom tray should be removed at this point and finished product recovered from the tray.

Remaining trays should be shifted downward in the cabinet, and a new tray with fresh product can be added to the top position. Subsequent drying of trays should generally occur every 3 hours during sunlight exposure; although new trays should never be loaded within 2 hours of sunset (8:00pm) as drying will not progress before nightfall. Product can remain in the solar dryer during inclement weather and at night

time. If actual drying does not complete as scheduled, adjust the loading density with either less or more fresh product.

### **Maintenance/Cleaning**

Drying trays should be washed and cleaned between use. All solid particulate should be removed and any remaining residues should preferably be cleaned with moist, soapy water. The trays should be allowed to dry before loading with product. This process should be repeated each time a tray is removed during operation of the solar dryer. The solar collector should also be cleaned each morning to remove moisture and debris.

**APPENDIX C**  
**OPERATING SCHEDULE**

<b>TIME OF DAY</b>	<b>NOTES</b>
<u>Sunrise</u> (7:00am)	Initial loading of the fresh mango slices
<u>Midday</u> (2:00pm)	Remove bottom tray as drying finishes Shift remaining trays downward in cabinet Add new tray with fresh product to top position
<u>Every 3 Hours</u> (5:00pm)	Next tray removed from bottom as drying finishes Add new tray with fresh product to the top position
<u>Sunset</u> (8:00pm)	Trays/product can remain in solar dryer over night (Do Not Add Fresh Product Within 2 Hours of Sunset)
<u>Sunrise</u> (7:00am)	Clear any debris/moisture from solar collector Check cabinet/product to ensure no problems exist
<u>Every 3 Hours</u> (10:00am, 1:00pm) (4:00pm, 7:00pm)	Remove bottom tray as drying finishes Shift remaining trays downward in cabinet Add new tray with fresh product to top position

## LIST OF REFERENCES

- Adebayo, S. & Irtwange, S. V. (2009). Development and performance of a laboratory-scale passive solar grain dryer in a tropical environment. *Journal of Agricultural Extension and Rural Development*, 1(2), 139-152.
- Adegoke, C. O. & Bolaji, B. O. (2000). Performance evaluation of solar-operated thermosyphon hot water system in Akure. *International Journal of Engineering Technology*, 2(1), 35-40.
- Ahmad, A., Saini, J. S., & Varma, H. K. (1996). Thermohydraulic performance of packed-bed solar air heaters. *Energy Conversation Management*, 37(2), 205-214.
- Akanbi, C. H., Adeyemi, R. S., & Ojo, A. (2006). Drying characteristics and sorption isotherm of tomato slices. *Journal of Food Engineering*, 73, 157-163.
- Akoy, El-A. O. M., Ismail, M. A., Ahmed, El-F. A., & Luecke, W. (2006). Design and construction of a solar dryer for mango slices. Conference of International Research on Food Security, Natural Resource Management and Rural Development (pp 1-7), University of Bonn, October 11-13.
- Al-Juamly, K. E. J., Khalifa, A. J. N., & Yassen, T.A. (2007). Testing of the performance of a fruit and vegetable solar drying system in Iraq. *Desalination*, 209, 163-170.
- Amir, E. J., Djaya, C., Esper, A., Grandegger, K., & Mühlbauer, W. (1991). Development of a multi-purpose solar tunnel dryer for use in humid tropics. *Renewable Energy*, 1, 167-176.
- Ampratwum, D. B. (1998). Design of solar dryer for date. *Agricultural Mechanization in Asia, Africa and Latin America*, 29(3), 59-62.
- Arata, A. & Sharma, V. K. (1991). Performance evaluation of solar assisted dryers for low temperature drying applications-I. plants description. *Renewable Energy*, 1(5), 729-735.
- Ayensu, A. (1997). Dehydration of food crops using a solar dryer with convective heat flow. *Solar Energy*, 59, 121-126.
- Ayrancı E., Ayrancı, G., & Dogantac Z. (1990). Moisture sorption isotherms of dried apricot, fig and raisin at 20 °C and 36 °C. *Journal of Food Science*, 55(6), 1591-1593.
- Bakeka, B. J. D., & Bilgen, E. (2008). Solar Collector systems to provide hot air in rural applications. *Renewable Energy*, 33, 1461-1468.

- Bala B. K., Mondol M. R. A., Biswas B. K., Chowdury B. L. D., & Janjai S. (2003). Solar drying of pineapple using solar tunnel drier. *Renewable Energy*, 28, 183–190.
- Bhandari, R., Gewali, M. B., & Joshi, C. B. (2005). Performance evaluation of a hybrid solar biomass cabinet dryer. *European Journal of Scientific Research*, 4(1), 25-33.
- Bolaji, B. K. & Olalusi, A. P. (2008). Performance evaluation of a mixed-mode solar dryer. *Assumption University Journal of Technology*, 11(4), 225-231.
- Bolin, H. R. (1980). Relation of moisture to water activity in prunes and raisins. *Journal of Food Science*, 45(5), 1190-1192.
- Brett, A., Cox, D. R., Simmons, R., & Anstee,G. (1996). Producing solar dried fruit and vegetables for micro and small-scale rural enterprise development. *Handbook 3: Practical Aspect of Processing*, Natural Resources Institute, Chatham, UK.
- Buchinger, J., & Weiss, W. (2002). Solar Drying. Austrian Development Cooperation: Institute for Sustainable Technologies.
- Buteau, J. M. (2009). Mango Exports. JMB S. A.: Premium Quality Export Produce.
- Castañeda N. P., Rodriguez F., & Lundy, M. (2011). Assessment of Haitian Mango Value Chain: A participatory assessment of mango chain actors in southern Haiti. Catholic Relief Services (CRS), United States Conference of Catholic Bishops.
- Chau, K. V., Baird, C. D., & Bagnall, L. O. (1980). Performance of a plastic suspended screen solar air heater. *Journal of Agricultural Engineering Resources*, 25, 231-238.
- Chaudhri, S., Kothari, S., & Panwar, N. L. (2009). Performance evaluation of exhaust air recirculation system of mixed mode solar dryer for drying onion flakes. *International Journal of Renewable Energy Technology*, 1(1), 29-41.
- Chen C. R., Sharma A., & Lam H. X. (2007). Experimental thermal performance studies of a forced flow solar dryer. SOLARIS, Third International Conference, New Delhi, India, 1, 293-297.
- Chen, C. R., Sharma, A., & Vu Lan, N. (2009). Solar-energy drying systems: A review. *Renewable and Sustainable Energy Reviews*, 13, 1185-1210.
- Chua, K. J., & Chou, S. K. (2003). Low-cost drying methods for developing countries. *Trends in Food Science & Technology*, 14, 519-528.

- Condori, M., Echazu', R., & Saravia, L. (2001). Solar drying of sweet pepper and garlic using the tunnel greenhouse drier. *Renewable Energy*, 22, 447-460.
- Datta, G., Garg, H. P., & Kumar R. (1998). Simulation model of the thermal performance of a natural convection-type solar tunnel dryer. *International Journal of Energy Resources*, 22, 1165-1177.
- Dauthy, M. E. (1995). *Fruit and Vegetable Processing*. FAO Agricultural Services Bulletin No. 119.
- De Jung, G. I. W., Van den Berg, C., & Kokelaar A. J. (1996). Water vapour sorption behavior of original and defatted wheat gluten. *International Journal of Food Science Technology*, 31, 519-526.
- Ekechukwu, O. V. & Norton, B. (1999). Review of solar-energy drying systems II: An overview of solar drying technology. *Energy Conversion and Management*, 40(6), 615-655.
- El-Sebaii, A. A., Aboul-Enein, S., Ramadan, M. R. I., & El-Gohary, H. G. (2002). Experimental investigation of an indirect type natural convection solar dryer. *Energy Conversion and Management*, 43, 2251-2266.
- Enebe, O. M. & Ezekoye, B. A. (2006). Development and performance of modified integrated passive solar grain dryer. *The Pacific Journal of Science and Technology*, 7(2), 185-190.
- Enibe, S. O. (2002). Performance of a natural circulation solar air heating system with phase change material energy storage. *Renewable Energy*, 27, 69-86.
- Ezeike, G. O. I. (1986). Development and performance of a triple-pass solar collector and dryer system. *Energy in Agriculture*, 5, 1-20.
- Ezekwe, C. I. (1981). Crop drying with solar air heaters in tropical Nigeria. *ISES Solar World Forum*, Brighton, UK, 997-1005.
- Falade, K. O. & Aworh, O. C. (2004). Adsorption isotherms of osmo-oven dried African star apple (*Chrysophyllum albidum*) and African mango (*Irvingia gabonensis*) slices. *European Food Resource Technology*, 218, 278-283.
- Falade, K. O., Olukini, I., & Adegoke, G. O. (2004). Adsorption isotherm and heat of sorption of osmotically pretreated and air-dried pineapple slices. *European Food Resource Technology*, 218, 540-543.
- Goswami, Y. (1986). *Alternative energy in agriculture*. CRC Press Incorporated, Florida, 2, 83-102.

- Goyal, R. K., & Tiwari, G. N. (1999). Performance of a reverse flat plate absorber cabinet dryer: a new concept. *Energy Conversion Management*, 40, 385-392.
- Henderson, S. M., & Perry, R. L. (1976). Agricultural process engineering (3<sup>rd</sup> ed.). Westport, Connecticut: The AVI Publishing Company, Inc.
- Hossain M. A., & Bala B. K. (2007). Drying of hot chilli using solar tunnel drier. *Solar Energy*, 81, 85–92.
- Jairaj, K. S., Singh, S. P., & Srikant, K. (2009). A Review of solar dryers developed for grape drying. *Solar Energy*, 83, 1698-1712.
- Janjai, S., Srisittipokakuna, N., & Bala, B. K. (2008). Experimental and modeling performances of a roof-integrated solar drying system for drying herbs and spices. *Energy*, 33, 91-93.
- Jayaraman K. S., Das Gupta D. K., & Babu Rao N. (2000). Solar drying of vegetables. *Developments in Drying: Food dehydration*, 1, 179–186.
- Jindal, V. K., & Gunasekaran, S. (1982). Estimating air flow and drying rate due to natural convection in solar rice dryers. *Renewable Energy Review*, 4(2), 1-9.
- Kader, A. A. (2005). Increasing food availability by reducing postharvest losses of fresh produce. *International Postharvest Symposium*, 5, Verona, Italy.
- Kandpal, T. C., & Kumar, A. (2005). Solar drying and CO<sub>2</sub> emissions mitigation: potential for selected cash crops in India. *Solar Energy*, 78, 321-329.
- Kandpal, T. C., Kumar, A., & Purohit, P. (2006). Solar drying vs. open sun drying: A framework for financial evaluation. *Solar Energy*, 80, 1568-1579.
- Keener H. M., Sabbah, M. A., Meyer, G. E., & Roller, W. L. (1977). Plastic film solar collectors for grain drying. *Proceedings of the Solar Grain Drying Conference*, Urbana-Champaign, IL, 56–77.
- Khedkar D. M., & Roy S.K. (1990). Histological evidence for the reconstitutional property of dried/dehydrated raw mango slices. *Journal of Food Science Technology*, 25, 47.
- Koyuncu, T. (2006). An investigation on the performance improvement of greenhouse-type agricultural dryers. *Renewable Energy*, 31(7), 1055-1071.
- Labuza, T. P. & Altunakar, L. (2008). Water activity prediction and moisture sorption isotherms, in water activity in foods: fundamentals and applications. Oxford, UK: Blackwell Publishing Ltd.

- Leon, M. A. , Kuman, S., & Bhattacharya, S. C. (2002). A comprehensive procedure for performance evaluation of solar food dryers. *Renewable and Sustainable Energy Reviews*, 6, 367-393.
- Li, Z., Zhong, H., Tang, R., Liu, T., Gao, W., & Zhang, Y. (2006). Experimental investigation on solar drying of salted greengages. *Renewable Energy*, 31, 837-847.
- Lush, T. (2010). Mangoes, Tasty and Popular, Offer Hope for Haiti. The Free Library/Associated Press, August 2010. Online Service. Available from: <http://www.mnn.com/your-home/organic-farming-gardening/stories/mangoes-tasty-and-popular-offer-hope-for-haiti>.
- Madamba, P. S., & Lopez, R.I. (2002). Optimization of the osmotic dehydration of mango (*Mangifera indica L.*) slices. *Drying Technology*, 20(6), 1227-1242.
- Madhlopa, A., & Ngwalo, G. (2007). Solar dryer with thermal storage and biomass-backup heater. *Solar Energy*, 81, 449-462.
- Medlicott, A. (2001). Postharvest improvement program for the Haitian mango industry. USAID/Haiti Hillside Agricultural Program, March 2001. Online Service. Available from: [http://pdf.usaid.gov/pdf\\_docs/PNACL742.pdf](http://pdf.usaid.gov/pdf_docs/PNACL742.pdf).
- Mohamed, L. A., Kouhila, M., Jamali, A., Lahsasni, S., & Mahrouz, M. (2005). Moisture sorption isotherms and heat of sorption of bitter orange leaves (*Citrus aurantium*). *Journal of Food Engineering*, 67, 491-498.
- Mohamed, L. A., Kane, C. S. E., Kouhila, M., Jamali, A., Mahrouz, M., & Kechaou, N. (2008). Thin layer modeling of Gelidium sesquipedale solar drying process. *Energy Conversion and Management*, 49, 940-946.
- Mohanraj, M., & Chandrasekar, P. (2008). Drying of copra in a forced convection solar drier. *Biosystems Engineering*, 99, 604-607.
- Mrema, G. C., Brenndorfer, B., Kennedy, L., Oswin-Bateman, C. O., Trim, D. S., & Wereko-Brobbey, C (1987). Solar Dryers—their Role in Post-Harvest Processing. Commonwealth Science Council, London, UK.
- Mumba, J. (1996). Design and development of a solar grain dryer incorporating photovoltaic powered air circulation. *Energy Conservation Management*, 37, 615-621.
- Mwithiga, G., &Kigo, S. N. (2006). Performance of a solar dryer with limited sun tracking capability. *Journal of Food Engineering*, 74, 247-252.

- National Academy of Sciences. (1978). Postharvest Food Losses in Developing Countries. National Academy of Sciences, Washington D.C., 202.
- Othieno, H., Grainger, W., & Twidell, J. W. (1981). Application of small scale solar crop driers to maize drying in Kenya. Proceeding of the 2<sup>nd</sup> Conference on Energy for Rural and Island Communities. London, UK: Pergamon Press, 377-386.
- Pande, P. C., & Thanvi, K. P. (1991). Design and development of a solar dryer cum water heater. *Energy Conversion Management*, 31, 419-424.
- Pangavhane, D. R., Sawhney, R. L., & Sarsavadia, P. N. (2002). Design, development and performance testing of a new natural convection solar dryer. *Energy*, 27, 579-590.
- Pawar, R. S., Takwale, M. G., & Bhide, V. G. (1995). Solar drying of custard powder. *Energy Conversion Management*, 36, 1085-1096.
- Pott, I., Neidhart, S., Mühlbauer, W., & Carle, R. (2005). Quality improvement of non-sulphited mango slices by drying at high temperatures. *Innovative Food Science Emerging Technology*, 6, 412-419.
- Prasad, J., Vijay, V. K., Tiwari, G. N., & Sorayan, V. P. S. (2006). Study on performance evaluation of hybrid drier for turmeric (*Curcuma longa L.*) drying at village scale. *Journal of Food Engineering*, 75, 497-502.
- Ranganna, S. (1986). Handbook of analysis and quality control for fruits and vegetable products. New Delhi: Central Food Technological Research Institute, Tata: McGraw-Hill Publishing Company.
- Rangel-Marrón, M., Welti-Chanes, J., Córdova-Quiroz, A. V., Cerón-Bretón, J. G., Cerón-Bretón, R. M., & Anguebes-Franceschi F. (2011). Estimation of moisture sorption isotherms of Mango Pulp Freeze-dried. *International Journal of Biology and Biomedical Engineering*, 5(1), 18-23.
- Sarsavadia, P. N. (2007). Development of a solar-assisted dryer and evaluation of energy requirement for the drying of onion. *Renewable Energy*, 32, 2529-2547.
- Sarsilmaz, C., Yildiz, C., & Pehlivan, D. (2000). Drying of apricots in a rotary column cylindrical dryer (RCCD) supported with solar energy. *Renewable Energy*, 21, 117-127.
- Shanmugam, V., & Natarajan, E. (2006). Experimental investigation of forced convection and desiccant integrated solar dryer. *Renewable Energy*, 31, 1239-1251.

- Shanmugam, V., & Natarajan, E. (2007). Experimental study of regenerative desiccant integrated solar dryer with and without reflective mirror. *Applied Thermal Engineering*, 27, 1543-1551.
- Sharma, V. K., Colangelo, A., & Spagna, G. (1995). Experimental investigation of different solar dryers suitable for fruit and vegetable drying. *Renewable Energy*, 6, 413-424.
- Shove, G. C. (1977). Solar energy collectors for drying grain. *Proceedings of the Solar Grain Drying Conference*. Urbana-Champaign, Illinois, 34-38.
- Shyam, S. S., Rahman, M. S., & Labuza, T. P. (2001). Measurement of Water Activity Using Isopiestic Method. *Current Protocols in Food Analytical Chemistry*. New York: John Wiley & Sons, A2.3.1-A2.3.10.
- Singh, K. K. (1994). Development of a small capacity dryer for vegetables. *Journal of Food Engineering*, 21, 19-30.
- Singh P. P., Singh, S., & Dhaliwal, S. S. (2004). Multi-shelf portable solar dryer. *Renewable Energy*, 29, 753-765.
- Singh P. P., Singh, S., & Dhaliwal, S. S. (2006). Multi-shelf domestic solar dryer. *Energy Conversion Management*, 47, 1799-1815.
- Smitabhindu, R., Janjai, S., & Chankong, V. (2008). Optimization of a solar-assisted drying system for drying bananas. *Renewable Energy*, 33, 1523-1531.
- Sodha, M. S., Bansal, N. K., Kumar, A., Bansal, P. K., & Malik, M. A. (1987). Solar crop drying, Vol. I and II. Boca Raton, Florida: CPR Press.
- Sodha, M. S., Dang, A., Bansal, P. K., & Sharma S. B. (1985). An analytical and experimental study of open sun drying and a cabinet type drier. *Energy Conversion Management*, 25, 263-271.
- Sreekumar A., Manikantan P. E., & Vijayakumar K. P. (2008). Performance of indirect solar cabinet dryer. *Energy Conversion Management*, 49, 1388-1395.
- Thoruwa, T. F. N., Smith, J. E., Grant, A. D., & Johnstone, C. M. (1996). Developments in solar drying using forced ventilation and solar regenerated desiccant materials. *Renewable Energy*, 9, 686-689.
- Tiris, C., Tiris, M., & Dincer, I. (1995). Investigation of the thermal efficiencies of a solar dryer. *Energy Conservation Management*, 36(3), 205-212.
- Tsami E., Marinos-Kovris D., & Maroulis Z.B. (1990). *Journal of Food Science*, 55, 1594.

Yahia, E. M. (1999). Postharvest Handling of Mango: Technical Report. Agricultural Technology Utilization and Transfer/RONCO. August 1998. Online Service. Available from: <http://www.manarasoft.com/pdf/P85.pdf>.

Zomorodian, A., Zare, D., & Ghasemkhani, H. (2007). Optimization and evaluation of semi- continuous solar dryer for cereals (Rice, etc). Desalination, 209, 129-135.

## BIOGRAPHICAL SKETCH

Drew Schiavone was born in Decatur, Georgia but he spent most of his youth in St. Augustine, Florida where he graduated with honors from Bartram Trail High School in 2003. While completing his undergraduate curriculum, Drew became interested in resource availability in a global context. At this time, he joined Engineers Without Borders to assist international communities with engineering applications. He earned his B.S. in agricultural and biological engineering in 2008; graduating cum laude, and spent several years working before returning to the ABE Graduate Program at UF.

Drew held several research positions at the University of Florida during his graduate program, including his position as a biological technician at the Interdisciplinary Center of Biotechnology Research and as a postharvest lab technician in the Horticultural Sciences Department. Drew has made an effort to improve the handling practices of fresh commodities in order to ensure higher quality products are available to a wider community. Through his academic and professional endeavors, Drew hopes to minimize postharvest losses, improve process efficiency and enhance product quality with practical, economical and environmentally responsible practices.

Upon completion of his M.S. program, Drew plans to pursue a Ph.D. program in agricultural engineering. Drew has been married to Jessica M. Schiavone for almost two years. They are expecting their first daughter in January 2012.